

PROCESS-BASED SIMULATIONS OF NEAR-SURFACE
HYDROLOGIC RESPONSE FOR A FORESTED UPLAND
CATCHMENT: THE IMPACT OF A ROAD

A THESIS
SUBMITTED TO THE DEPARTMENT OF GEOLOGICAL
AND ENVIRONMENTAL SCIENCES
AND THE COMMITTEE ON GRADUATE STUDIES
OF STANFORD UNIVERSITY
IN PARTIAL FULFILLMENT OF THE REQUIREMENTS
FOR THE DEGREE OF
MASTER OF SCIENCE

Anona L. Dutton
April, 2000

© Copyright by Anona L. Dutton 2000
All Rights Reserved

ACKNOWLEDGMENTS

This thesis reflects a collection of the support that I received from friends, peers, and advisors that made a crazy little idea I had after spending a summer in the woods a reality. Beverley Wemple, then a PhD. student at Oregon State, and now a professor at the University of Vermont, instigated my interest in this project and provided me with contacts and information that I would have otherwise had no access to. My advisor, Keith Loague, put forth a supreme effort from the initiation of this thesis until its completion, providing guidance both academically and in the field. The opportunity to work with the individuals in the “hydro” group has left me inspired and awestruck. They are truly an amazing collection of scientists who have been invaluable to my thesis work and to my overall education as a graduate student. The modeling component of this study would not have been possible without the brilliance and patience of Mike Pinto, who took hours of his time to help me. Beverley, Leigh Soutter, and Iris Stewart were dedicated to my efforts in the field and continue to provide me with perspective and mentorship. George Mader was kind enough to be my second reader and provide me with the insight that a reader from another discipline can bring. I also thank the folks at the H.J. Andrews Experimental Forest who let me borrow their equipment and drill holes in their land.

My thanks also go out to my friends and family who have loved and supported me through the roughest times down this thesis road. My deepest thanks to the folks at DEAL who have made a home together that includes the warmth of friendship and family dinners, to team GLD and our adventures and aspirations, to my “girls” Felicia Chu, Noelle Marquis, and Katherine Greig who I know as deeply as I know myself, to my brother, Pascual Dutton, who I will always be chasing in awe, to my parents, Peter and Rhonda Dutton, who I value above all else, and to Paul Hagin who I learn from each and everyday and who makes me laugh more and louder than I ever have.

The funding for this study was provided in part by the Wright Fund and by the Center for Earth Science Information research (CESIR). Without these funding sources, this effort would not have been possible. Computing facilities used in this study were provided, in part, by an equipment grant to Steven Gorelick and Keith Loague (i.e. the Stanford Hydrogeology Group) from the National Science Foundation.

ABSTRACT

Forest management practices, specifically logging road construction, create seepage faces and hydraulic conductivity contrasts that can significantly affect the hydrologic response, accelerate the near-surface evolution of a hillslope catchment, and increase erosion and mass wasting events. The objective of this study is to understand the physical, topographic, and hydrologic controls that drive subsurface flow at Watershed 3 (WS3) in the H.J. Andrews Experimental Forest, Blue River, OR and the role logging roads play in altering the hydrologic processes. This study combines a field component, process-based numerical simulation of near-surface hydrologic response, and slope stability analyses to address the impact of a road in a typical steep forested catchment.

The fieldwork conducted at WS3 characterized hillslope morphology, soil depth, and soil properties of a single hillslope (C3) within WS3. The modeling component of this study had four objectives: (i) identify what part of the WS3 and C3 hillslope systems were most drastically effected by the presence of a road using NUM5, a simple 2-D finite-difference model; (ii) isolate that portion of the flow domain for more detailed simulation with VS2DT, a 2-D transient, saturated-unsaturated, finite-difference model; (iii) compare the results from the VS2DT simulations with observed piezometric levels and hydrograph data for precipitation events in 1995; (iv) use the factor of safety criterion to assess if pore pressure buildup in specific areas of C3 during a series of hypothetical events would be enough to trigger a mass movement event.

In general, the results from this study show that slope stability decreases as a function of rainfall intensity and/or duration, with increased slope angle, with higher antecedent soil-water content conditions, and with increased hydraulic conductivity contrast between the high conductivity soil and the compacted soil beneath the road. The vertical hydraulic conductivity contrast below the road acts to impede the slope-parallel subsurface flow and water builds up behind the low permeability zone and creates a region of groundwater mounding. The increased pore pressure leads to an increased risk of failure that propagates upslope from the road.

TABLE OF CONTENTS	
ACKNOWLEDGMENTS	i
ABSTRACT	ii
TABLE OF CONTENTS	iii
LIST OF TABLES	vii
LIST OF FIGURES	ix
CHAPTER ONE: INTRODUCTION	1
OBJECTIVE	2
INTRODUCTION	2
STUDY SITE DESCRIPTION	3
Geology	8
Climate	10
Vegetation	10
Prior Work in the H.J. Andrews Experimental Forest	10
Coos Bay Case Study	16
<i>Instrumentation</i>	16
<i>Findings</i>	16
BACKGROUND	19
Streamflow Generation	19
Hillslope Hydrogeology	19
Roads	21
Hydrologic Impacts	23
Sedimentation Impacts	24

Landslides	27
NUMERICAL MODELING	28
FACTOR OF SAFETY ANALYSIS	30
CONCLUSIONS	31
CHAPTER TWO: METHODS	33
FIELDWORK	34
Topographic Mapping	34
Soil Depth	38
Hydraulic Conductivity	38
<i>Surface and near-surface</i>	38
<i>Saturated sub-surface</i>	41
Soil-water Content	41
Characteristic Curves	41
NUMERICAL MODELING	43
Finite-difference Method	43
<i>NUM5</i>	44
Assumptions	46
Boundary Value Problem	48
WS3	48
C3	52
<i>VS2DT</i>	52
VS2DT Equations	55
Boundary Value Problem	56
VS2DT Testing	60
Simulated Events	63
FACTOR OF SAFETY ANALYSIS	66

Sensitivity Analysis	70
Boundary Value Problem	70
<i>NUM5</i>	70
<i>VS2DT</i>	74
CHAPTER THREE: RESULTS	75
FIELDWORK	76
NUM5	76
<i>Soil Depth</i>	76
<i>Saturated Hydraulic Conductivity</i>	76
VS2DT	80
<i>Saturated Hydraulic Conductivity</i>	80
Surface and Near-surface	80
Saturated Sub-surface	87
<i>Soil-water Content</i>	87
<i>Characteristic Curves</i>	90
NUMERICAL MODELING	90
NUM5	90
WS3	94
Hydraulic Head	94
Flow Paths	96
Pressure Distribution	98
C3	98
Hydraulic Head	98
Flow Paths	101
Pressure Distribution	101
<i>Discussion</i>	102
<i>Factor of Safety Analysis</i>	104
VS2DT	108
<i>Model Testing</i>	108
<i>Rainfall Events</i>	110

<i>Factor of Safety Analysis</i>	117
<i>Simulated Events</i>	120
<i>Rainfall Events</i>	121
Hydrologic Response	121
Case 1	123
Case 2	126
Cases 3-5	126
Case 6	127
<i>Factor of Safety Analysis</i>	127
Sensitivity Analysis	127
Rainfall Events	131
Case 1	131
Case 2	131
Cases 3-5	133
Case 6	133
Case 7	133
<i>Discussion</i>	134
CHAPTER FOUR: CONCLUSIONS	138
SUMMARY	139
DISCUSSION	141
IIPLICATIONS	142
REFERENCES	145

LIST OF TABLES

Table 1. Major plant species found at C3 (from Hawk and Dyrness, 1969).	11
Table 2. A sampling of previous work and key results from studies done on the impact of roads on hydrology.	25
Table 3. A sampling of previous work and key results from studies done on the impact of roads on sedimentation.	26
Table 4. Summary of the field data collected for C3. For the location of the measurement points see Figures 11, 12, and 13.	35
Table 5. Summary of the simulations conducted using NUM5.	45
Table 6. Assumptions made in this study related to the NUM5 simulations for WS3 and C3.	47
Table 7. Summary of three storm events and discharge recorded at C3 for 1995. (a) Ranked in terms of the maximum half-hour precipitation intensity. (b) Ranked in terms of the total precipitation. (c) Ranked in terms of the maximum discharge. (d) Ranked in terms of the average precipitation intensity.	61
Table 8. Summary of the case studies used to determine the sensitivity of the C3 hillslope to failure.	65
Table 9. Parameter values used in this study for the factor of safety analysis at the C3 hillslope.	71
Table 10. Summary of the FS input data used in a sensitivity study to assess the sensitivity of (a) Pore pressure development and (b) Factor of safety to the hydraulic conductivity contrast along the failure plane. The Ks value representing the compacted soil beneath the road was 1×10^{-7} m/s in the NUM5 simulations.	73
Table 11. Description of the soil types that dominate WS3 (from Hawk and Dyrness, 1969).	77
Table 12. Saturated hydraulic conductivity values that represent the different geologic layers in the NUM5 simulations. The values in bold were the values used in this study.	79

Table 13. Summary of the Ks values measured for the top meter of soil using the Guelph permeameter.	82
Table 14. Saturated hydraulic conductivity values estimated using slug tests. See Figure 14 For the piezometer locations.	85
Table 15. Pore pressure simulated at each measurement point throughout the C3 hillslope when the system was subject to different initial conditions and/or rainfall rates. See Table 8 for case descriptions and Figure 25 for measurement locations.	125

LIST OF FIGURES

Figure 1. Location of WS3 within the H.J. Andrews Experimental Forest The H.J. Andrews occupies the Lookout Creek watershed in Oregon's Western Cascades (from Wemple, PhD. Thesis, 1998).	4
Figure 2. Map of the C3 hillslope. (a) Location of the C3 hillslope within WS3. (b) Enlarged view of the C3 hillslope showing its relation to the road and to the adjacent catchments within WS3.	6
Figure 3. Relief map of the C3 hillslope.	7
Figure 4. Schematic illustration of the WS3 geologic profile.	9
Figure 5. Location of WS1, WS2, and WS3 in the H.J. Andrews Experimental forest.	12
Figure 6. Schematic of the various types of mass movements associated with road construction.	15
Figure 7. Map of the Coos Bay catchment showing the topographic contours and the location of the piezometers (from Montgomery, 1997).	17
Figure 8. Schematic illustration of the ways that a road can impact the hydrologic and geomorphic processes within a watershed (after Wemple, 1998).	22
Figure 9. Schematic illustration of groundwater flow being intercepted by the roadcut.	29
Figure 10. Relief map of the C3 hillslope showing the 13 transects used in the topographic mapping.	36
Figure 11. Plan view of the C3 hillslope showing the elevation contours and the location of the transects and measurement locations.	37
Figure 12. Relief map of the C3 hillslope showing the location of the soil depth measurements.	39
Figure 13. Relief map of the C3 hillslope showing the location for the hydraulic conductivity and soil-water content data.	40
Figure 14. Relief map of the C3 hillslope showing the location of the piezometers.	42

Figure 15. Finite-difference grid used for the NUM5 simulations in this study ($\Delta y = 10\text{m}$, $\Delta z = 2\text{m}$).	49
Figure 16. Boundary value problem for the WS3 hillslope. (a) Homogeneous hillslope. (b) Homogeneous hillslope with roadcut.	50
Figure 17. Boundary value problem for the WS3 hillslope. (a) Heterogeneous hillslope. (b) Heterogeneous hillslope with roadcut.	51
Figure 18. Boundary value problem for the C3 hillslope. (a) Homogeneous hillslope. (b) Homogeneous hillslope with roadcut.	53
Figure 19. Boundary value problem for the C3 hillslope. (a) Heterogeneous hillslope. (b) Heterogeneous hillslope with a roadcut.	54
Figure 20. The portion of the C3 hillslope simulated in NUM5 that defined the BVP for the VS2DT simulations.	57
Figure 21. Finite-difference mesh used for the VS2DT simulations ($\Delta y = 0.42\text{m}$, $\Delta z = 0.05\text{m}$) in this study.	58
Figure 22. The boundary value problem representing the portion of the C3 hillslope simulated with VS2DT.	59
Figure 23. Simulated versus observed precipitation intensity and duration for the three 1995 storm events recorded at C3 and used to calibrate the VS2DT model. (a) November 24 event. (b) November 29 event. (c) December 28 event.	62
Figure 24. Location of the four piezometers and six measurement points for the VS2DT simulations.	64
Figure 25. Schematic illustration of the forces acting on a point along the potential failure plane surface (after Selby, 1993).	67
Figure 26. Schematic illustration of the shearing versus resisting as they act on a rectangular block resting on a shear plane. β is the slope angle and W is equal to $l\gamma z \cos\beta$.	68
Figure 27. Boundary value problem used in the Factor of safety analysis. (a) The C3 hillslope simulated by NUM5. (b) The portion of the C3 hillslope simulated with VS2DT.	72
Figure 28. Soil depths measured at C3 using a soil drive probe. See Figure 12 for measurement locations.	81

Figure 29. The C3 saturated hydraulic conductivity values for (a) Surface soils as measured with a pressure infiltrometer and (b) The top meter of soil as measured using a guelph permeameter. See Figure 13 for measurement locations.	83
Figure 30. The kriged map of the spatial distribution in the hydraulic conductivity values over the C3 hillslope.	85
Figure 31. A geostatistical realization of the spatial variation in the hydraulic conductivity values over the C3 hillslope.	86
Figure 32. Falling head slug test results for saturated hydraulic conductivity in the saturated zone at five locations. The locations are shown on Figure 14. (a) 3P4. (b) 4P2. (c) 4P4. (d) 4P1. (e) 4P3. (f) 3P10.	88
Figure 33. Plan View of the TDR measurements taken at three different depths over C3. The location of the measurement sites is shown on Figure 13.	89
Figure 34. Comparison of the C3 characteristic curve of soil-water retention to the six curves for Coos Bay. (a) CB site 1. (b) CB site 2. (c) CB site 3. (d) CB site 4. (e) CB site 5. (f) CB site 6. The locations of the CB sites are given by Torres et al. (1998).	91
Figure 35. (a) Average characteristic curve of soil-water retention at six sites on the Coos Bay catchment (CB), both wetting and drying. See Figure 34 for the original curves. (b) Comparison of characteristic curve of soil-water retention for C3 and the average characteristic curve (wetting).	92
Figure 36. Characteristic curve of hydraulic conductivity as a function of pressure head based upon the Van Genuchten (1980) approach.	93
Figure 37. WS3 hydraulic head distribution simulated using NUM5. (a) Homogeneous. (b) Heterogeneous. (c) Homogeneous with road. (d) Heterogeneous with road.	95
Figure 38. WS3 flowlines simulated using NUM5. (a) Homogeneous. (b) Heterogeneous. (c) Homogeneous with road. (d) Heterogeneous with road.	97
Figure 39. WS3 pore pressure distribution simulated using NUM5. (a) Homogeneous. (b) Heterogeneous. (c) Homogeneous with road. (d) Heterogeneous with road.	99
Figure 40. Hydraulic head distribution for the C3 hillslope as simulated using NUM5. (a) Homogeneous. (b) Heterogeneous. (c) Homogeneous with road. (d) Heterogeneous with road.	100

Figure 41. Flowlines for the C3 hillslope as simulated using NUM5. (a) Homogeneous. (b) Heterogeneous. (c) Homogeneous with road. (d) Heterogeneous with road.	102
Figure 42. Pore pressure distribution for the C3 hillslope as simulated using NUM5. (a) Homogeneous. (b) Heterogeneous. (c) Homogeneous with road. (d) Heterogeneous with road.	103
Figure 43. Factor of safety analysis based on the NUM5 simulation results. Above the road FS values are less than one indicating imminent slope failure under fully saturated conditions.	105
Figure 44. Comparison of the impact that the Ks value for the compacted soil beneath the road has on the (a) Pore pressure distribution and (b) FS values. See Table 10 for case descriptions.	107
Figure 45. Comparison of VS2DT simulated results to the observed volumetric discharge at the C3 hillslope during the three storm events used for model calibration. (a) Simulated versus observed volumes of water discharged at the roadcut face. (b) Potential error in simulated estimates related to observed data.	109
Figure 46. The piezometric response simulated by VS2DT compared to that recorded at C3 during the November 24, 1995 storm event. See Figure 14 for piezometer locations. (a) 3P4. (b) 3P6. (c) 3P8. (d) 3P9.	111
Figure 47. The piezometric response simulated by VS2DT compared to that recorded at C3 during the November 29, 1995 storm event. See Figure 14 for piezometer locations. (a) 3P4. (b) 3P6. (c) 3P8. (d) 3P9.	112
Figure 48. The piezometric response simulated by VS2DT compared to that recorded at C3 during the December 8, 1995 storm event. See Figure 14 for piezometer locations. (a) 3P4. (b) 3P6. (c) 3P8. (d) 3P9.	113
Figure 49. Hydraulic head distribution throughout the C3 hillslope during the November 24, 1995 storm event as simulated by VS2DT.	114
Figure 50. Water table location throughout the C3 hillslope at different times during the November 24, 1995 storm event as simulated by VS2DT.	115
Figure 51. Partial flownet throughout the C3 hillslope during the November 24, 1995 storm event as simulated by VS2DT.	116
Figure 52. Pore pressure distribution throughout the C3 hillslope during the November 24, 1995 storm event as simulated by VS2DT.	118

Figure 53. Factor of safety values measured at one-day intervals along the potential failure plane during the simulated 1995 storm events. (a) November 24 storm event. (b) November 29 storm event. (c) December 28 storm event.	119
Figure 54. Total volumetric discharge recorded at the C3 hillslope as the rainfall rate varied over four orders of magnitude. (a) Base case. (b) Case 1. (c) Case 2. (d) Case 3. (e) Case 4. (f) Case 5. See Table 8 for case descriptions.	122
Figure 55. Pore pressure values simulated at six points on the C3 hillslope as the rainfall rate varied over four orders of magnitude. (a) Base case. (b) Case 1. (c) Case 2. (d) Case 3. (e) Case 4. (f) Case 5. See Figure 24 for the locations of the measurement points. See Table 8 for case descriptions.	124
Figure 56. Impact of storm duration on the C3 hydrologic response. (a) Volumetric discharge recorded at C3 at the end of each event. (b) Pore pressure response to each storm event. (c) Factor of safety distribution over the C3 hillslope.	128
Figure 57. Sensitivity of the Factor of safety values to adjusting individual parameters by +10% and -10%. (a) The thickness of the failure slab. (b) The root cohesion. (c) The slope angle. (d) The angle of internal friction. (e) The soil cohesion.	130
Figure 58. Factor of safety values simulated at the C3 hillslope as the rainfall rate varied over four orders of magnitude. (a) Base case. (b) Case 1. (c) Case 2. (d) Case 3. (e) Case 4. (f) Case 5. See Table 8 for case descriptions.	132
Figure 59. Pore pressure values simulated throughout the C3 hillslope subject to rainfall events varying over four orders of magnitude. (a) Base case. (b) Discharge at roadcut face routed over the road to recharge the downslope side of the C3 system.	135
Figure 60. Factor of safety values as the rainfall rate varied over four orders of magnitude. (a) Base case. (b) Water routed over the road and recharging the system on the downslope side.	136

CHAPTER ONE: INTRODUCTION

pressures. Depending on the degree of saturation, the colluvium thickness, and the intensity of a given rainfall event, periodic failure of hillslopes can be triggered that can scour the hollows down to bedrock.

It is now widely recognized that forest management practices, including timber harvesting and road construction, can significantly affect the hydrologic response, accelerate the near-surface evolution of a hillslope catchment, and increase sediment loading to downstream areas. Roads pose a significant contribution to cumulative watershed effects (CWE), and are implicated in ecosystem disturbance, accelerated nutrient and sediment transport, and degraded water quality issues. Specifically, prior work has identified logging roads as a significant factor in the increased incidence of shallow landsliding and the increased rate of fine sediment production in previously undeveloped mountainous areas (Harr, 1976; Swanson and Dyrness, 1975; Reid and Dunne, 1984). Roads act, via their geomorphic impacts, to degrade habitats in mountainous regions, to physically damage private and public property, and to endanger lives.

Roads are an integral part of silvicultural systems, but their impacts on watershed function can be isolated from other forest harvesting activities to assess their individual contributions to geomorphic events, changes in near-surface hydrology, and increased sediment production. Determining the conditions under which subsurface flow will be intercepted by a roadcut or the impermeable surface of a road to become surface flow has many implications for land use practices and for making informed land-use management decisions, especially in the Pacific Northwest.

STUDY SITE DESCRIPTION

The field component of this study was conducted on a 2-ha convergent hillslope within Watershed 3 (WS3), a 10.23-ha watershed in the U.S. Forest Service's H.J. Andrews (HJA) Experimental Forest that is shown in Figure 1. The HJA was established in 1932 to study the effects of logging and related forest management practices on watershed function. The HJA encompasses the Lookout Creek watershed in the Western Cascades about 80 kilometers east of Eugene, Oregon. Logging and road construction

OBJECTIVE

The objective of this study is to understand the physical and hydrologic processes that control subsurface flow in a steep forested catchment within the H.J. Andrews experimental forest and the role logging roads play in altering the near-surface hydrologic processes. This study combines fieldwork, hydrologic modeling, and slope stability analysis to address the impact of a road in a typical forested Western Oregon catchment.

INTRODUCTION

The suite of hydrologic and geomorphic processes operating in steep, forested catchments are extremely complex. The groundwater conditions and the soil properties within a hillslope are of interest to geomorphologists and engineers in their efforts to understand the three-dimensional form of hillslopes and the related hydrogeologic and geomorphic processes. Physical processes, including interactions between the saturated and unsaturated systems, perched water tables, and multiple seepage faces influence shallow landsliding and other mass movements (Rulon et al., 1985). Both large scale mass wasting events that occur over a short period of time and slow creeping soil movements impose important controls on landscape evolution and ultimately determine hillslope morphology (Dietrich and Dunne, 1982; Dietrich et al., 1986). Hillslope form, geology, and land use history can strongly influence the near-surface hydrologic response (Dunne et al., 1975). Recognition of the feedback loop between slope form, hydrologic response, runoff generation, and shallow landsliding is fundamental to understanding the geomorphology of mountain watersheds (Montgomery et al., 1997).

The convergent and steeply sloping hollows typical of the forested catchments of the Western Cascades are often filled with colluvium and are overlain by high permeability soils (B. Wemple, personal communication, 1999). Hillslope debris moves downslope slowly as a result of various hillslope processes (i.e. soil creep and rainsplash), but where overland flow and erosion ^{are} is minimal, colluvium accumulates at an increased rate along the axis of convergent hollows (Dietrich and Dunne, 1982). These fill and surface materials have a higher saturated hydraulic conductivity than the underlying layers of saprolite and bedrock. The concave topography and the conductivity contrast at the colluvium-bedrock contact are conducive to the formation of elevated pore

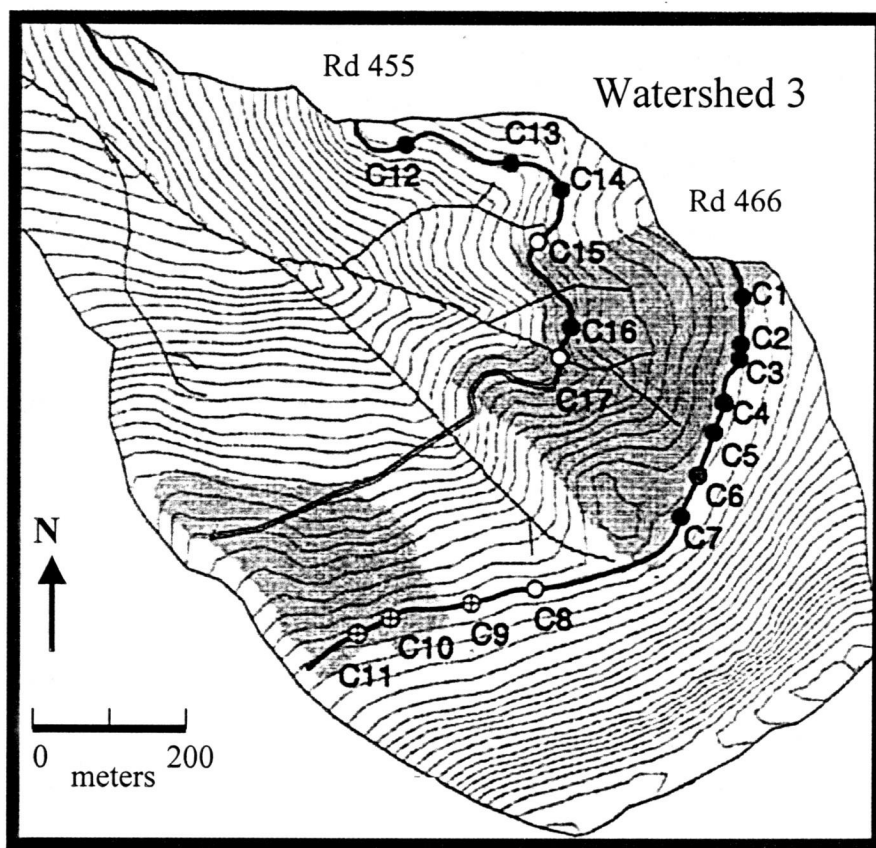
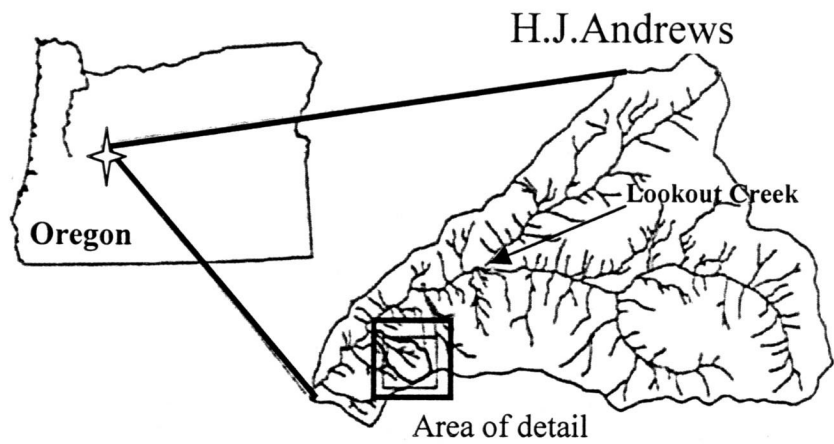


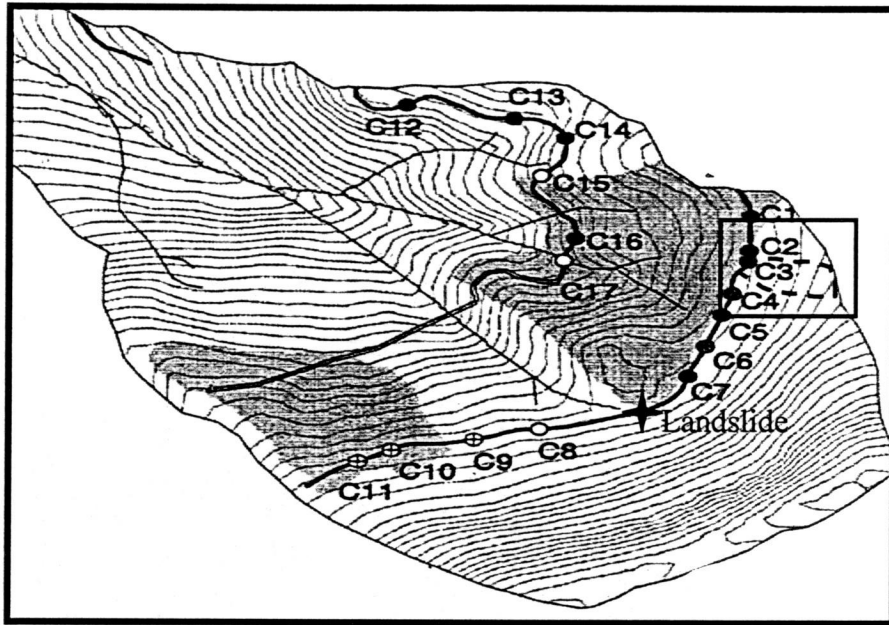
Figure 1. Location of WS3 within the H.J. Andrews Experimental Forest. The H.J. Andrews occupies the Lookout Creek watershed in Oregon's Western Cascades (from Wemple, 1998).

have resulted in a patchwork of harvest units on 25% of the land area and a road density of approximately 3 km/km² (Jones and Grant, 1996). WS3 is a tributary to Lookout Creek. The WS3 watershed has a Northwest aspect and ranges in elevation from 490 m to 1070 m with slopes of 60-100% (Rothacher et al., 1967; Jones and Grant, 1996). There is a precise record of the land use history for WS3 because of its part in a long-term paired watershed experiment. The watershed study was initiated in the early 1950s to compare the impacts of different forest harvest practices on ecosystem disturbance and streamflow (e.g. Jones and Grant, 1996; Thomas and Megahan, 1998).

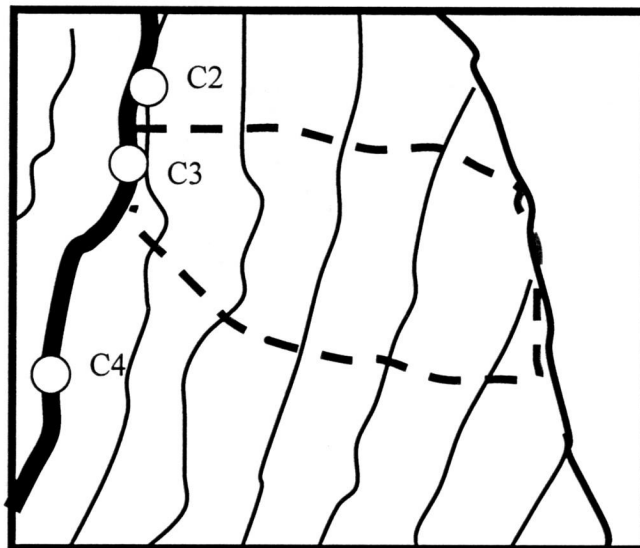
Prior to the field work done in this study, the concave 2-ha hillslope above Culvert 3 (C3) in Watershed 3 (WS3), (see Figure 2), was mapped and instrumented by other workers (eg. Dyrness, 1967; Wemple, 1996), but not at the detail of the work reported here. Figure 3 shows the C3 study area that is located above the upper road and extends to the ridge-top with an average gradient of 20°. At the road cut face the slope is greater than 45° but the gradient decreases moving towards the ridge. The North side of the catchment is considerably steeper than the southern nose and so the soil and hydrologic properties are expected to be different not only from the top of the ridge to the road, but from nose to nose of the catchment. Overland flow has not been observed for this catchment, but significant seepage has been observed and measured at the roadcut face (B. Wemple, personal communication, 1999). The C3 site was selected for the study reported here because of pre-existing instrumentation, the concave nature of the topography, and the lack of understory vegetation that made fieldwork feasible.

The C3 hillslope is intercepted by a six-meter wide service road (see Figure 2) that was built in 1959 using cut and fill engineering techniques. Under Megahan's (1987) classification scheme, which is derived from Idaho National Forest Classification schemes, this type of road can sustain traffic with expected speeds of 8-16 km/hr. Because the road was built prior to any specifications for the width and design of logging roads it is wider than current service roads. In 1996 a major landslide initiated on the downslope side of the upper road in WS3 (see Figure 2) and scoured a convergent hollow down to bedrock. This large-scale mass movement occurred in a similar topographic and geologic setting as C3 and was obviously related to the logging road carved through the WS3 catchment.

(a)



(b)



- C3 boundary
- Road
- Culvert

Figure 2. Map of the C3 hillslope. (a) Location of the C3 hillslope within WS3. (b) Enlarged view of the C3 hillslope showing its relation to the road and to the adjacent catments within WS3.

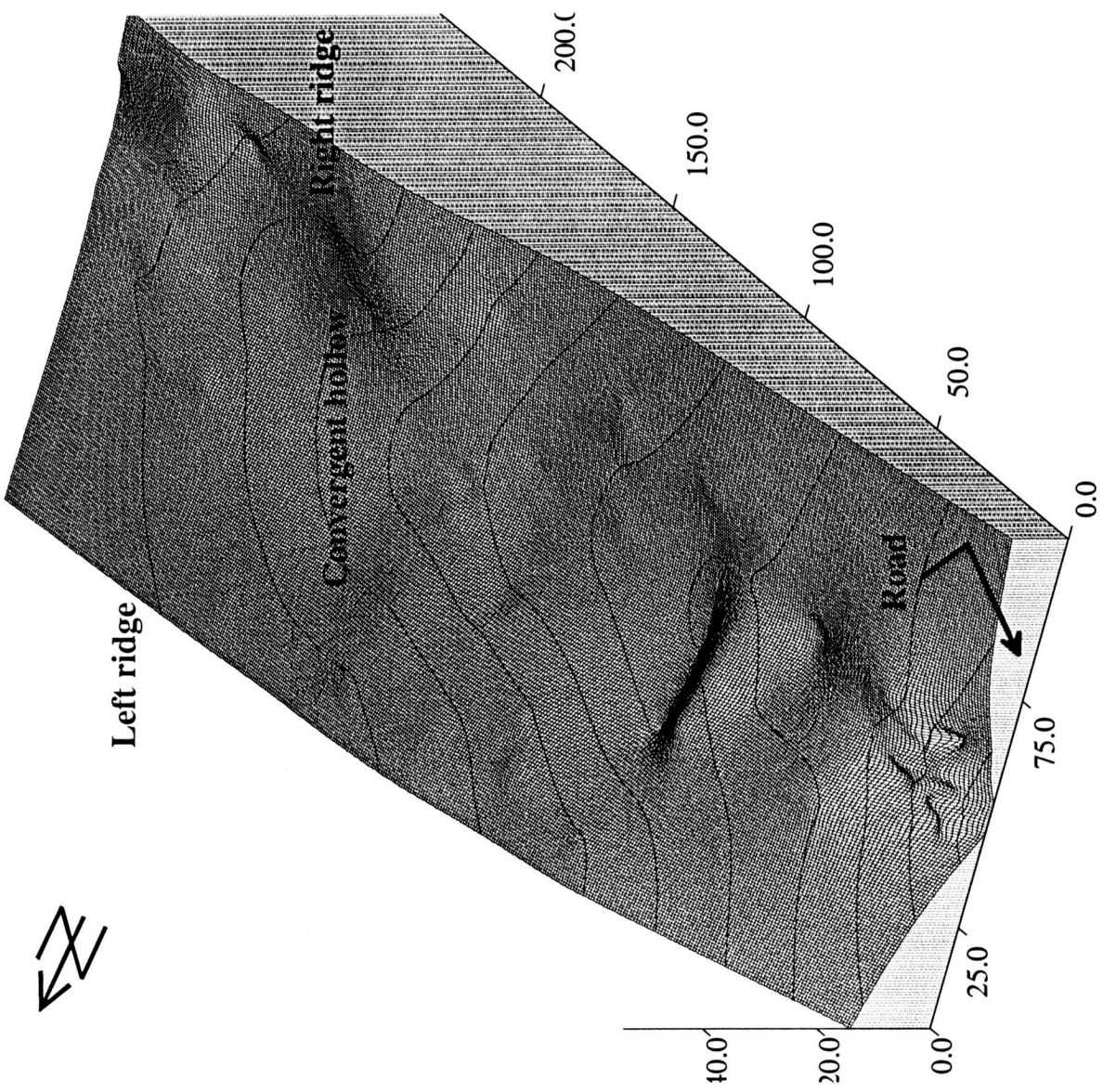


Figure 3. Relief map of the C3 hillslope.

Geology

The WS3 (including the C3 study area) is underlain by Tertiary and Quaternary volcanic rocks, primarily andesites and basalts, with some glacial deposits and lava flows (Rothacher et al., 1967). The general near-surface stratigraphic trend for the HJA watersheds is shown in Figure 4. Typically, as shown in Figure 4, there is slightly more than one meter of relatively poorly developed soil underlain by 2-7 meters of subsoil (saprolite) consisting of highly-weathered coarse volcanic breccias which formed as a result of mudflows and pyroclastic flows (Swanson and James, 1975). The bedrock of the HJA is predominantly volcanic in origin and constitutes most of the higher ridges and side slopes (Jones and Grant, 1996). The lower elevation slopes in the HJA are underlain by pyroclastic tuffs, breccias, and agglomerates deposited during the Oligocene and Miocene epochs (Jones and Grant, 1996).

Dyrness (1963) conducted a comprehensive soil survey in three watersheds in the HJA. Dyrness found that soil-water storage and transfer in WS3 was characterized by high porosity, high percolation rates, and high infiltration rates. The soils in WS3 were derived from Andesite and in general have a loamy to sandy-loamy texture with little evidence of mature profile development (Dyrness, 1963). The thin, very porous WS3 soils have a high percentage of organic matter and deeply weathered parent materials that typically overlie a less permeable subsoil or bedrock (Dyrness, 1969). The WS3 surface soils are well structured and range in color between dark brown and very dark brown. Most of the WS3 soils are at least moderately stony, with stone content showing a positive correlation with slope (Dyrness, 1969).

Typical of the steep, forested basins in the Cascades, the highly porous, well-aggregated WS3 surface soils readily accept all precipitation and transmit the water to lower soil depths where its steep slopes are conducive to rapid, shallow subsurface flow. The surface horizons of the Budworm soil series, the dominant soil series in C3, has such a high percolation rate that Dyrness (1969) reported that it was impossible to maintain a head of water on the surface of a soil core during lab tests. Due to the high permeability and infiltration capacity of the WS3 soils, Horton overland flow (HOF) rarely occurred (Dyrness, 1969). HOF is characterized by the rainfall intensity exceeding the saturated hydraulic conductivity of the soil.

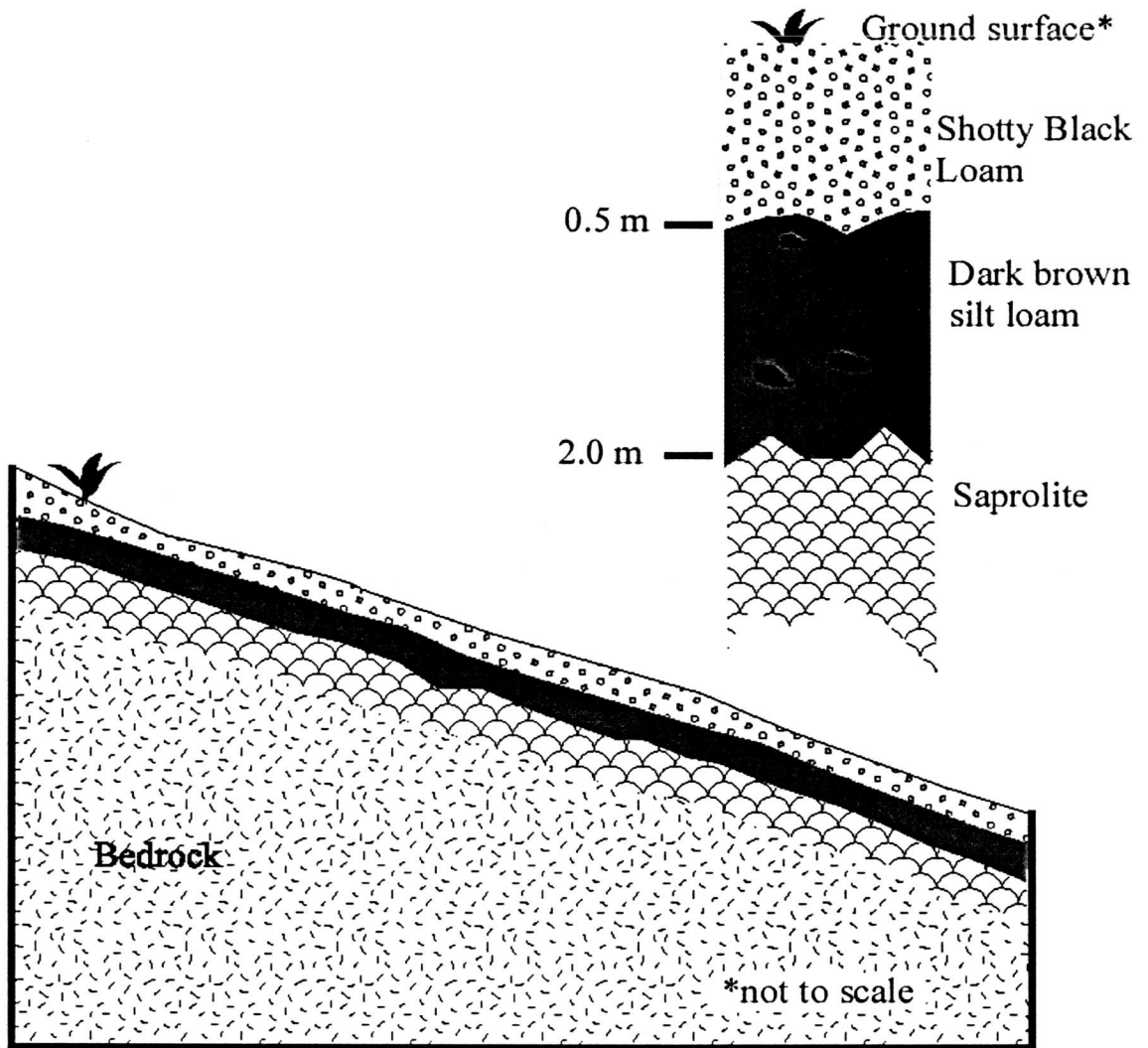


Figure 4. Schematic illustration of the WS3 geologic profile.

Table 1. Major plant species found at C3 (from Hawk and Dyrness, 1969).

Species	Common name	Areal cover (%)	Areal cover normalized (%)
Overstory Tree Layer			
<i>Tsuga heterophylla</i>	Western hemlock	20	
<i>Pseudotsuga menziessii</i>	Douglas fir	35	
<i>Thuja plicata</i>	Western redcedar	3	
	Total	58	36.5
Small Tree/Shrub Layer			
<i>Tsuga heterophylla</i>	Western hemlock	25	
<i>Thuja plicata</i>	Western redcedar	2	
<i>Acer circinatum</i>	Vine maple	15	
<i>Rhododendrum macrophyllum</i>	Rhododendrum	2	
<i>Castanopsis chrysophylla</i>	Chinquapin	2	
<i>Taxus brevifolia</i>	Pacific yew	10	
<i>Vaccinium parvifolium</i>	n/a	2	
	Total	58	36.5
Low Shrub Layer			
<i>Berberis nervosa</i>	Oregon grape	28	
<i>Gaultheria shallon</i>	Salal	5	
<i>Rubus nivalis</i>	n/a	10	
	Total	43	27.0

Deeper in the WS3 soil profile there is a noticeable reduction in porosity relative to the highly conductive surface soil. The unsaturated drainage of the soil in WS3 creates a discontinuous, ephemeral, saturated zone that routed groundwater flow downslope. The water flows predominately through non-capillary sized pores, especially in the topsoil and this translatory flow emerged as seeps in stream banks and road cuts, and contributed to peak flow discharges (Harr, 1977). Dyrness (1969) found that for WS3 soil-water in retention storage was located in large non-capillary pores and that moisture retention capacity was predominantly a function of the stone content.

Climate

The climate in the HJA is humid with mean temperature ranging from 39°F in January to 65°F in the summer. Precipitation rates are high varying from 226 cm/yr. in lower watersheds to 356 cm/yr along the highest ridges (Jones and Grant, 1996). Average precipitation intensities above 2 mm/hr and total precipitation depths of greater than 40 meters are necessary to produce runoff hydrographs at most sites. For WS3, only storms occurring as either rain or as rain on snow produced measurable runoff (Wemple, 1996).

Vegetation

The overstory vegetation within C3 is predominately Douglas Fir [*Pseudotsuga menziesii*] interspersed with western hemlock [*Tsuga heterophylla*] and western red cedar [*Thuja plicata*]. The understory vegetation consists of rhododendron [*Rhododendrum macrophyllum*], Oregon grape [*Berberis nervosa*], salal [*Gaultheria shallon*], vine maple [*Acer ciccinatum*], and sword fern [*Polystichum munitum*] (Hawk and Dyrness, 1970). The percentage of C3 occupied by the different types of vegetation is listed in Table 1.

PRIOR WORK IN THE H.J. ANDREWS EXPERIMENTAL FOREST

A long-term paired watershed study in the HJA was initiated in 1952 to compare the effects of clearcutting and road construction on hydrologic response and sedimentation (Jones and Grant, 1996). Watershed one (WS1), Watershed two (WS2), and WS3 locations are shown in Figure 5. Two of three adjacent watersheds, one of which (WS3) includes the study area, were subjected to treatments while the third was

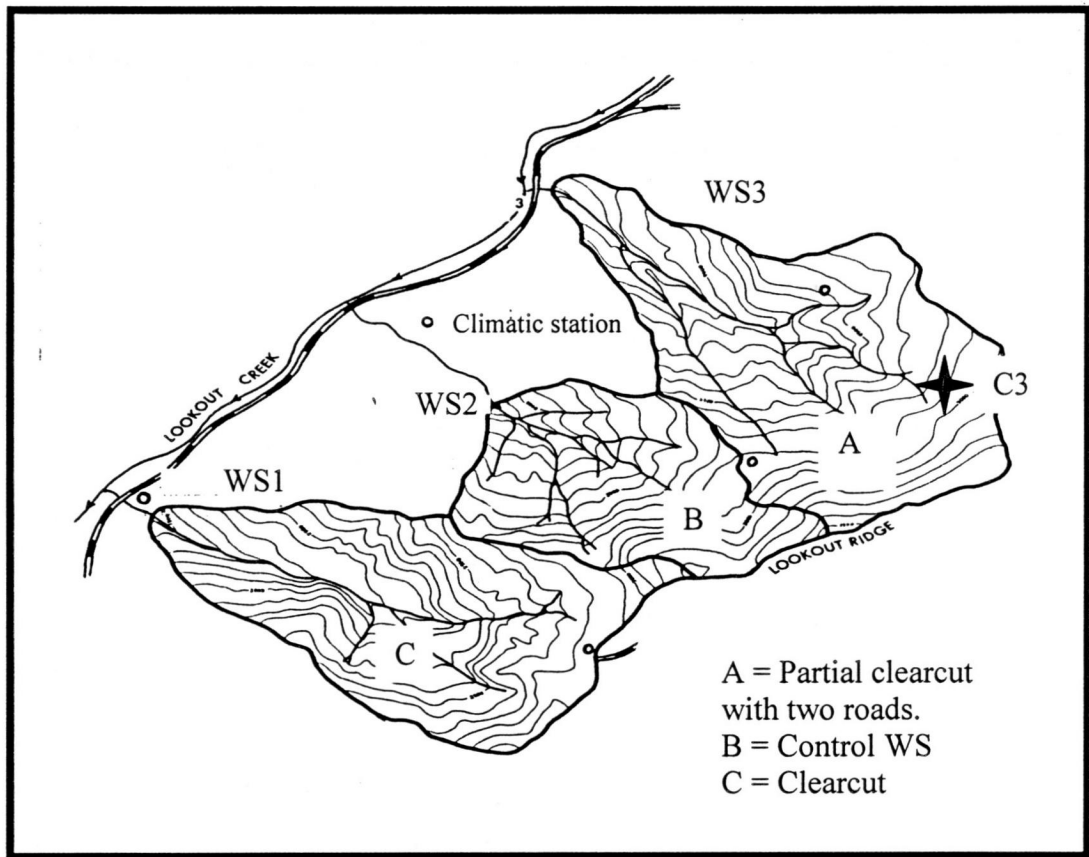
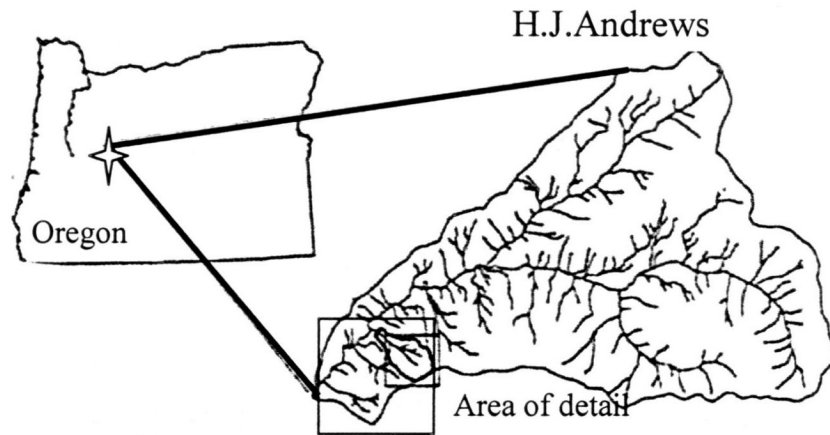


Figure 5. Location of WS1, WS2, and WS3 in the H.J. Andrews Experimental forest. A, B, and C refer to the different treatments imposed upon the watersheds.

untouched and remained the control watershed. WS1 was completely clear-cut. WS3 was partially clear cut with two roads constructed (one mid-slope and the other upslope). WS2 was left in its natural state. For the next few decades, the discharge at the bottom of each watershed was monitored. These data have been interpreted by several researchers (e.g. Jones and Grant, 1996; Thomas and Megahan, 1998; Dyrness, 1969). It should be noted that no trees were logged from the C3 hillslope itself but scars on the trees indicate that there had been a fire in the past.

Extensive research has been conducted in the HJA on the local geology, soil properties, vegetation distribution, streamflow, and precipitation (Dyrness, 1969). The hydrologic processes of steep forested watersheds (Harr and McCorison, 1979; Jones and Grant, 1996), the increased rates of landsliding relative to forested conditions (Swanson and Dyrness, 1975), the disturbance cascades initiated by road construction (Swanson et al., 1998), and the increased rates of sediment production (Wemple, 1998) have all been evaluated and are comparable to studies performed elsewhere (Megahan, 1972; Ziemer, 1981; Reid and Dunne, 1984; Ziegler and Giambelluca, 1997; Thomas and Megahan, 1998).

Harr (1976) performed extensive reconnaissance fieldwork in the HJA to understand the local hydrogeology. Harr found that subsurface storm flow contributes 96-98% of the storm runoff in watersheds of the western Cascade Range of Oregon. Using tensiometers to measure pressure head, Harr determined that the magnitude of water flux was much greater in the top meter of soil than in the subsoil. Harr concluded that a lateral (i.e. slope parallel) component of flow is expected wherever a vertical decrease in permeability (i.e. low conductivity layer) occurs in sloping soil.

Following a major storm event of 1964-1965 Dyrness (1967) conducted a reconnaissance survey of all of the mass soil movements that had occurred in the HJA. The purpose of the Dyrness study was to describe the mass movements. Dyrness classified the type of movement and its resulting damage, and attempted to identify the relationship between the mass soil movement and man's disturbance or site factors such as the geology, the soil, the elevation, and the slope aspect. The most common type of mass movement at the HJA was roadfill failure (Dyrness, 1967). Large amounts of rainfall or improper fill compaction allowed fill material to flow when the roadfill

embankment became saturated. A second common failure event was roadcut failure which predominately occurred when the mantle was saturated and mostly took the forms of slumps. A third road-related event was mass movement caused by concentration of road drainage water or the failure of the road drainage system. Figure 6 shows the different types of landslides commonly associated with roads.

Based upon a summary of the Dyrness work, the influence of roads on mass movements within the HJA is clear. At the time of the Dyrness study only 1.8% of the forest was occupied by roads, this area accounted for 72% of the mass movement events (Dyrness, 1967). In contrast, only 11% of the mass movements occurred in completely undisturbed areas. Slope, geology, and elevation were also found to have a significant impact on the areas found to be susceptible to sliding in the HJA. Of the events inventoried by Dyrness, 94% occurred on materials with low internal strength, sufficient water for saturation, and at least moderately steep slopes were most susceptible to failure. Mass movements tended not to occur in areas with slopes less than 45% and predominated in areas characterized by deep soils and well-weathered bedrock. All but two events inventoried occurred at elevations below 884 meters, with the largest proportion occurring at elevations between 600-800 meters. The location of the mass movements is correlated with the fact that most deposits of unstable materials such as tuffs and breccias occurred at lower elevations and the presence of snow cover added additional moisture to the system.

Swanson and Dyrness (1975) performed a field survey of the HJA and found that erosion related to landslides has been 30 times greater than undisturbed conditions once a road was built. Swanson (1975) detailed the geologic and geomorphic history of the HJA with emphasis on the relationship between bedrock geology and mass wasting events. Swanson showed that a significant portion of the mass wasting events were shallow landslides that occurred along the contact between the bedrock and the soil. In comparison to the overlying shallow, stony soils, the bedrock was relatively impermeable and in some places, highly jointed. Consequently, water moved rapidly through the marginally stable soil and this rapid influx during heavy storms caused high pore pressure and the increased probability of mass movement (Swanson and Dyrness, 1975).

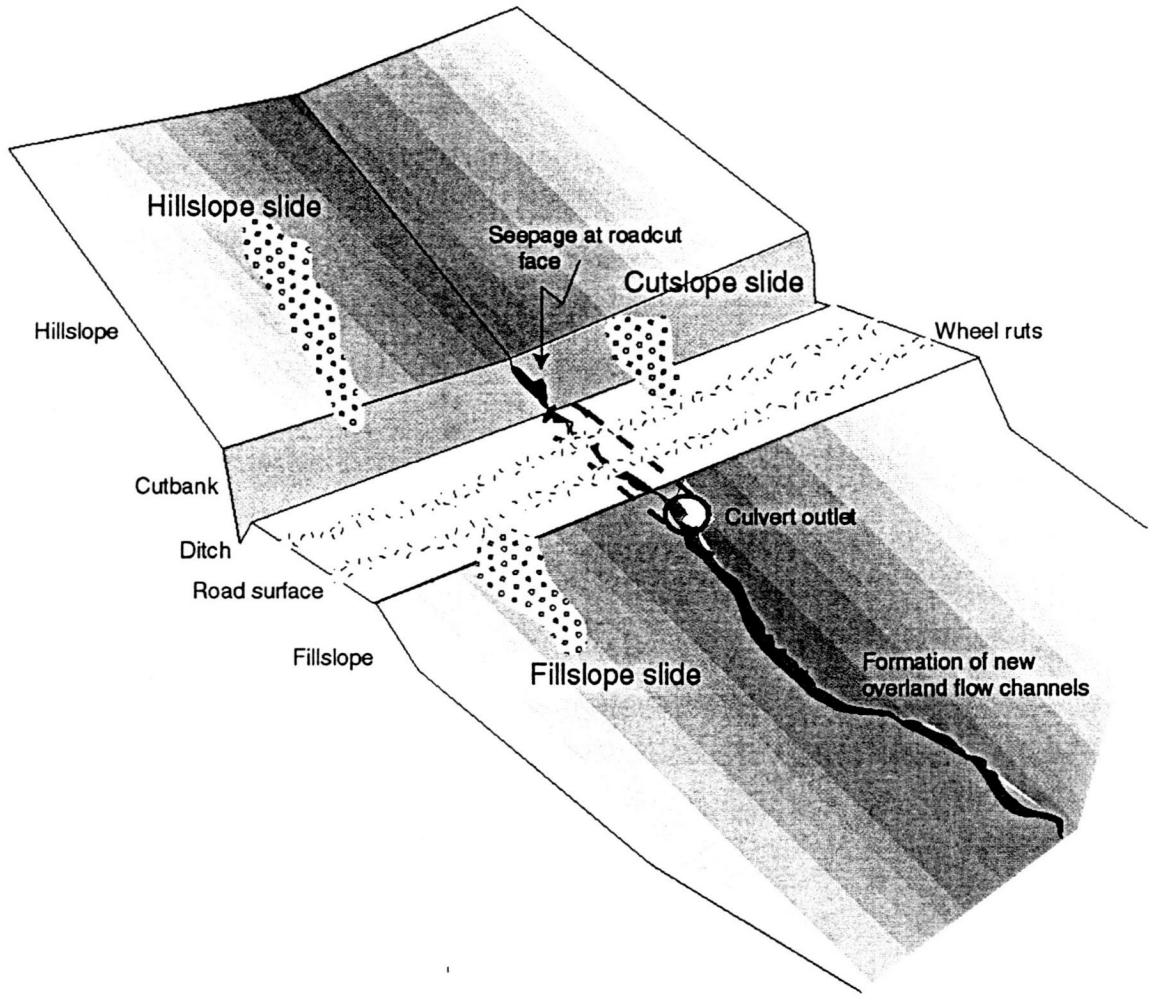


Figure 6. Schematic of the various types of mass movements associated with road construction (after Wemple, 1998).

COOS BAY CASE STUDY

The study repeated here was approached as a small-scale replica of the extensive work done at an experimental catchment located in the Oregon Coast Range near Coos Bay (CB), Oregon. The purpose of the CB study was to determine the relationship between hillslope hydrology and geomorphology i.e. mass movements in steep zero-order catchments. The workers (Anderson et al., 1997a, 1997b; Montgomery et al., 1997; Torres et al., 1998) conducted several controlled irrigation experiments in an attempt to assess the near-surface hydrologic response to rainfall events as a precursor to mass soil movements in steep zero-order catchments.

Site description

The (CB) catchment was 860 m² with a slope that averaged 43-45° (Montgomery et al., 1997) (see Figure 7). The soils were characterized as low-density silty sands that overlay fractured and weathered sandstone that became more massive and impermeable with depth. The soil profiles on the interfluves yielded to thicker soils along the axis of the convergent hollow.

Instrumentation

Workers at the CB site constructed a complex instrumentation infrastructure for gathering climatic, water balance, topographic, chemical, and near-surface and subsurface soil-water and soil tension data (see Anderson et al., 1997a, 1997b; Montgomery et al., 1997; Torres et al., 1998 for detailed descriptions of instrumentation and data collection). In summary, the instrumentation at CB included two weirs, 195 piezometers in 86 nests, 100 tensiometers, tipping bucket rain gauges, and an array of lysimeters, time domain reflectometry stations, and instruments for measuring evapotranspiration. Falling head conductivity tests were conducted at the piezometer nests and soil cores were analyzed. Three total site irrigation experiments were conducted.

Findings

Although the sprinkler experiments conducted at CB did not address the impact of a road on near-surface hydrologic response, the work at CB was considered to be an

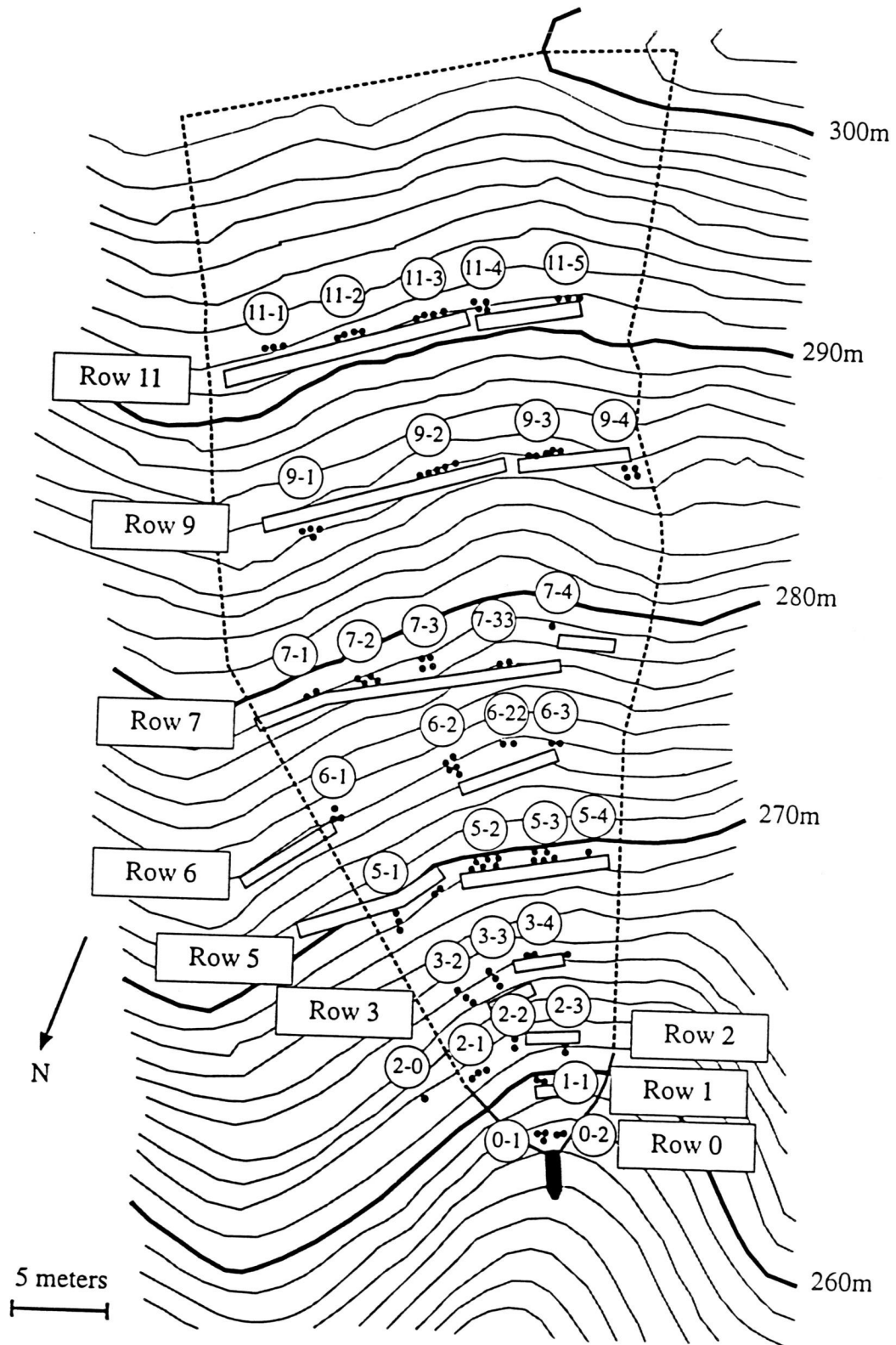


Figure 7. The Coos Bay catchment showing the topographic contours and the location of the piezometers (from Montgomery, 1997).

applicable analog to the study reported here because both catchments are steep, zero-order catchments with concave topography. In much the same manner, although not at the same density, the C3 hillslope in this study was instrumented to gather soil and piezometric data. Both C3 and CB have very similar subsurface stratigraphy i.e. both have high permeability colluvium overlying relatively impermeable bedrock that is very conducive to subsurface storm flow. In addition, both hillslopes have some history of land-use disturbance (CB was clear cut and had a road on the ridge above it and C3 was partially clear-cut and has a road dissecting the catchments midpoint). Comparison of the characteristic curves for the CB and C3 catchments (see Chapter 3) shows that the soils have similar properties. Also, the piezometer response recorded during individual storms is similar between the two catchments (see Chapter 3).

The CB study highlighted the role of the unsaturated zone in determining hydrologic response and the potential triggering of mass movements (Torres et al., 1998). Montgomery et al. (1997) discussed the importance of the convergence of subsurface flow in steep, unchanneled valleys. This convergence of flow makes colluvium filled hollows especially prone to instability and contributes to their observed periodic colluvial infilling and excavation by landsliding (Reid, 1988; Coates, 1990; Montgomery, 1991). The CB work also demonstrated that a rainfall event on nearly saturated soil produces a slight change in pressure. Due to the nature of the soil-water retention curve, the pressure head change corresponds to a dramatic increase in soil-water content.

The observations of piezometric response at CB during storm events demonstrated the important role that the fractured bedrock played in groundwater flow, runoff generation, and pore pressure development (Montgomery et al., 1997). The CB findings have been a guide for the approach and interpretations of the results of this study. However, there are many other studies regarding hillslope hydrogeology that have provided background and insight to the characterization of the hydrogeologic and geomorphic processes at work in steep, forested catchments (eg. Megahan, 1972; Stephenson and Freeze, 1974; Harr, 1979; Beven, 1981; Wiczorek, 1987; Reid et al., 1988; Montgomery and Dietrich, 1995; Wemple et al., 1998).

BACKGROUND

Streamflow Generation

In the study of hillslope hydrology there are three distinct forms by which lateral inflow reaches a channel within a catchment (Dunne, 1978; Freeze, 1980): (i) groundwater discharge, (ii) subsurface stormflow, and (iii) overland flow. Groundwater discharge provides the sustaining baseflow component to a stream hydrograph between storm periods. The flashy response of stream flow can be ascribed to either subsurface stormflow or overland flow. In general, the primary source of rapid lateral inflow is due to overland flow that can only occur after surface ponding has occurred. This surface saturation can occur by two distinct mechanisms: Horton overland flow and Dunne overland flow. For the Horton mechanism, the rainfall intensity must exceed the saturated conductivity of the surface soil long enough for ponding to occur. The Dunne mechanism occurs when the rainfall duration exceeds the time needed for a shallow water table to reach the surface. Horton overland flow is commonly found in the low conductivity areas in the upslope of a catchment (or on a compacted road surface). Dunne overland flow is found in near-channel lowlands, convergent hollows, and other areas with shallow watertables. Both the Horton and Dunne mechanisms can lead to variable source areas that expand and contract through wet and dry periods.

Hillslope Hydrogeology

Hillslope hydrogeology, as a function of the hillslope geometry, soil properties and heterogeneity, land use history, and climatic conditions is the controlling factor for slope stability in steep forested catchments. In general, hillslopes and catchments consist of a variety of shapes and materials. The water table is often well represented as a subdued replica of the topography (see Toth, 1963). Subsurface stratigraphy and the resulting subsurface variations in saturated hydraulic conductivity can exist in an infinite variety. This geological heterogeneity can have a profound effect on regional groundwater flow (Freeze and Cherry, 1979). Reid and Iverson (1992) showed that most of the potential pore-pressure changes occurred in regions marked by a hydraulic conductivity contrast of several orders of magnitude. Studies have shown that even slight decreases in saturated hydraulic conductivity within a hillslope can impede fluid flow,

locally elevate pore pressures, and lead to slope failure (e.g. Hodge and Freeze, 1977; 1994; Rulon et al., 1985; Wilson and Dietrich, 1987; Reid et al., 1988; Montgomery et al., 1991; Reid and Iverson, 1992; Reid, 1998).

To understand how changes in land use, including selective forest harvesting, clear-cutting, and road building, can accelerate the landscape evolution process and increase the sediment loading to downstream areas, one must have knowledge of the physical and hydrologic properties of the site. The subsurface movement of water through a hillslope is critical because it can affect the earth materials so as to exceed their threshold of stability. Previous studies have indicated that rainfall-induced positive pore pressures in hillslopes were caused by (i) water perched above low permeability layers, (ii) ground-water flow convergence controlled by surface or bedrock topography, (iii) bedrock water contributions, and (iv) spatial variations in soil properties (see Swanson, 1970; Freeze 1971, 1972; Campbell, 1975; Beven, 1977; Anderson and Burt, 1978; Rulon et al., 1985; Reid, 1988, 1998). Localized increases in pore pressures and the expansion of saturated zones can reduce the soil cohesion and dramatically increase the likelihood of mass movement. Steep channel heads, low order channels, and convergent hollows are especially prone to instability and contribute to the cycle of periodic colluvial infill and excavation by shallow landsliding in the watersheds that feed channel networks (see Dietrich and Dunne, 1982, Dietrich et al., 1986; Reid et al., 1988). The geomorphic process of landsliding in colluvium-filled hollows and the subsequent delivery of sediment to downslope streams can be accelerated by timber harvesting and the associated road construction.

Studies have confirmed that, because the hydraulic conductivity of the surface soils in steep, forested landscapes is so great, subsurface stormflow (SSF) is the dominant flow mechanism (see Harr, 1977; Dunne, 1978; Beven, 1981; Montgomery and Dietrich, 1995). Pore pressure response in steep hollows mantled by a highly conductive soil has been measured and simulated and it is now well established that unsaturated zone processes can control the timing and magnitude of positive pore pressure development and peak discharge (Torres et al., 1998). Researchers have found that, even in convergent hollows, unsaturated flow was predominately vertical (Harr, 1977; Humphrey, 1982). Thus, in regions where SSF is the dominant mechanism by which water reaches a

channel, all incident precipitation must flow through a largely unsaturated profile before contributing to runoff. The infiltrating precipitation may reach the soil-bedrock boundary or another low-conductivity zone at the base of the root mat and be forced to flow laterally through macropores (root channels or larger pipe-like systems in the soil) or along the low conductivity contact (see Jones, 1971; Coates, 1990; Smetten et al., 1991; Montgomery and Dietrich, 1995; Montgomery et al., 1997).

Roads

The modifications of hydrologic flowpaths that are associated with a road are a function of the road location, substrate, and design. The likelihood for creating slope failure is influenced by the depth of the roadcut (into the soil profile) and the volume of water intercepted at the roadcut (and routed through the ditch system or new surface flow paths) (King and Tennyson, 1984). For example, the amount of subsurface stormflow intercepted along road cuts and the magnitude of the response it precipitates will typically increase with increasing upslope flow contributions (King and Tennyson, 1984). In addition, runoff on a ridge top road is more likely to be dispersed and re-infiltrate, while mid-slope roads have the greatest potential for affecting runoff by intercepting subsurface flow and rainfall and dumping it into a side channel (Wright et al., 1990). The geology of an area greatly influences slope stability. Ridgetops tend to be underlain by more stable bedrock while unstable materials tend to be predominate on the lower and mid-slopes. Thus, a road built high on a ridge is less prone to instability than one built in less consolidated substrate.

There may be a threshold precipitation rate or a water table depth below which a roadcut will not intercept groundwater or macropore flow (Wemple, 1998). As seen in Figure 8, road surfaces, cutbanks, ditches, and culverts can all act as interfaces to convert subsurface flow to surface flowpaths (Harr et al., 1975; King and Tennyson, 1984; Wemple, 1996). If sufficiently deep, forest roads incised into the soil profile may intercept SSF (Megahan, 1972; Jones and Grant, 1996) and the lower permeability of the road surface may be conducive to the generation of overland flow (Reid, 1981; Ziegler and Giambelluca, 1997). Ditch systems and relief culverts can concentrate surface runoff, alter the natural surface flow paths, and reroute water along some alternative surface/

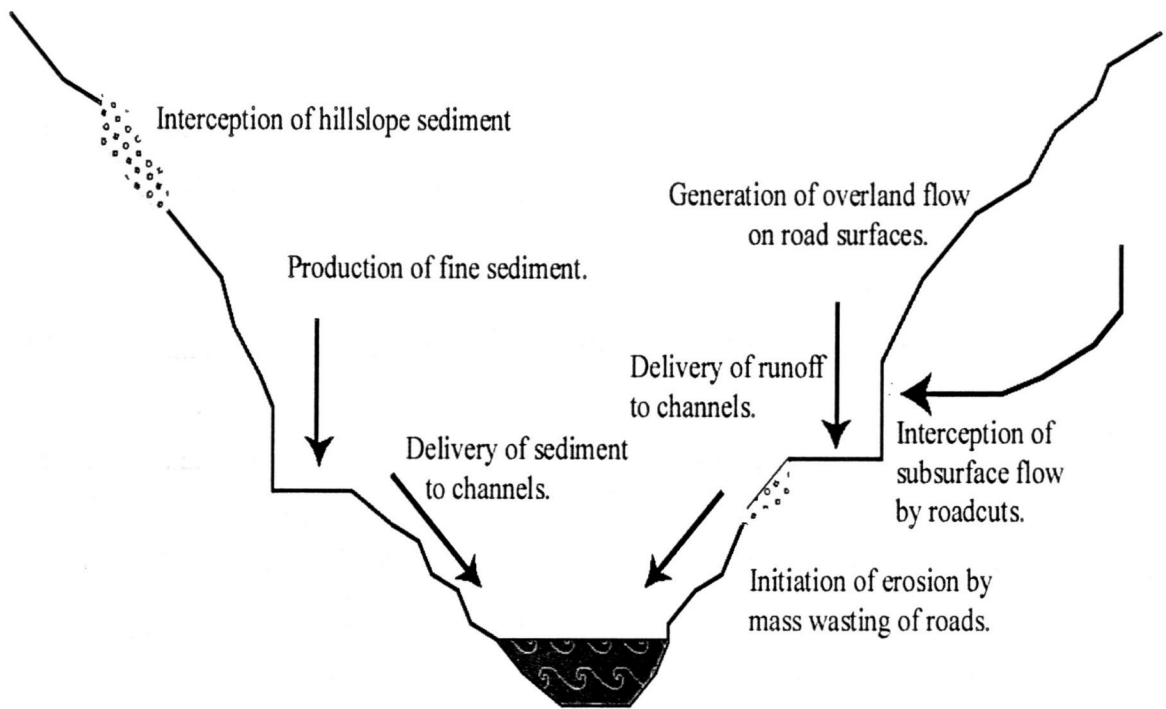


Figure 8. Schematic illustration of the ways that a road can impact the hydrologic and geomorphic processes within a watershed (after Wemple, 1998).

subsurface flowpaths until it re-infiltrates the system in an area of concentrated recharge. Theoretically, this additional influx of water can locally increase the pore-pressures, reduce the shear strength of the hillslope, and instigate shallow landsliding in the area below the road (i.e. the fillslope).

The increase in runoff generation and concurrent accelerated soil erosion on unpaved roads are the two major road-related impacts that have been the focus of extensive research in steep forested watersheds. Several researchers have studied the impacts of roads on the hydrologic and geomorphologic systems of forested watersheds (e.g. Megahan and Kidd, 1972, Megahan, 1974, 1978, 1987; Swanston, 1974; Swanston, 1981; Reid and Dunne, 1984; Ziegler and Giambelluca, 1997; Reid, 1998; Thomas and Megahan, 1998). These researchers have found that the disturbances created by road construction and use may impact the hydrology and geomorphology of a watershed by the alteration of streamflow and channel networks, the destabilization of slopes and mass wasting, and the increased sedimentation of downstream reaches and watersheds relative to background levels.

Hydrologic Impacts

One goal of many researchers has been to assess the hydrologic impacts associated with roads by measuring changes in runoff and streamflow in the watersheds where roads have been built. Field work and observation stations (e.g. wiers) have served as inputs and as checks to numerical and empirical models at several different sites in areas affected by forest management practices. Tables 2 and 3 summarize some of the prior work related to the impact of roads. In general, in the areas disturbed by roads, peak flows are expected to increase and the time to peaks flows to decrease relative to observed background levels (Jones and Grant, 1996; Ziemer, 1981).

Roads may be expected to modify storm flow peaks by two principle mechanisms: (i) compaction of road surface may reduce infiltration and allow rapid surface runoff, and (ii) interception of subsurface flow, as well as capturing surface runoff, and channeling it more directly to streams (Megahan and Clayton, 1983; Megahan, 1987, Ziemer, 1981). The infiltration rates on roads can be decreased because of compaction, removal of permeable surface soils, and increased gradients on cut and fill

slopes. However, in the studies where the impact of roads alone on streamflow response have been evaluated, any changes following road construction have been variable and, in general, statistically non-significant (Ziemer, 1981). Peak flows appear to be increased when roads and other compacted areas occupy on the order of 12% of the total watershed area (Harr et al., 1975). Other workers have found that the water yield increases significantly following logging and associated road construction, but that the system recovers within a year to background levels (Douglas, 1993).

Ziemer (1981) conducted a paired watershed study at Caspar Creek near Fort Bragg in Northern California to assess the impacts of road building and logging on storm flow response. Ziemer found that road construction resulted in no change in any of the storm flow parameters measured because the percentage of area covered in roads was so small that any impact they might have had was drowned out. Wright et al. (1984) performed a study similar to Ziemer's study at the same location, and with similar results.

Sedimentation Impacts

A second suite of road-related issues that has been extensively studied is the increase in sediment production and the accelerated landscape evolution. These issues are a direct consequence of the increased incidence of mass movements and road surface erosion that have been identified to be a result of road construction and usage (Reid, 1981; Reid and Dunne, 1984). Several researchers have measured the amount of sediment removed from roads or the occurrence of road-related mass wasting (Reid and Dunne, 1984; Reid, 1981; Anderson and MacDonald, 1998; Swanson and Dyrness, 1975; Megahan, 1987).

The overall significance of a road as a sediment source is a function of both road type and length (Reid and Dunne, 1984). Topographic surveys of road segments and observations during storms show that 16% of the runoff generated on a typical road surface is diverted off the outer side of the road as sheet flow. The remainder of the runoff eventually flows into an inboard ditch, through a culvert, and in 75% of the cases, into a stream (Reid and Dunne, 1984). Road surface erosion is extremely sensitive to traffic levels. The contribution of sediment from off-road sources is small compared to that from an active road surface (Reid and Dunne, 1984). Other studies have found that

Table 2. A sampling of previous work and key results from studies done on the impact of roads on hydrology.

Author	Fieldwork	Model	Intercepted/ Runoff Rerouted	Flow	Time to Peak Flow	Magnitude of Peak Flow	Infiltration	Area in Roads	Evaporation
Rothacher (1971)	X	LSR				inc.		>15%	
Harr (1975)						inc.		12%	
Harr (1979)						inc.		15%	
Ziemer (1981)	X	LSR			no ch.	no ch.		5%	
Bosch and Hewlett (1982)			inc.			inc.		>15%	dec.
King and Tennyson (1984)	X	LSR		X	dec.	inc.			
Rulon et al. (1985)		2-D	inc.	X					
Megahan (1987)	X			X			dec.		dec.
Coates (1990)	X	2-D		X					
Wright et al. (1990)	X		no ch.	no ch.	no ch.	no ch.		5%	no ch.
Cullen et al. (1991)	X		inc.				dec.		
Grayson et al. (1993)	X				no ch.	inc.			
Montgomery (1994)	X		inc.	X			dec.		
Ziegler and Giambelluca (1997)	X			X			dec.		
Jones and Grant (1996)		LSR			dec.			6%	
Thomas and Megahan (1998)		LSR				inc.			

inc. = increase
 dec. = decrease
 no ch. = no change
 LSR = Least squares regression model
 2-D = Two – dimensional model
 X = This was done as part of the study.

Table 3. A sampling of previous work and key results from studies done on the impact of roads on sedimentation and mass wasting.

Author	Fieldwork	Model	Traffic	Substrate	Location	Surface flow	Surface erosion	Mass erosion
Megahan and Kidd (1972)	X						inc.	inc.
O'Loughlin (1972)	X							inc.
Megahan (1974)		X					inc.	inc.
Megahan (1978)	X							inc.
Harr (1975)	X							
Swanson and Dyrness (1975)	X		X	X	X		inc.	inc.
Harr (1976)	X							
Swantson et al. (1977)	X							inc.
Megahan (1978)	X							inc.
Gray and Megahan (1981)	X							inc.
Reid et al. (1981)							inc.	inc.
Megahan (1983)						X		inc.
King and Tennyson (1984)						X		
Reid and Dunne (1984)	X	X					inc.	inc.
Megahan (1987)		X	X		X		inc.	inc.
Bilby et al. (1989)			X	X	X			
Coates (1990)								inc.
Cullen et al. (1991)	X	X	X				inc.	
Montgomery (1991)	X						inc.	inc.
Grayson et al. (1993)	X	X	X	X			inc.	
Mongomery (1994)	X	X			X		inc.	inc.
Ziegler and Giambelluca (1995)			X	X			inc.	inc.
Anderson & MacDonald (1998)	X	2-D					inc.	inc.

inc. = Increase

X = This was studied

2-D= Two-dimensional model

erosion rates from roads were greater than those in undisturbed conditions and that heavily used segments could contribute as much as 130-1000 times more sediment than abandoned roads (Reid and Dunne, 1981; Reid and Dunne, 1984).

Bilbly et al. (1989) found that sediment production from roads was a function of traffic, road steepness, depth of the roadcut, and the surfacing. Roads have been found to be a source of fine-grained sediment derived directly from road surfaces because the surface material breaks down and vehicular traffic causes the upward forcing of fine-grained sediment from the roadbed. This fine sediment is the size that is most harmful to fish and water quality (Targart, 1976; Cederholm et al., 1981). Cederholm et al. (1981) attributed 18-26% of the increased sediment loading to streams to sediment derived directly from the road surface. Anderson (1972) found that when 0.6% of a watershed was converted to roads, the sediment yield increased by 24%.

Landslides

Shallow mass wasting damages roads, removes soil from tree-growing sites and may lead to degradation of water quality and stream habitat (Swanson and Dyrness, 1975). Factors that are determinant in hillslope failure are: hillslope gradient, depth of the saturated soil zone relative to total soil depth, soil or parent material strength properties including cohesion and friction angle, and strength provided by vegetation roots. Vegetation removal for road right-of-way increases soil-water contents due to reduced evapotranspiration, root decay diminishes root strength, and cut and fill slopes increase slope gradients and may increase the relative depth of the saturated zone (Megahan, 1987).

A landslide is more likely to occur in an environment with high initial soil-water contents and low soil-water tensions. Soil tension refers to the matrix suction exerted on the interstitial water. The drier the soil, the higher the suction is as the water is held tightly within the soil matrix. Subject to wet antecedent conditions, a wave of infiltrating precipitation can propagate rapidly through the soil creating a sudden rise in pore pressure, an expansion of the saturated zone, and consequently, an increased risk of slope instability (Torres et al., 1997). Many researchers have studied the rainfall events leading up to a mass movement (eg. Cannon and Ellen, 1985; Wiczorek, 1987; Neary and Swift,

1987). In general they found that long duration (i.e. wet antecedent conditions) coupled with spikes of high intensity rainfall most often triggered slope failures.

Reid (1981) found that landslides are responsible for 60% of the sediment production. Montgomery (1994) did a similar field survey and found that the drainage area required to support a channel head was much smaller for road-related runoff than that on undisturbed slopes. Montgomery also found that landslide-related sediment transport accelerated dramatically after road building and forest clearance with most of the failures associated with road drainage concentration. Harden (1992) incorporated roads into watershed scale simulations of hydrologic response and erosion and found that they had implications that were disproportionate to their areal extent.

NUMERICAL MODELING

A common approach to studying the subsurface component of watershed systems is numerical simulation of two-dimensional (vertical slice), steady-state, saturated or saturated-unsaturated flow. Many authors have used two-dimensional flow models to analyze how groundwater flow can be constrained by slope-parallel low conductivity layers or by vertical conductivity contrasts (e.g. Rulon et al., 1985; Rulon and Freeze, 1985; Iverson and Major, 1986; Reid, 1988; Coates, 1990; Iverson and Reid, 1992; Reid and Iverson, 1992; Montgomery, 1994; Reid, 1998). Figure 9 shows the impact that having a low-conductivity road (or vertical barrier) has on a groundwater flow system. The compacted area below the surface of the road acts as a vertical impediment to groundwater flow. Directly above the road there will be a localized and dramatic rise in pore pressure levels because water will build up on the up-gradient side of the low conductivity zone below the road and seepage will be directed outward from the slope.

Rulon et al. (1985) combined two-dimensional saturated-unsaturated numerical simulations with laboratory experiments in a sandbox to explore the link between hydraulic conductivity contrasts in layered hillslopes and the creation of multiple seepage faces and perched water tables. Rulon found that the hydraulic head distribution and the percentage of total flow through the system that is discharged across a seepage face was highly dependent on the rainfall rate, the location and geometry of the impeding layer, and the magnitude of the conductivity contrast. Rulon and Freeze (1985) also found that

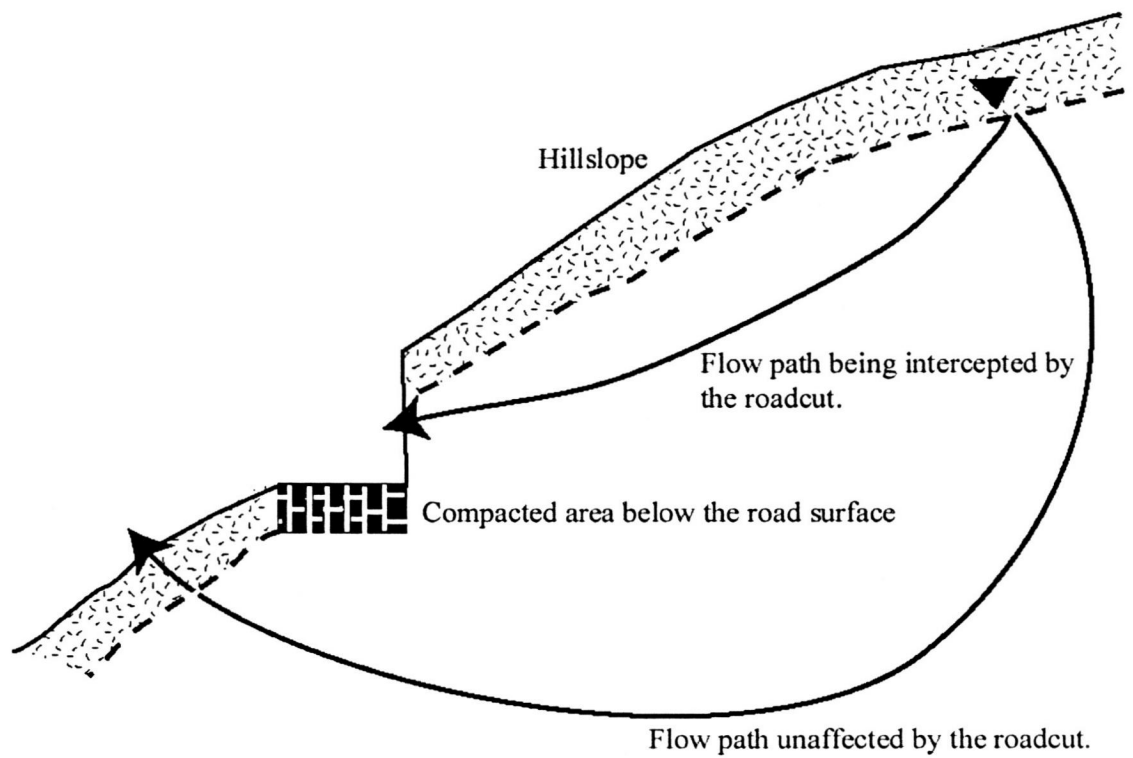


Figure 9. Schematic illustration of groundwater flow being intercepted by the roadcut (after Coates, 1990).

seepage faces and multiple seepage faces, as produced by logging roads, can potentially have tremendous impacts in steep, forested catchments.

Reid (1998) used a simple two-dimensional saturated hillslope model to assess the importance of small changes in hydraulic conductivity on the groundwater flow fields, effective stress fields, and slope stability. Reid also studied and compared the effects of vertical, slope parallel, and horizontal hydraulic conductivity contrasts of varied orders of magnitude. Reid found that materials with low hydraulic conductivity that impede the downslope groundwater flow could create unstable zones with locally elevated pore pressures. The most dramatic increases in pore pressure and the resultant magnitude and orientation of the seepage force vectors occurred directly upslope of the vertical impermeable boundaries (i.e., the low conductivity zone below the road).

FACTOR OF SAFETY ANALYSIS

Slope profiles and hydraulic conductivity contrasts have the most pronounced and diverse effects on groundwater seepage forces, effective stress, and slope failure potentials (Reid and Iverson, 1992). Although it does not provide a comprehensive picture of the effective-stress field distribution throughout a hillslope, one method for quantifying slope stability is limit equilibrium analysis. The limit-equilibrium method uses the factor of safety (FS) criterion to estimate the de-stabilizing effects of different hydraulic conductivity contrasts, material properties, and slope angles (Reid, 1998). A factor of safety analysis evaluates the ratio of the shear strength to the shear stress required for equilibrium along a predetermined failure plane. When FS is less than 1 slope failure is eminent.

Iverson and Reid (1992) used a comprehensive mathematical model to quantify and systematically examine the influence of gravity-driven, topography controlled groundwater flow on effective stress and slope failure potential. Iverson and Reid found that groundwater flow increased the failure potential in the near-surface region, and that increases were largest at the toe of a slope. Seepage pressure is exerted in the direction of groundwater flow and is a function of the hydraulic head (Coates, 1990; Reid and Iverson 1992). The seepage pressure and velocity increases as you move from higher terrain towards the foot of a slope and regions of concentrated discharge where the seepage

forces were directed outward are particularly susceptible to failure. Under saturated conditions the interstitial pore-water pressure has increased, decreasing the strength of the hillslope materials and making them subject to seepage pressures conditions (Coates, 1990).

A variety of analytical and numerical solutions are often employed to demonstrate the influence of topography on the magnitude and orientation of the principle stresses within a hillslope (Duncan and Dunlop, 1969; Savage et al., 1985; Iverson and Major, 1986). Using conventional limit-equilibrium methods other researchers have concluded that groundwater flow fields strongly influence slope stability (Hodge and Freeze, 1987; Rulon et al., 1985; Rulon and Freeze, 1985). Field observations have confirmed this phenomena (Iverson and Major, 1986) and a statistically determinate infinite slope analysis by Iverson and Major (1986) showed that both the magnitude and the direction of groundwater flow influenced the potential for slope instability.

Montgomery and Dietrich (1994) coupled soil moisture and slope stability models with digital terrain data to predict the steady-state rainfall necessary for slope failure within a catchment. They found that steep, convergent areas, such as low order channels and hollows, were most susceptible to failure followed by steep side slopes and low-gradient hollows.

CONCLUSIONS

It is crucial to understand how pervasive the effect of a land use change is on the overall watershed and hydrologic system functioning. To assess the susceptibility of a hillslope to shallow landsliding, one must have a thorough knowledge of the hydrology, the near-surface and hydrogeologic properties, the topography, the slope, the failure plane, and the land use history. However, because there can be tremendous variability in the near surface soil and hydrogeologic properties, this can be very difficult. For example, just the saturated hydraulic conductivity within a given hillslope can easily vary over several orders of magnitude (both vertically and horizontally) depending on the scale and the geologic variability of the site.

Admittedly there exists disparity between the quantitative results that interested researchers have generated about the impacts of roads on watershed functioning in their

respective studies. For example, some workers have disputed the importance of subsurface flow as a dominant mechanism (e.g. Stephenson and Freeze, 1974; Torres et al., 1998) and offer alternatives such as fractured bedrock flow as a means of transporting infiltrating water downgradient. They argue that gravity driven flow is predominant in the subsurface zone as opposed to lateral flow. Be those differences a function of different methods employed, different study locations, or different data analysis and interpretations, it remains indisputable that roads have a significant impact on the hydrology and sediment budget of watersheds.

This study will explore the effect of a road in a steep forested watershed. Over time the road will become compacted under the weight of vehicular traffic and thus, relatively impermeable to surface infiltration and groundwater flow. Depending on the location of the road, the slope, the conductivity contrast between the road surface and the hillslope, the height of the road cut, and the depth to the water table, the impact on the hydrologic system will differ. In this study, a large-scale landslide occurred 500 meters from the study site along the same road in a very similar topographic regime. The thrust of this study, given information on the soil, topographic, climatic, and limited hydrologic conditions, is to assess whether a series of two-dimensional simulations can simulate the conditions necessary to trigger such an event. Many other researchers have studied the impacts of roads in altering near-surface landscape processes (e.g. Reid et al, 1981; Reid and Dunne, 1984; Coates, 1990; Montgomery, 1994). This research is unique in that it quantitatively explores the interactions of a road cut in steep terrain with a subsurface flow system.

CHAPTER TWO: METHODS

FIELDWORK

To assess how a road can potentially modify the surface and near-surface hydrologic response in a steep forested landscape one must first analyze the processes controlling groundwater flow at the hillslope scale. After characterizing the site one can attempt to quantitatively determine how a road (or road cut) will interact with the site hydrogeology to potentially alter the flow system. Some site-specific characteristics that need to be considered to understand the hydraulically driven hillslope morphology are the geology, the soil properties, and the magnitude and direction of flow in the subsurface before, during, and after storm events. Characterization of the near-surface hydrologic response and the relative importance of unsaturated and saturated flow during different storm events will indicate the hydrologic conditions under which slope failure at the C3 hillslope could be imminent.

The objective of the fieldwork conducted at C3 was to characterize the hillslope morphology, the soil depth, and the soil properties (i.e. hydraulic conductivity and soil-water content). Using a combination of techniques (see Table 4) new site-specific data was collected for the C3 hillslope. In cases where the results of the C3 field data showed significant scatter, the spatial variability of the site was quantitatively characterized using geostatistical techniques (i.e. Kriging and sequential simulation). The use of geostatistics created a more realistic representation of the hydrogeologic properties of the C3 hillslope by recognizing and accounting for the heterogeneity inherent to the system. The C3 data set was compared to larger data sets collected at related sites (i.e., Coos Bay and other watersheds (WS1, WS2, WS10) within the HJA) to assess the accuracy and consistency of the data gathered for this study.

Topographic Mapping

The initial fieldwork at C3 concentrated on mapping the site topography. The 13 transects used to characterize the C3 topography are shown Figures 10 and 11. The transects were laid out at approximately twenty meter intervals from the top of the ridge to the roadcut and then each transect was marked at five meter increments. Using an autolevel, the elevation was measured at each point along these transects and these values were referenced to a point at the roadcut that marked the (0,0,0) coordinate point for the

Table 4. Summary of the field data collected for C3. For the location of the measurement points see Figures 11, 12, and 13.

Field data	Method of collection	Number of measurements
Topography	Total station	13 transects
Soil depth	Soil drive probe	10
Saturated hydraulic conductivity	Pressure infiltrometer	36
	Guelph permeameter	36
	Falling head slug tests	12
Soil-water content curve	Time Domain Reflectrometer (TDR)	108
	Tensiometers, TDR	3

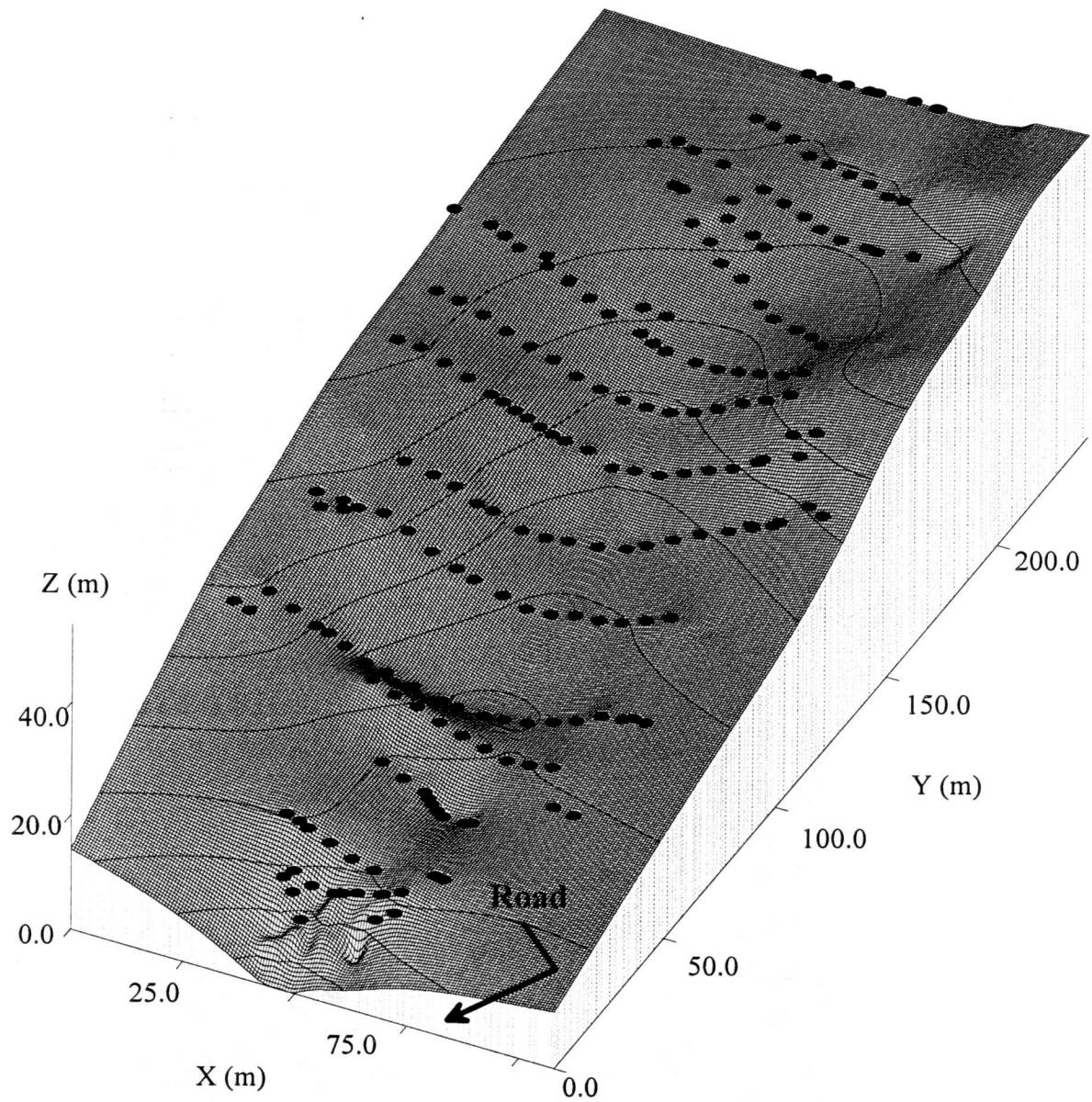


Figure 10. Relief map of the C3 hillslope showing the 13 transects used in the topographic mapping.

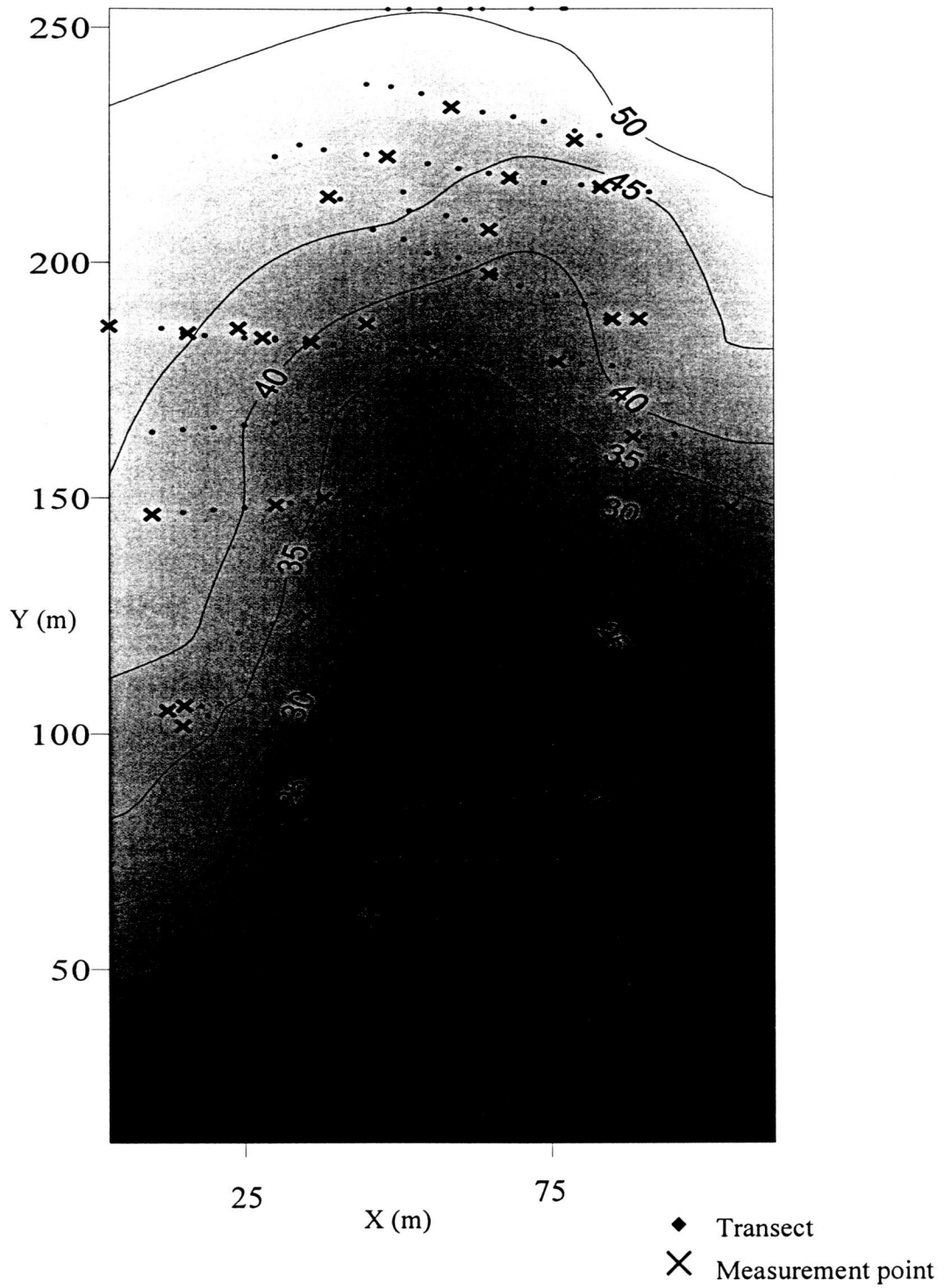


Figure 11. Plan view of the C3 hillslope showing the elevation contours and the location of the transects and measurement locations.

grid describing the catchment. The elevation (z-coordinate) values, along with their respective x- and y- coordinate values were plotted with the program Surfer (Golden Software Inc., 1999). The 3-dimensional map of the C3 hillslope that resulted from the topographic mapping is shown in Figure 3.

Soil Depth

Soil-probe tests were conducted to determine the approximate soil depth at nine measurement sites across C3. Three transects were established at approximately twenty meter intervals from the ridge to the road. Three measurements were made per transect: one on the mid-slope of the left ridge, one on the mid-slope of the right ridge, and one along the axis of the central hollow. The locations of the soil-depth measurements are shown in Figure 12. The steel probe was driven into the ground with a 15kg weight as deeply as possible. When the probe would not penetrate the ground any further it was assumed that the saprolite layer had been reached. The color, texture, and stone content of the soil at different depths were observed during these tests to aid in the soil and site characterization.

Hydraulic Conductivity

Surface and near-surface

The hydraulic properties that control flow into and through unsaturated soil are the saturated hydraulic conductivity (K_s) and the unsaturated hydraulic conductivity – pressure head relationship $K(\psi)$. Field tests were conducted in a semi-regular gridded pattern across C3 using a Guelph Permeameter (GP) to determine the K_s of the soil at depth (Erlick and Reynolds, 1992). A Pressure Infiltrometer (PI) (Erlick and Reynolds, 1992) was used to make the surface infiltration measurements. The locations of the 35 in situ K_s measurements made with the GP are shown in Figures 11 and 13. Approximately three measurements were taken along each transect: one at the axis of the convergent hollow and one on each of the bounding ridges. Some of factors that might have influenced the accuracy of the GP measurements included smearing, or compaction of the well-surface during auguring and small scale soil heterogeneity. Insertion of the PI ring into the soil can alter the soil structure or truncate non-vertical pores.

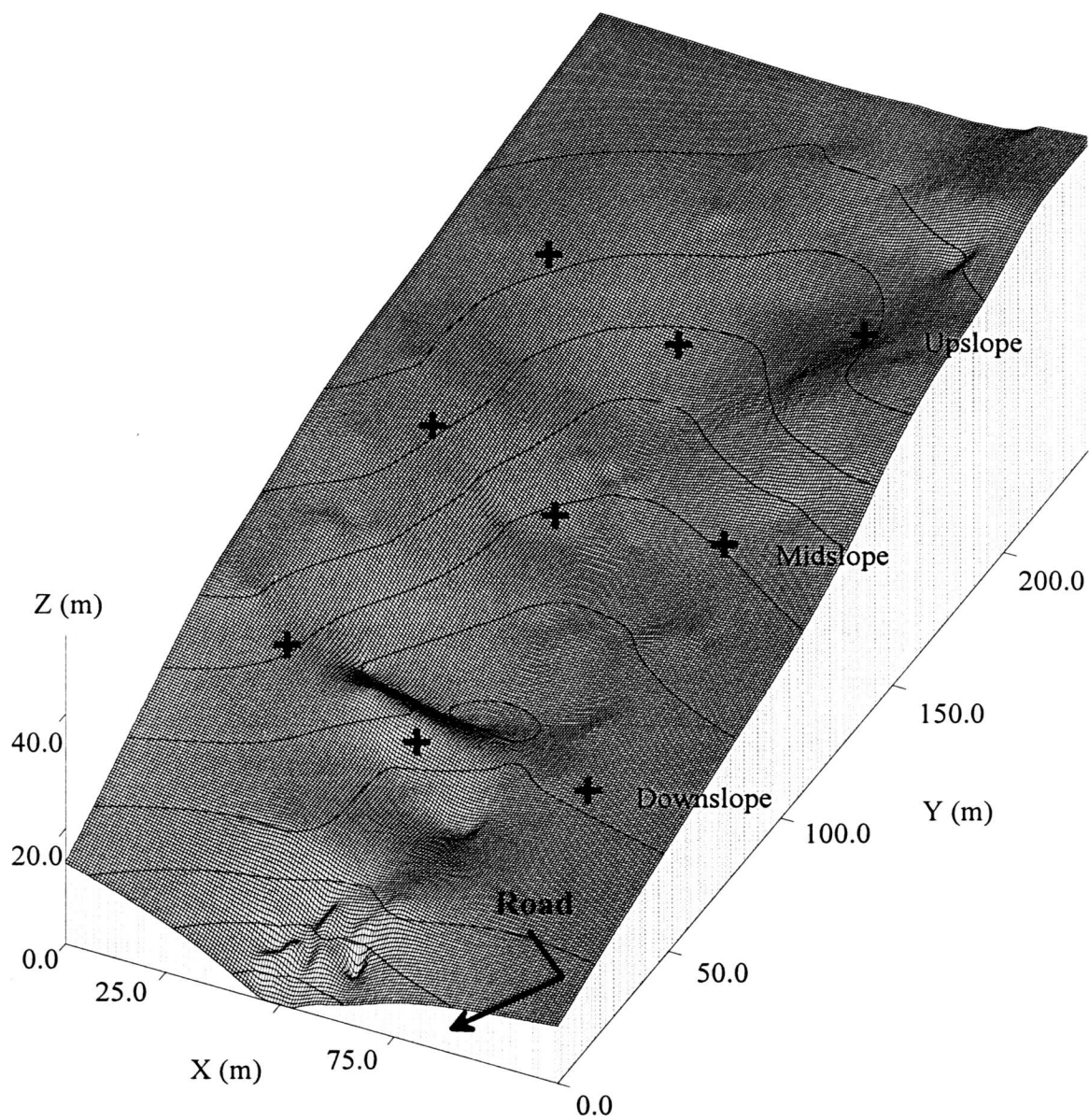


Figure 12. Relief map of the C3 hillslope showing the location of the soil depth measurements.

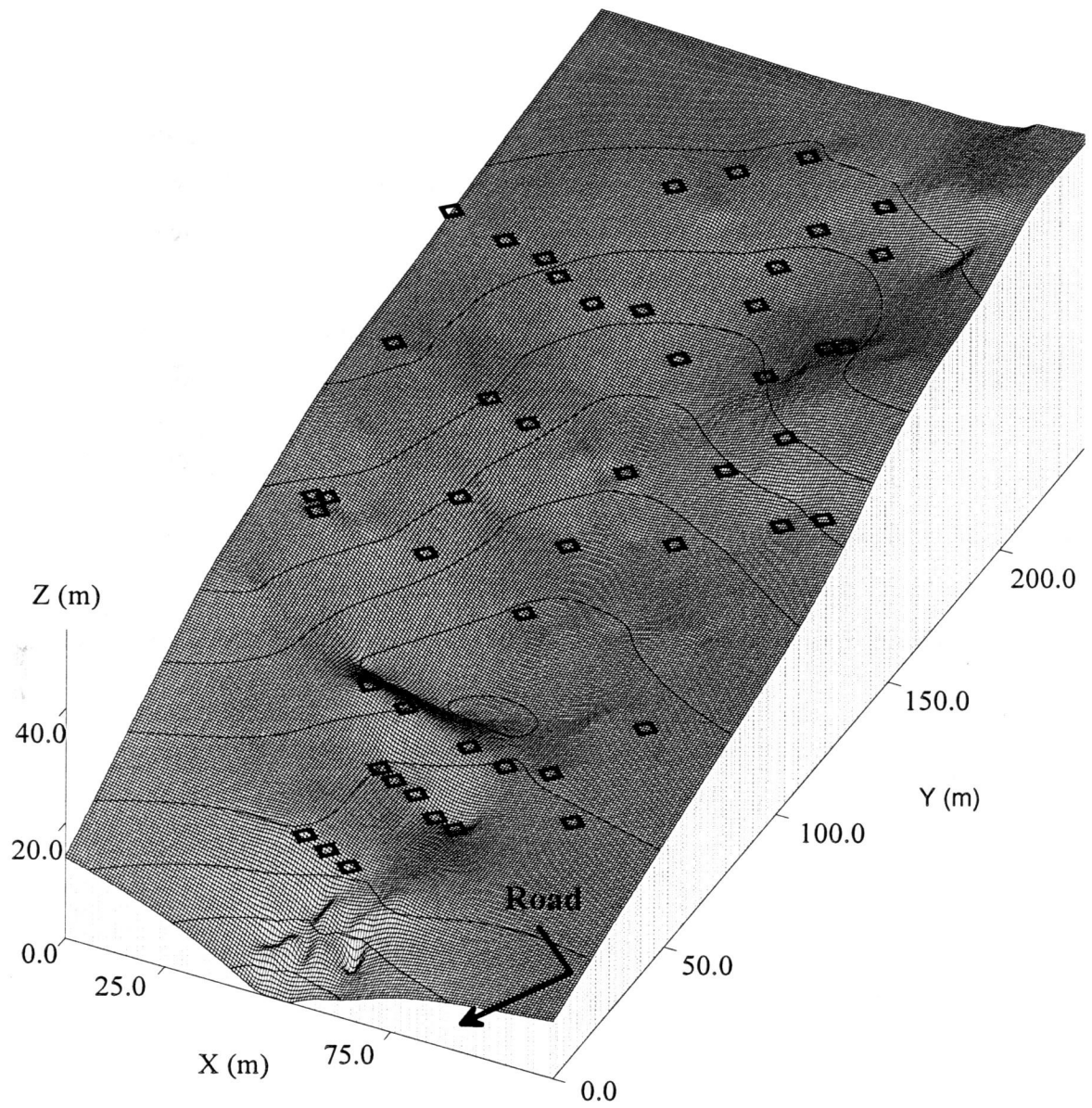


Figure 13. Relief map of the C3 hillslope showing the location of the measurement points for the hydraulic conductivity and soil-water content data.

Saturated subsurface

Twelve slug tests were conducted, using the Hvorslev (1951) (i.e. falling head) method, to attain a preliminary in situ estimate of K_s in the saturated zone. Two tests were conducted at each of the six piezometers installed at both C3 (see Figure 14) and in the adjacent catchment C4 (see Figure 2) by Wemple (1996). A slug of water was rapidly introduced to the piezometer, the highest water level was recorded, and then subsequent levels at a given time increment were measured as the water height returned to the pre-test level. The major disadvantage of using a slug test was that it only provided an estimate of K_s for the zone immediately adjacent to the piezometer. Therefore, large-scale heterogeneity, fractures, and other anomalies did not contribute to the measured value of K_s unless they were within close proximity to the measurement site.

Soil-water content

To set up the correct boundary value problem (BVP) for a numerical model of the C3 hillslope, one must establish the spatial variability of the initial soil-water content conditions as they vary both over the surface and with depth. Soil moisture measurements were taken at the same locations throughout the C3 hillslope as the GP and PI measurements (see Figures 11 and 13) using a TRASE Time Domain Reflectometer (TDR) (Soilmoisture Equipment Corp., 1989). The soil-water content was measured for three different depths (0.15, 0.30, and 0.45m) at each location. Because the TDR data was collected during the month of August in 1998 it represented the minimum seasonal soil-water content prior to any rainfall.

Characteristic Curves

A series of field experiments were performed to establish unique characteristic curves for the soils at C3. Successive and simultaneous TDR (soil-water content) and tensiometer (pressure head) measurements were taken at a small plot under constant irrigation as the soil was wetting. The technique is similar to the method applied by Torres et al. (1998) at Coos Bay. Plotted against each other, the pressure head and the soil-water content data comprise the wetting soil-water characteristic curve. The timed experiments were performed at three sites at three different soil depths (i.e., 0.15, 0.30,

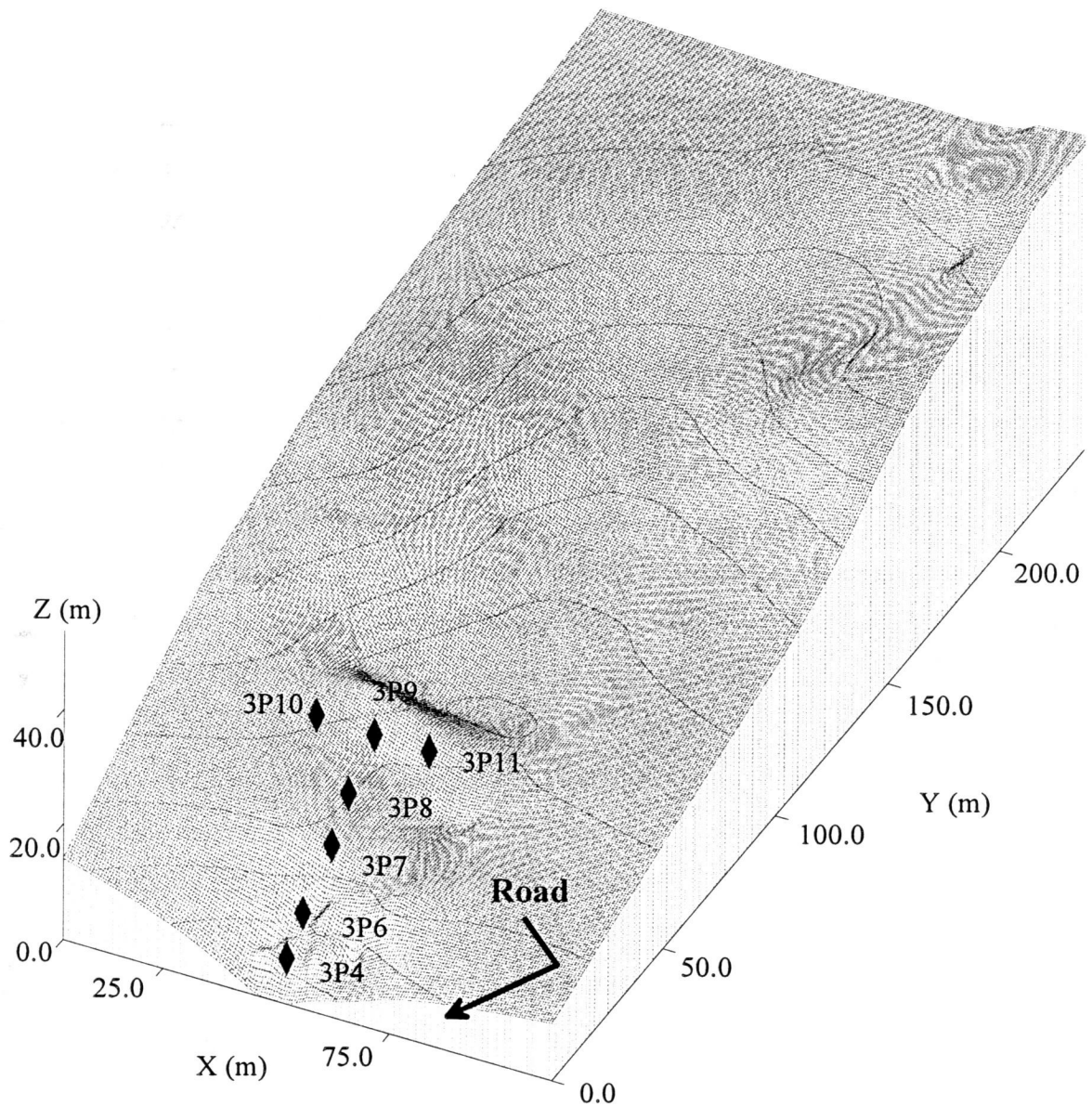


Figure 14. Relief map of the C3 hillslope showing the location of the piezometers.

0.45m). The results of these three experiments were combined to generate a single characteristic curve.

NUMERICAL MODELING

Finite-Difference Method

In general, the rainfall-runoff process can be divided into three water transport phases describing (i) flow into, through, and out of saturated/unsaturated porous media, (ii) overland flow, and (iii) open channel flow. On a two-dimensional hillslope the processes of infiltration, subsurface storm flow, and exfiltration are generally described by the equations of saturated and unsaturated porous media flow. The assessment of the groundwater component within a hillslope (i.e. the water table configuration and the distribution of hydraulic head or pore pressures) requires a complex saturated-unsaturated analysis if the heterogeneity of the system is to be accounted for (Rulon et al., 1985). Transient modeling accounts for different antecedent soil-water content conditions and different recharge mechanisms such as rain vs. rain-on-snow.

In general, there are two motivations for using numerical simulation in hydrogeology: (1) prediction with a calibrated and validated model, and (2) process-based conceptual development. In this study deterministic-conceptual simulation is employed to address field-scale saturated and unsaturated-saturated, steady-state, and transient subsurface flow boundary value problems. The simulation component of this study had four major steps:

- To identify with a relatively simple 2-D numerical model (NUM5) the portion of the C3 hillslope flow system that is most impacted by the introduction of a road.
- To simulate the portion of the flow domain that is most impacted by the road (using the NUM5 results) in greater detail using a 2-D transient, saturated-unsaturated, finite-difference model (VS2DT).
- To compare the piezometric response and the total discharge values simulated by VS2DT against observed piezometric and hydrograph data recorded at C3 during three precipitation events in 1995.

- Perform a sensitivity analysis of the different boundary and initial conditions for the VS2DT simulations and assess if, using the factor of safety criterion, the pore pressure increase in specific areas on the C3 hillslope could ever be sufficient to trigger a mass movement event.

NUM5

The first of the two physics-based finite-difference models used in this study is known as NUM5. NUM5 is a two-dimensional (vertical slice), steady-state, saturated subsurface flow model that was developed by R. Allan Freeze (K. Loague, personal communication, 1998). NUM5, which solves the two-dimensional groundwater flow equation, was employed to determine the distribution of hydraulic heads (and subsequently the pore-pressure values) throughout the long profile of the convergent hillslope system above and below the road at WS3 and at C3 system. Table 5 summarizes the different BVPs that were used with NUM5 to simulate regional and local groundwater flow patterns and to determine the hydrologic impacts associated with road construction. The pore pressure distributions throughout the C3 hillslope that were generated using NUM5 were coupled with a factor of safety analysis to determine the C3 hillslope's susceptibility to failure. The results from the long profile simulations (i.e. steady-state saturated) were used to identify the boundary value problem for the transient unsaturated-saturated simulations with VS2DT (Lappala et al., 1986).

There are two separate governing equations for the two different types of NUM5 simulations. The first type of simulation was two-dimensional, steady-state groundwater flow in a vertical slice assuming an isotropic and homogeneous hillslope. This system can be described by Laplace's Equation:

$$\frac{\partial^2 h}{\partial y^2} + \frac{\partial^2 h}{\partial z^2} = 0 \quad (1)$$

where h is hydraulic head (L) and y and z (L) defined the spatial domain that is modeled.

The second type of simulation involves two-dimensional, steady state groundwater flow in a vertical slice in an isotropic but heterogeneous hillslope. This system can be described by:

Table 5. Summary of the simulations conducted using NUM5. (a) WS3. (b) C3.

(a)

Simulation Description		Results
Base case	Homogeneous and isotropic	Base case, standard Toth flow regime
Case 1	Homogeneous and isotropic with road	Standard Toth flow regime, shows little impact of roadcut
Case 2	Heterogeneous and isotropic	Concentrates flow in high conductivity zones
Case 3	Heterogeneous and isotropic with road	Directs seepage outward at roadcut and creates high pressure zones in the vicinity of the road

(b)

Simulation Description		Results
Base case	Homogeneous and isotropic	Base case, standard Toth flow regime
Case 1	Homogeneous and isotropic with road	Standard Toth flow regime, noticeable impact of roadcut
Case 2	Heterogeneous and isotropic	Concentrates flow in high conductivity zones
Case 3	Heterogeneous and isotropic with road	Directs seepage outward at roadcut and creates high pressure zones in the vicinity of the road

$$\frac{\partial}{\partial y}(K_y(y, z) \frac{\partial h}{\partial y}) + \frac{\partial}{\partial z}(K_z(y, z) \frac{\partial h}{\partial z}) = 0 \quad (2)$$

where K is saturated hydraulic conductivity (L/T).

With the addition of flow lines perpendicular to the lines of hydraulic head estimated from either (1) or (2), one can construct a flow net that can in turn be used to calculate the discharge through the system using Darcy's law, given by:

$$q = -K \frac{\partial h}{\partial y} \quad (3)$$

The hydraulic relationships that were used to get the information for slope stability estimates from NUM5 simulations are as follows. The values of hydraulic head calculated in (1) and (2) are related to the elevation and pressure head based on the relationship given by:

$$h = \psi + z \quad (4)$$

where ψ is the pressure head (L), and z is the elevation head (L). The relationship between the pressure head and the pore pressure, not accounting for the changes in temperature and pressure with depth, is given by:

$$p = \rho g \psi \quad (5)$$

where p is the pore pressure (M/L^2), ρ is the density of water at standard temperature, and pressure (M/L^3), and g is the acceleration due to gravity (L/T).

Assumptions

Table 6 summarizes the approximations that were made to simulate a complex hillslope system with NUM5. In general, the assumptions listed in Table 6 did not detract from the fundamental goal of understanding how water moves through the WS3 hillslope prior to and after the construction of the road. It should be pointed out that the

Table 6. Assumptions made in this study related to the NUM5 simulations for WS3 and C3.

Model Assumption	Actual Condition	Comment
2-D (y,z)	3-D system	Simplified representation of the system
Heterogeneous	Heterogeneous	
Isotropic	Anisotropic	
Saturated	Unsaturated and Saturated	
Vertically averaged properties	Variable permeability	
Steady-State	Transient	
Water table at surface	Flux boundary	
Porous media	Porous media	Reasonable assumption for groundwater flow at regional scale
No flow boundaries	Flow divides along ridges	Reasonable assumption for modeling catchment morphology and delineating catchment boundary
Impermeable base	Bedrock (low K_s ¹) base	
Vertically averaged properties	Variable permeability	Generally valid for permeable zone at a regional scale
K_s decreases with depth	K_s decreases with depth	Reasonable model of flow system
Road is impermeable	Road has very low K_s	Reasonable approximation

¹ K_s is the saturated hydraulic conductivity.

assumptions upon which the NUM5 simulations are based did not affect the characterization of the boundary value problem for the VS2DT simulations that followed.

Use of NUM5 in this study was based upon the assumption that the material is fully saturated. The water table was assumed to be at the surface and each point had a specified total head equal to its elevation at the surface. In reality, the water table was perched along the bedrock contact but the depth to the water table rarely exceeds two meters during the rainy season. Because the water table is so shallow, this approximation is reasonable relative to the thickness of the entire hillslope. Simulating WS3 as a steady-state system is a reasonable assumption during the winter rainy season because it rains consistently for several months (also the ground might be covered by a snow layer that helps to keep the system stable for longer periods of time). The assumption that the horizontal spatial distribution of K_s is uniform within each layer is sufficient for the purposes of determining where the water is infiltrating and exfiltrating the system.

Boundary Value Problem

WS3

The finite-difference grid used for the NUM5 simulations is shown in Figure 15. The space increments for the grid shown in Figure 15 (i.e. $\Delta y=10\text{m}$, $\Delta z=2\text{m}$) were uniform for both the WS3 and C3 cases. The slope of the long profile was equal to 20° for both cases. The boundary conditions for WS3 were assigned assuming that natural flow divides, or no-flow boundaries, occurred along the lateral edges of the C3 catchment and along the bottom at the bedrock contact. To determine flow patterns at a regional scale it was sufficient to simulate WS3 with a constant slope equal to the median value.

The boundary value problem for the WS3 hillslope, illustrated in Figure 16, constitutes the region starting at the WS3 ridgetop (elevation of 1100 m) and dropping to approximately 950 m above sea level. The flow region defined by ABCD in Figure 16a represents a homogeneous, two-dimensional, vertical cross section through the long profile of WS3 under fully saturated steady-state conditions. The boundaries AB, BC, and CD represent impermeable, or no-flow boundaries while the AD boundary represents a water table boundary. Figure 16b is the same hillslope shown in Figure 16a, but with the addition of a road. Figure 17a shows the layers of different hydraulic conductivity

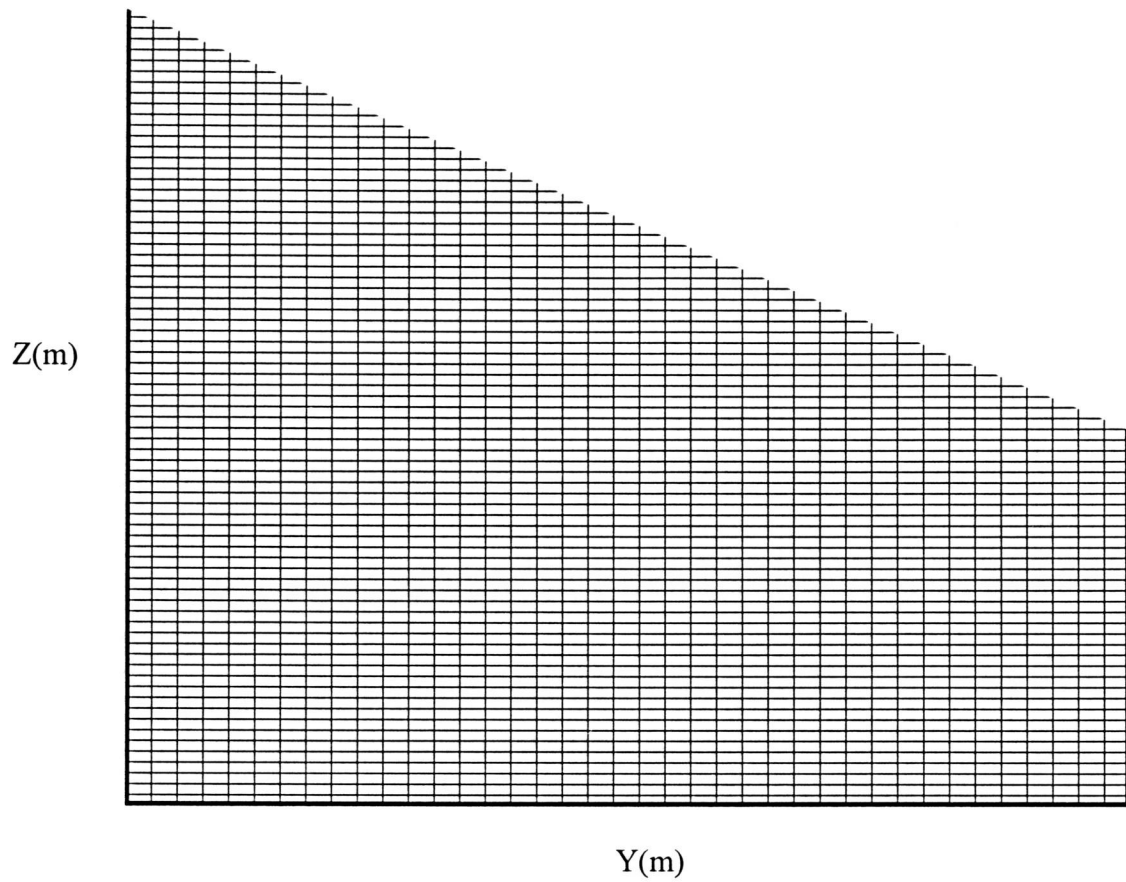


Figure 15. Finite-difference grid used for the NUM5 simulations in this study ($\Delta y = 10\text{m}$, $\Delta z = 2\text{m}$).

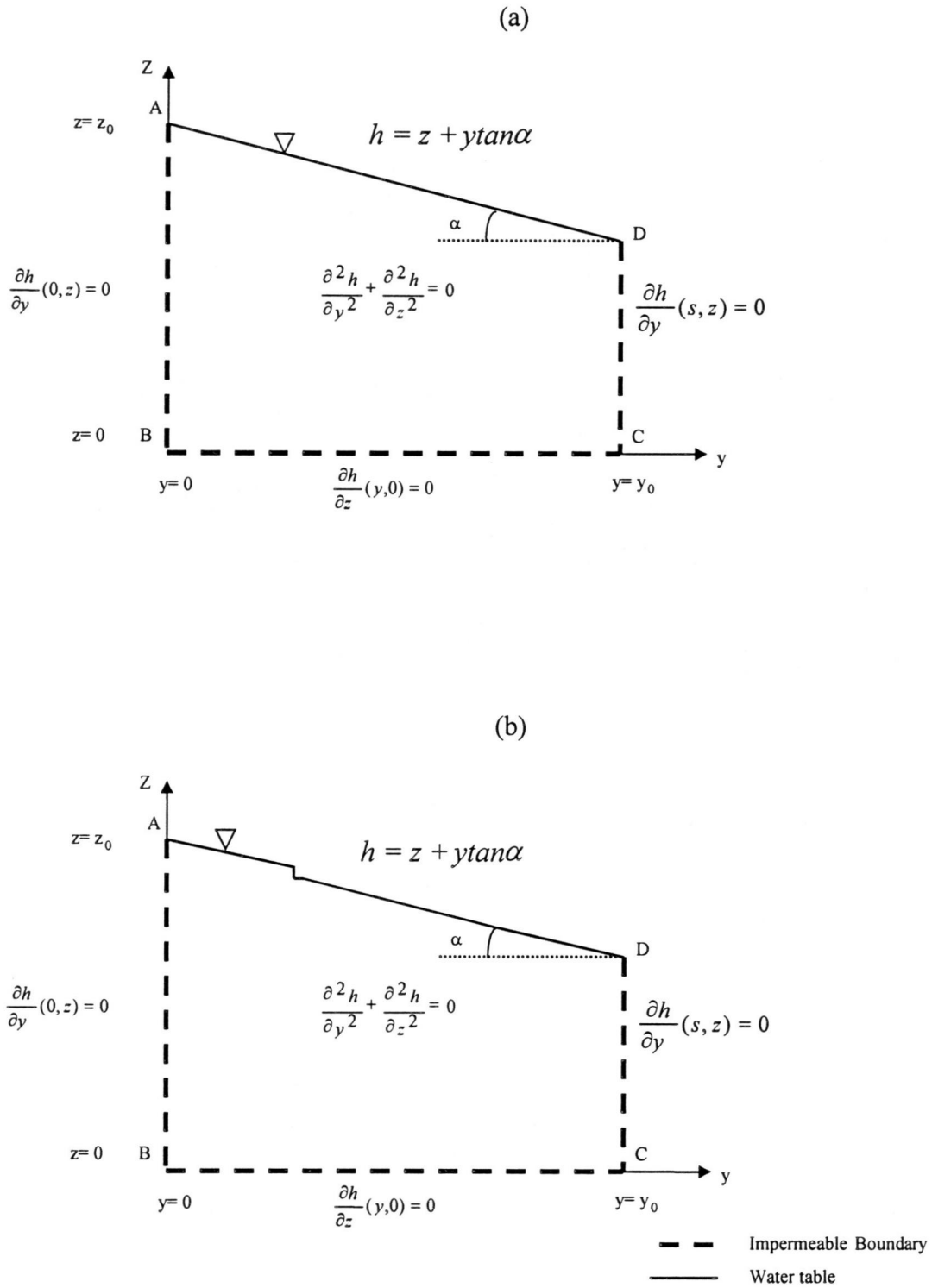


Figure 16. Boundary value problem for the WS3 hillslope. (a) Homogeneous hillslope. (b) Homogeneous hillslope with roadcut.

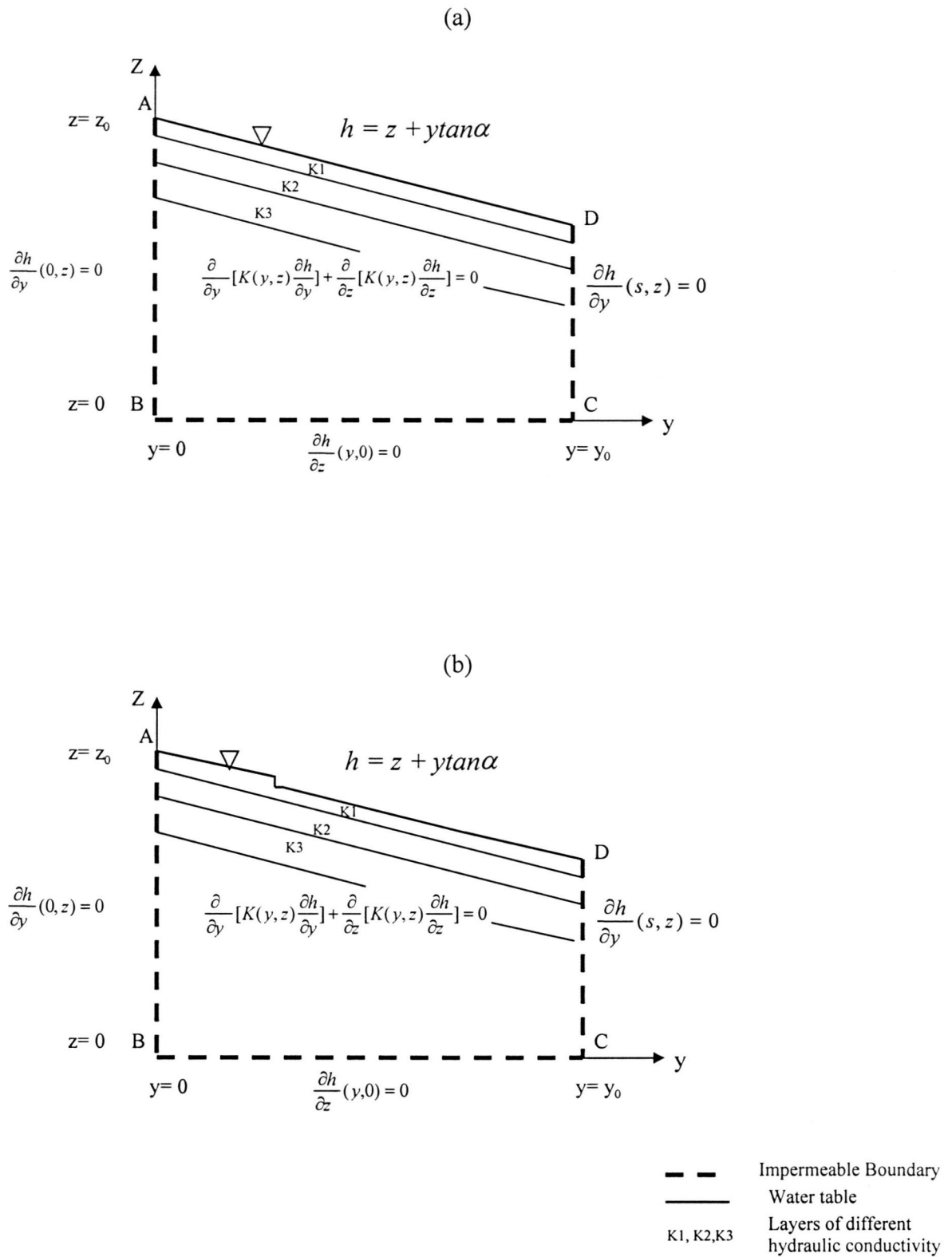


Figure 17. Boundary value problem for the WS3 hillslope. (a) Heterogeneous hillslope. (b) Heterogeneous hillslope with roadcut.

representing the different soil layers and geologic units at WS3. The individual geologic units in the layered slope were considered homogeneous and isotropic with respect to the hydraulic conductivity. Figure 17b shows a roadcut in the heterogeneous C3 hillslope system.

C3

When the large scale WS3 system was modeled, the impact of the road on altering the near-surface hydrologic response was not as apparent as it might be when modeled at a smaller scale. Therefore, a smaller portion of WS3 representing only the convergent hollow directly above the road, was the physical basis for the next series of hillslope scale simulations. Figure 18 shows the C3 hillslope as homogeneous with (Figure 18b) and without the addition of a road (Figure 18a). The boundaries AB, BC, and CD in Figure 18 represented impermeable, or no-flow boundaries while the AD boundary represented the water table. Figure 19 shows the C3 hillslope as heterogeneous with (Figure 19b) and without the roadcut (Figure 19a). The layers of different hydraulic conductivity represent the different soil layers and geologic units at C3. The individual geologic units in the layered slope were each considered homogeneous and isotropic with respect to the hydraulic conductivity.

VS2DT

Based on the results from the steady-state NUM5 simulations, the spatial extent and the magnitude of the impact of a road in the WS3/C3 system were determined. The next phase of the modeling component of this study incorporated the results from the fully saturated watershed-scale WS3 (NUM5) and hillslope-scale C3 (NUM5) systems, into a small-scale, unsaturated-saturated system that focused on the area of interest above and below the road.

In natural hillslope systems recharge occurs through the unsaturated near-surface. The unsaturated flow component of the hydrologic response affects the timing and magnitude of water table response, the influence of evapotranspiration and evaporation, and the importance of non-capillary flow channels on subsurface flow. To understand the effect of the road on the near-surface hydrologic response, the model VS2DT (Lappala et al., 1987) was employed. VS2DT is a block-centered, two-dimensional finite-difference

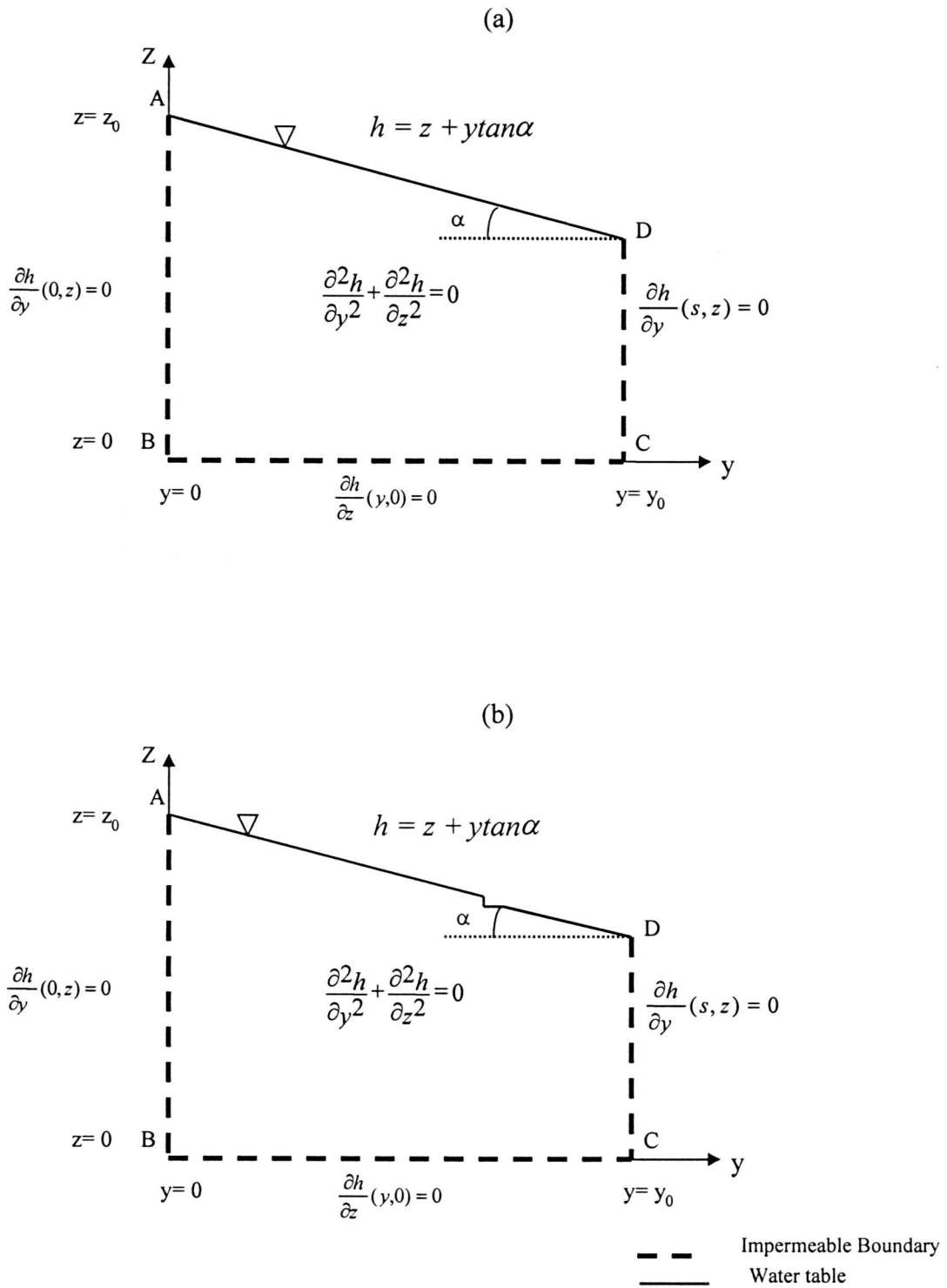


Figure 18. Boundary value problem for the C3 hillslope. (a) Homogeneous hillslope. (b) Homogeneous hillslope with roadcut.

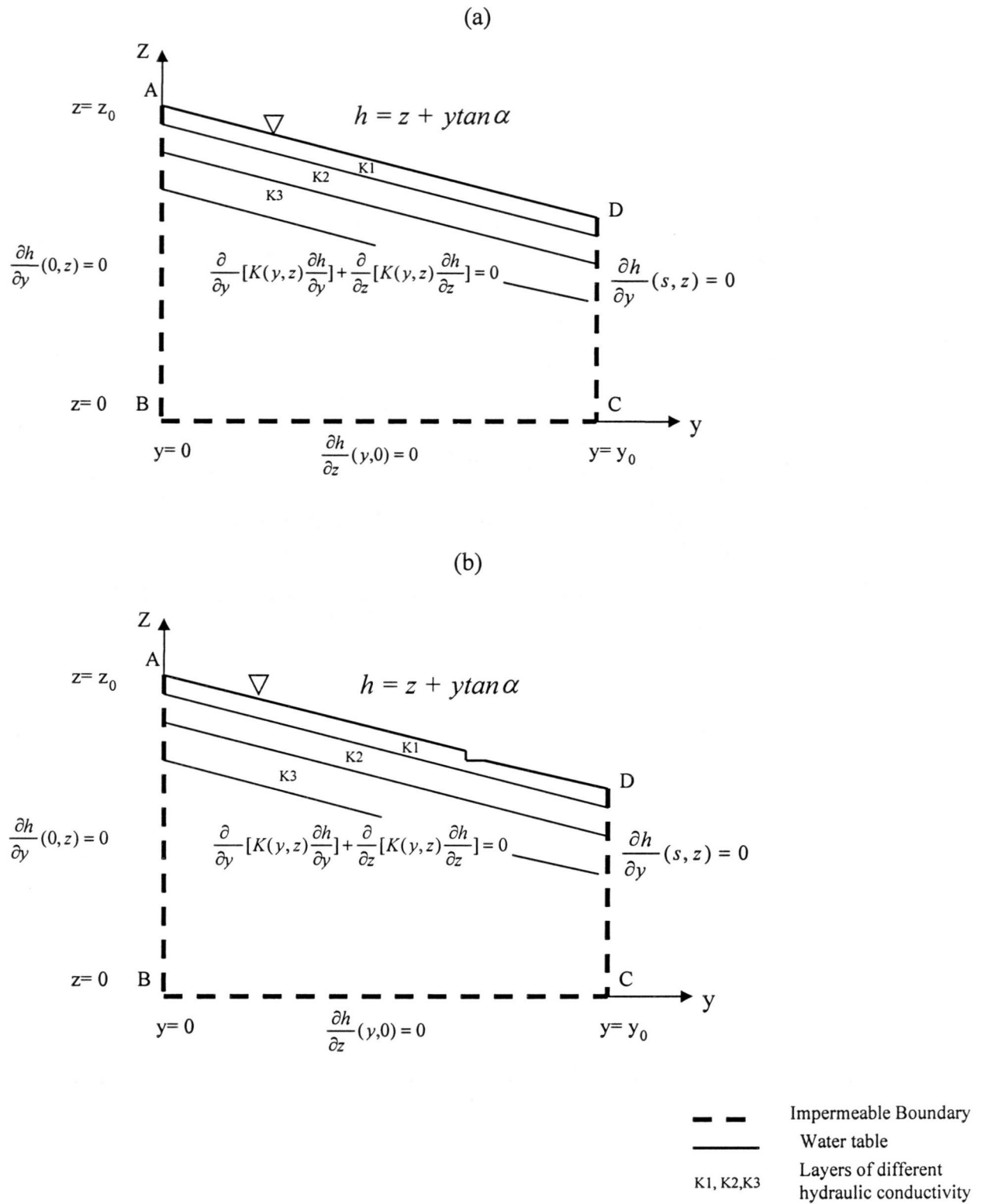


Figure 19. Boundary value problem for the C3 hillslope. (a) Heterogeneous hillslope. (b) Heterogeneous hillslope with a roadcut.

code designed to solve transient flow problems in variably saturated porous media. The data from the storm events in 1995 were used to calibrate VS2DT to the C3 hillslope.

VS2DT Equations

Subsurface fluid flow within a two-dimensional vertical slice of variably saturated media is described by:

$$\frac{\partial}{\partial y} (K_{yy}(\psi) \frac{\partial \psi}{\partial y}) + \frac{\partial}{\partial z} (K_{zz}(\psi) \frac{\partial \psi}{\partial z} + 1) = C(\psi) \frac{\partial \psi}{\partial t} \quad (6)$$

where y is the horizontal direction (L), z is the vertical direction (L), t is time (T), ψ is the pressure head (L), $C(\psi)$ is the specific moisture capacity of the material, and $K(\psi)$ is the hydraulic conductivity of the material (L/T).

The interface between the unsaturated and saturated zone occurs when the pressure head is equal to zero (i.e., $\psi=0$). Along this interface the total head equals the elevation head. The psi-based, non-linear equation flow solved by VS2DT is

$$v\{\rho[c_m + \theta S_s]\} \frac{\partial h}{\partial t} - \rho \sum_{k=1}^m A_k K K_r(\psi) \frac{\partial h}{\partial n_k} - \rho q v = 0 \quad (7)$$

where c_m is the specific moisture capacity (the slope of the soil-water retention curve), ψ is the pressure head (L), K is the saturated hydraulic conductivity (assuming constant density and viscosity) (L/T), h is the total head (L), $K_r(\psi)$ is the unsaturated hydraulic conductivity as a function of the pressure head (L/T), v is the volume for which (4) was solved (L^3), S_s is the specific storage (which is a function of the matrix compressibility and the fluid compressibility) (M^{-1}), ρ is the fluid density (M/L^3), θ is liquid saturation, and q is the volumetric source sink term accounting for the volume of liquid added or taken away from the volume (v) per unit time (L^3/T).

Boundary Value Problem

The C3 system is simulated with VS2DT as a two-dimensional vertical slice down the central axis of the convergent hollow. Because the dominant seepage face occurs at the mouth of the convergent hollow and feeds the v-notched wier at the base of the roadcut face, a two-dimensional representation of the system that neglects topographically driven lateral inflow is sufficient to represent the near-surface hydrologic flow field. The topography is represented by linear interpolation between data points measured on site with an auto-level.

The focus of the questions posed in this study about the impact of roads is the portion of the C3 hillslope above and below the road shown in Figure 20 and accounts for approximately seventy meters of the hillslope. This area includes the highest nest of piezometers on the hillslope and extends approximately 10 meters downslope of the road. By assigning these boundary conditions to this problem, the majority of the field data collected at C3 could be utilized for calibration and to test model performance (i.e. the piezometer and hydrograph readings for each storm event are compared to model output). The finite difference grid that was used in the VS2DT simulations is shown in Figure 21. The Δy and Δz were uniform throughout the C3 grid and equal to 0.42 and 0.05 meters respectively. As a function of the VS2DT input structure, the C3 BVP was set up as a horizontal domain and then rotated by 30° to establish the correct slopes and geometry to represent the problem.

The C3 VS2DT BVP is shown in Figure 22. Based on the on-site soil depth analysis and information obtained from the literature (see Wemple, 1996; Dyrness, 1976) the most active region for near-surface hydrologic response (i.e., the high conductivity layer) was contained within the first 1.0-1.5m of soil. Based on the Coos Bay work of Torres et al., (1998) and Montgomery et al., (1997) the first few meters of fractured bedrock and saprolite are expected to be hydrologically active as well. Therefore, the C3 VS2DT simulations in this study were only for the near- surface system, which included approximately the top 8m of the soil profile. To avoid numerical instability in the unsaturated zone, the vertical space increment was required to be 0.05m. The base of the C3 BVP (B-C) in Figure 22 was treated as a constant flux boundary that leaked at a rate equal to the hydraulic conductivity of the bedrock.

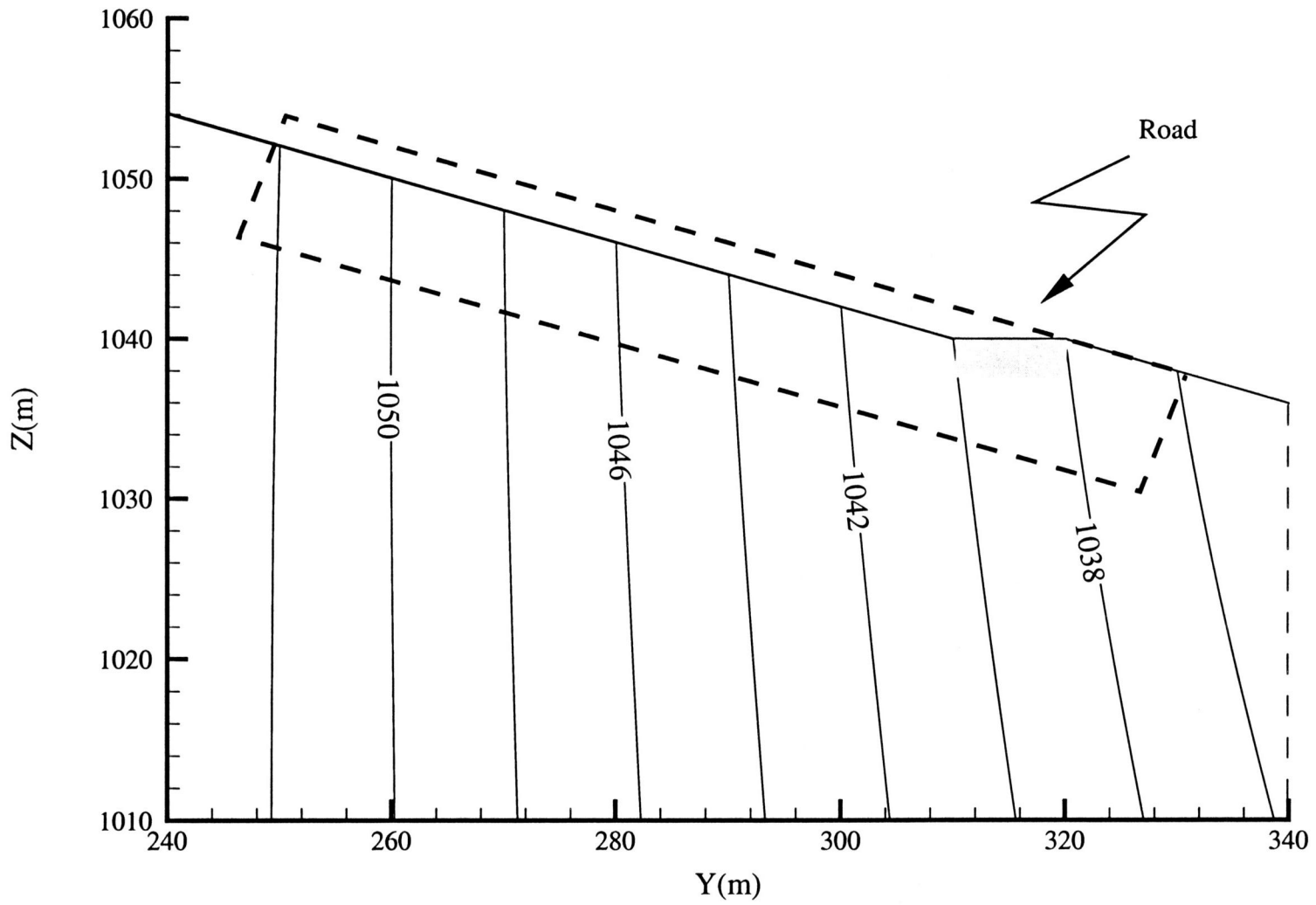


Figure 20. The portion of the C3 hillslope simulated in NUM5 that defined the BVP used for the VS2DT simulations.

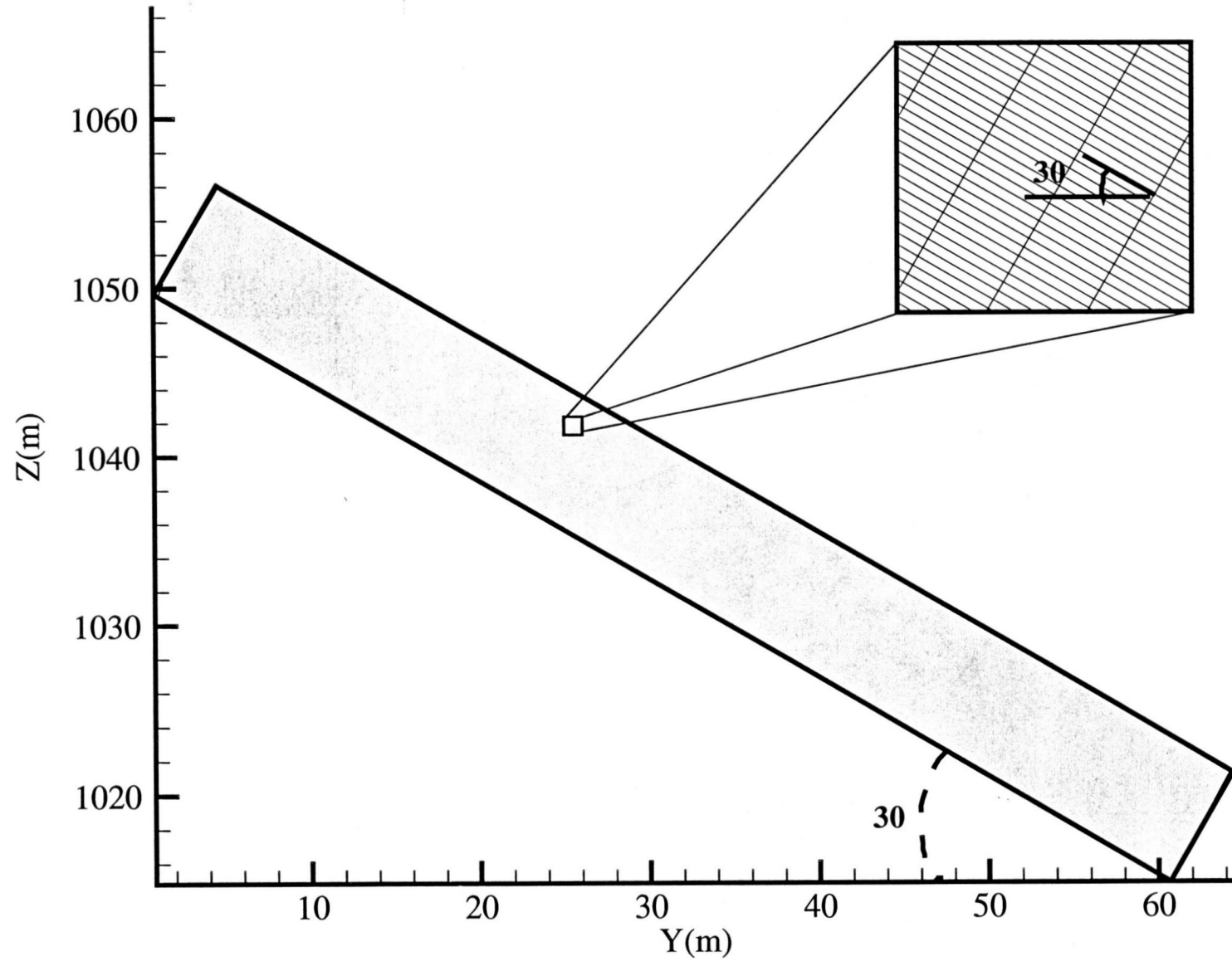


Figure 21. The finite-difference grid used for the VS2DT simulations ($D_y = 0.42m$ and $D_z = 0.05m$).

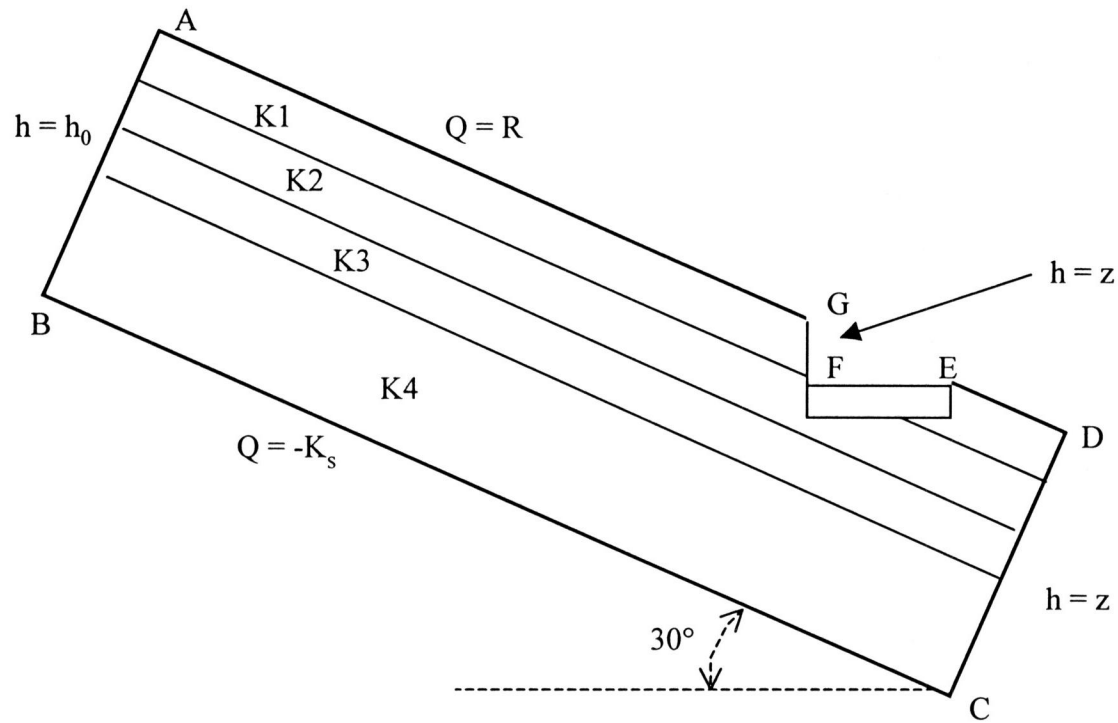


Figure 22. The boundary value problem representing the portion of the C3 hillslope simulated with VS2DT. K1, K2, K3, and K4 represent layers of different hydraulic conductivity (L/T), R is a constant flux equal to the rainfall rate (L^2/T), h is equal to the hydraulic head (L), and Q is a constant flux equal to the hydraulic conductivity of the bedrock (L^2/T).

The upgradient boundary of the system (A-B) in Figure 22 was treated as a constant head or Dirichlet boundary; the value of which was determined as a function of the initial water table location. The surface boundary condition (A-D) in Figure 22 was treated as a constant flux boundary with a flux rate equal to the recharge rate. The cutslope above the C3 road (F-G) and the downgradient side (C-D) in Figure 22 were treated as seepage faces. The surface in Figure 22 (E-F) represents the road surface that was considered relatively impermeable in contrast to the high conductivity soil it intercepted.

The initial conditions for the VS2DT simulations of C3 were obtained by letting the fully saturated system drain until an equilibrium profile was obtained. The pressure head distribution was used as the initial condition inputs for all of the successive simulations. Once the pressure head distribution was known, the water table location, soil-water content distribution, and the direction of flow could be determined.

VS2DT testing

The VS2DT simulations for C3 were compared against the observed data for three different storm events during the winter of 1995-1996. Piezometer and hydrograph data collected at C3 for all events by Wemple (1998) was used in the comparisons of observed versus simulated results. The magnitude and duration of the storms were measured at one-half hour intervals using a tipping bucket rain gauge at the WS3 meteorological station (see Figure 5). Table 7 shows the ranking of the rainfall events according to storm size, average rainfall rate, and maximum rainfall rate. For the VS2DT input each C3 rainfall event was subdivided into periods with similar rainfall rates. Figure 23 compares the hyetographs of the simulated versus the observed rainfall events.

The hydrograph produced by the continuous record of the stage height on the wier located at the base of the C3 roadcut face served as one check that the BVP describing the C3 hillslope accurately described the hydrologic response recorded for the individual storm events. The area beneath the hydrograph recorded at C3 for each storm event was integrated to determine the total volume of water discharged at the roadcut face. To compare the model results against the observed data the mean height of the seepage face above the road was measured at sequential times during each storm event. The local

Table 7. Summary of three storm events and discharge recorded at C3 for 1995.
 (a) Ranked in terms of the maximum half-hour precipitation intensity. (b) Ranked in terms of the total precipitation. (c) Ranked in terms of the maximum discharge. (d) Ranked in terms of the average precipitation intensity.

(a)

Storm date	Total precipitation (mm)	Average precipitation intensity (mm/hr)	Maximum half-hour intensity (mm/hr)	Maximum Discharge (ml/s)
December 28	165	2.6	9.1	11000
November 24	103	1.5	7.1	4800
November 29	51	2.5	6.1	10000

(b)

Storm date	Total precipitation (mm)	Average precipitation intensity (mm/hr)	Maximum half-hour intensity (mm/hr)	Maximum Discharge (ml/s)
December 28	165	2.6	9.1	11000
November 24	103	1.5	7.1	4800
November 29	51	2.5	6.1	10000

(c)

Storm date	Total precipitation (mm)	Average precipitation intensity (mm/hr)	Maximum half-hour intensity (mm/hr)	Maximum Discharge (ml/s)
December 28	165	2.6	9.1	11000
November 24	51	2.5	6.1	10000
November 29	103	1.5	7.1	4800

(d)

Storm date	Total precipitation (mm)	Average precipitation intensity (mm/hr)	Maximum half-hour intensity (mm/hr)	Maximum Discharge (ml/s)
December 28	165	2.6	9.1	11000
November 24	51	2.5	6.1	10000
November 29	103	1.5	7.1	4800

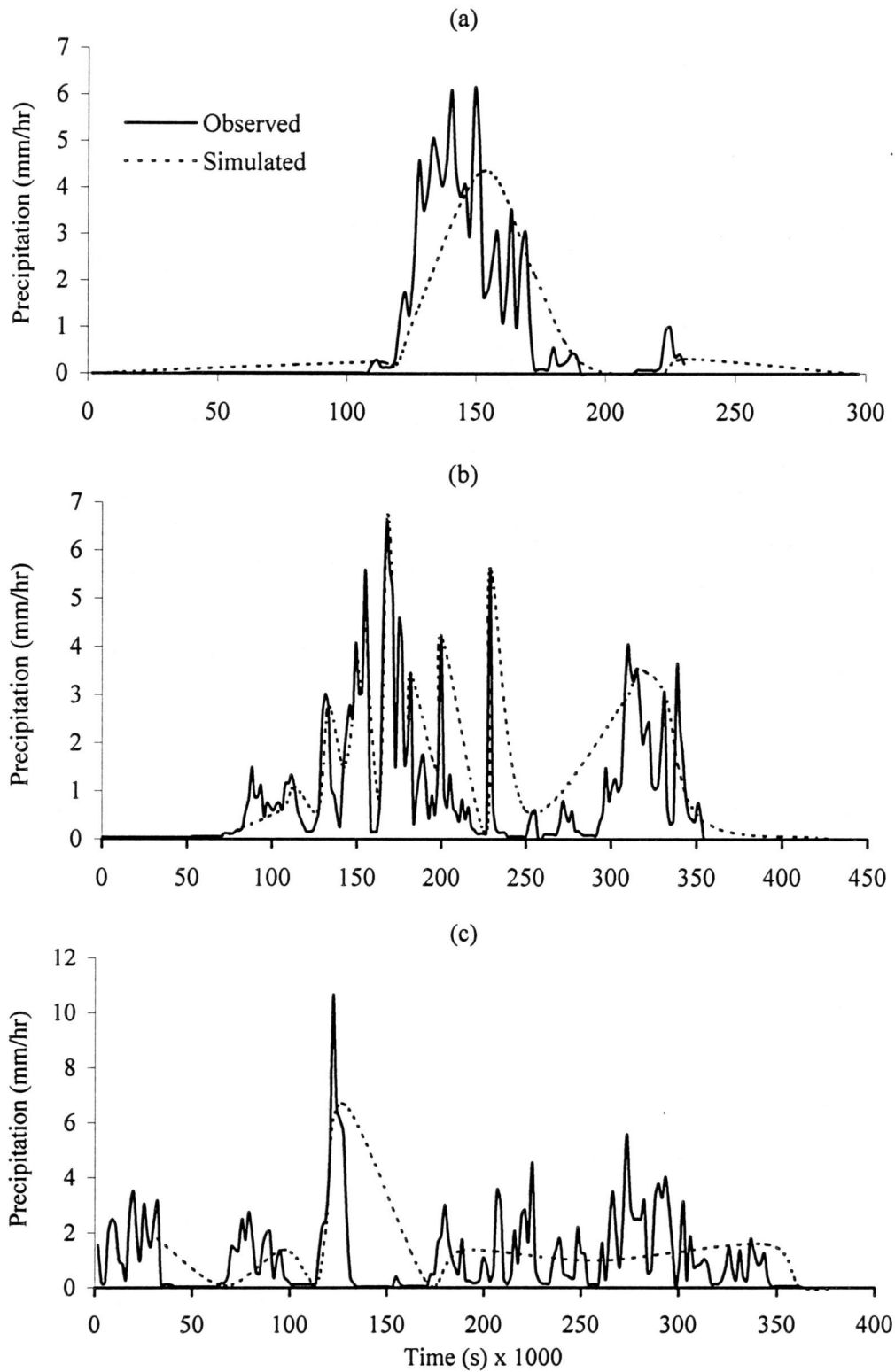


Figure 23. Simulated versus observed precipitation intensity and duration for the three 1995 storm events recorded at C3 and used to calibrate the VS2DT model. (a) November 24 event. (b) November 29 event. (c) December 28 event.

hydraulic gradient at the seepage face was calculated, and assuming a unit width and using Darcy's law (4) the discharge across the cross-sectional area of the roadcut face was determined. The same convention was applied to the cross sectional area at the downslope boundary (line CD in Figure 22) through which water flowed out of the C3 system. The discharge across the roadcut face was calculated as a percentage of the total discharge recorded for each storm event during the VS2DT simulations.

The response of four piezometers (i.e., 3P4, 3P6, 3P8, and 3P9) located along the axis of the convergent C3 hollow (see Figure 14 for locations) served as another check of model performance. Figure 24 shows the location of the four measurement points established within the VS2DT framework that corresponded to the depth and locations of the C3 piezometers.

Simulated Events

The thrust of this research was to understand the hydrologic response of the C3 hillslope to different rainfall events and to assess the corresponding slope stability condition. Based upon the match between the volume of water discharged at the roadcut face and the piezometric response during the three storm events described above, the C3 BVP was assumed to be a reasonable approximation of the C3 hillslope system. Under this assumption, the sensitivity of the C3 system to different factors that would influence slope stability could be assessed. Table 8 summarizes the different case studies applied to the C3 hillslope. In addition, a series of hypothetical events (i.e. rainfall events of different intensity and duration) were imposed upon the system and the resultant hydrologic response was evaluated in terms of its impact on slope stability. The impact of the slope gradient, hydraulic conductivity contrasts, and initial conditions, for the VS2DT simulations, were evaluated in terms of their influence on the simulated hydrologic response and the factor of safety value (i.e. ratio of shearing to resisting forces) estimated for C3.

Six measurement points (both upslope and downslope of the road) were established throughout the C3 hillslope (see Figure 24). The pore pressure response was calculated four times during each hypothetical rainfall event to assess how the different rainfall intensities and different sets of boundary value or initial conditions impacted the

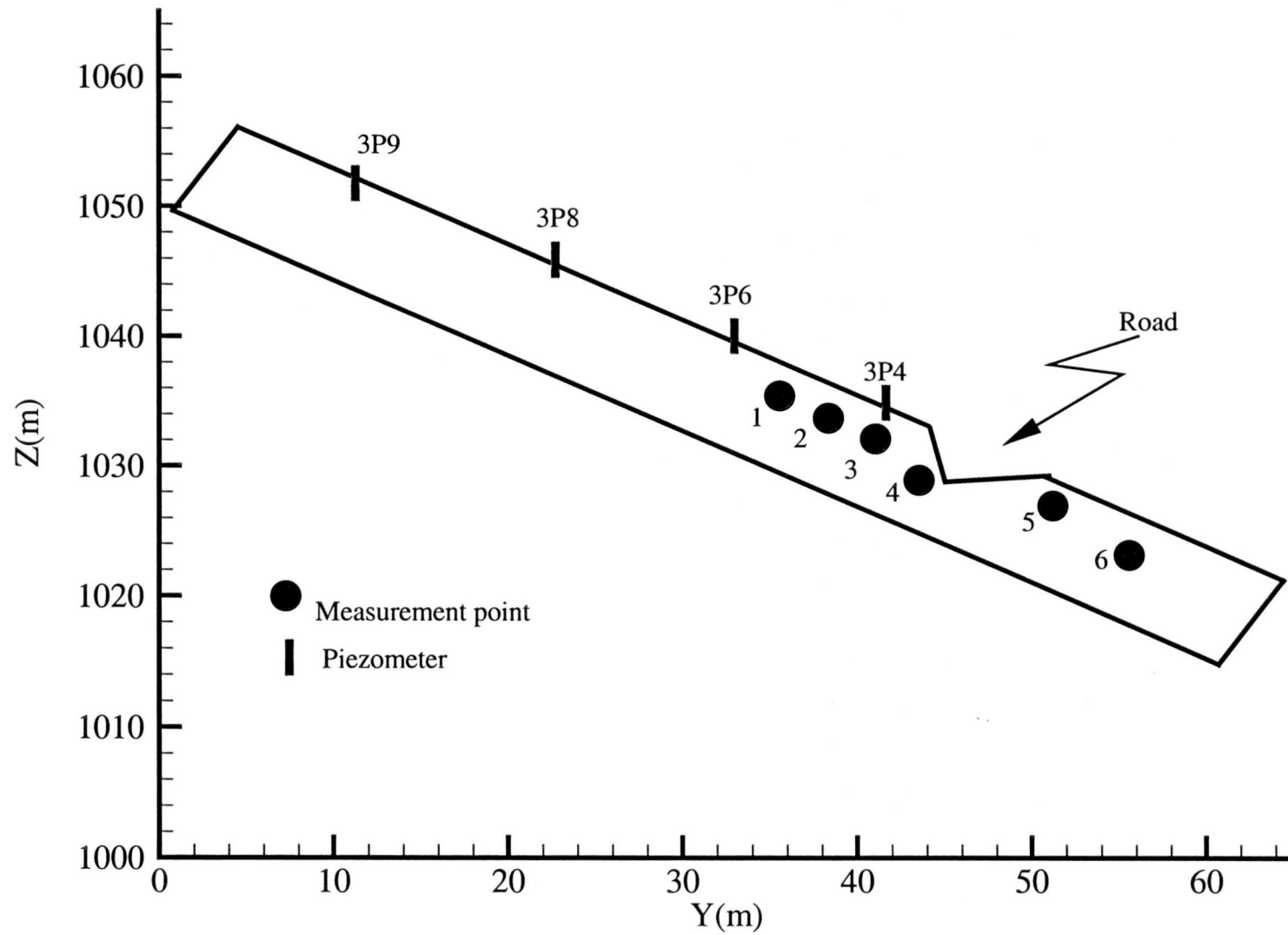


Figure 24. Location of the four piezometers and six measurement points for the VS2DT simulations.

Table 8. Summary of the case studies used to determine the sensitivity of the C3 hillslope to failure.

Case	Rainfall rate (mm/hr)	Rainfall duration (days)	Case description
Base case	0.36	1	Heterogeneous hillslope with roadcut.
	3.60	1	
	36.0	1	
	360.0	1	
Case 1	0.36	1	Slope angle increased to 35 degrees.
	3.60	1	
	36.0	1	
	360.0	1	
Case 2	0.36	1	Hydraulic conductivity of compacted area below road decreased by one order of magnitude.
	3.60	1	
	36.0	1	
	360.0	1	
Case 3	0.36	1	Water table height increased to 1.6 m below the surface.
	3.60	1	
	36.0	1	
	360.0	1	
Case 4	0.36	1	Water table height increased to 1.0 m below the surface.
	3.60	1	
	36.0	1	
	360.0	1	
Case 5	0.36	1	Initial conditions changed so water table is 1.0 m below the surface.
	3.60	1	
	36.0	1	
	360.0	1	
Case 6	0.36	1	Rainfall duration increased.
	3.60	2	
	36.0	3	
	360.0	4	
Case 7	0.36	1	Water rerouted to downslope side of road.
	0.36	1	
	0.36	1	
	0.36	1	

pore pressure development throughout the slope. The total discharge from the system for each simulated event was recorded as well.

FACTOR OF SAFETY ANALYSIS

Increases in pore pressure can have a destabilizing impact in fully or partially saturated materials with frictional strength. These effects are highlighted under conditions of steady-state groundwater flow and uniform hydraulic boundary conditions. Performing a factor of safety analysis can assess the destabilizing effects of conductivity contrasts and of a roadcut. In this study the infinite slope method was used for the two-dimensional FS slope stability analysis for the C3 hillslope. The region of the hillslope susceptible to failure was represented as a rectangular soil block with uniform thickness and hydraulic properties. Soil cohesion, root cohesion, permeability, viscosity, and density were assumed be constant within each of the C3 soil layers in the heterogeneous system. The slope angle and angle of internal friction were considered uniform throughout the C3 hillslope.

The homogeneous soil block in the C3 slope rests on a failure plane representing the conductivity contrast between the high conductivity soil and the saprolite layer. At equilibrium, the forces imposed on the block were taken to be equal and opposite in direction and magnitude. As seen in Figure 25 the forces that act on a point on the shear plane of a potential slide are (i) the gravitational stress acting vertically, (ii) the normal stress applied normal to the shear plane, (iii) the shear stress that acts downward along the shear plane, (iv) the shear strength of the soil, and (v) the buoyancy force created by the pore-water pressure.

Where a block of soil rests on a slope (see Figure 26), the normal force acting on the shear plane that maintains the block's position is estimated as

$$\sigma_n = W \cos \beta \quad (8)$$

where W is a product of the block's mass and the gravitational force given by $l\gamma z \cos \beta$ (ML^2), γ is the unit weight of the soil (M), z is the soil depth (L) and β is the slope angle. It should be pointed out that since an infinite slope stability analysis is employed in this study, the length l of the block is irrelevant and will be omitted in further analysis.

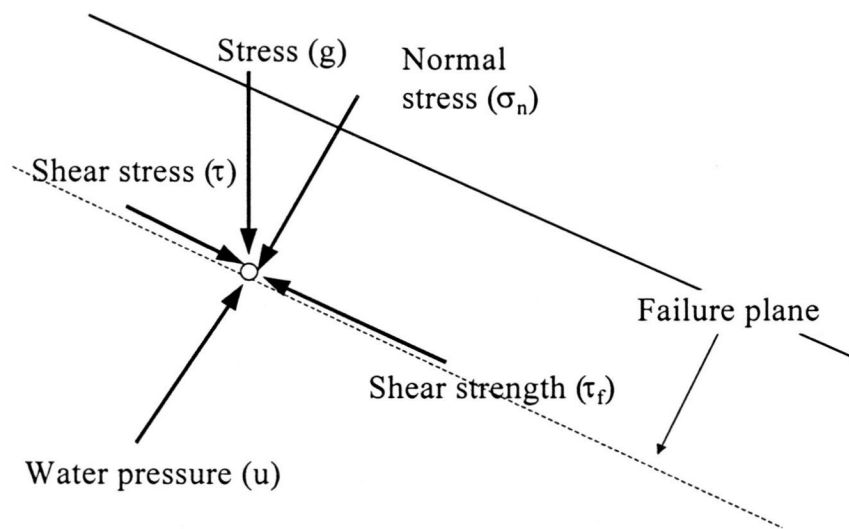


Figure 25. Schematic illustration of the forces acting on a point along the potential failure plane surface (after Selby, 1993).

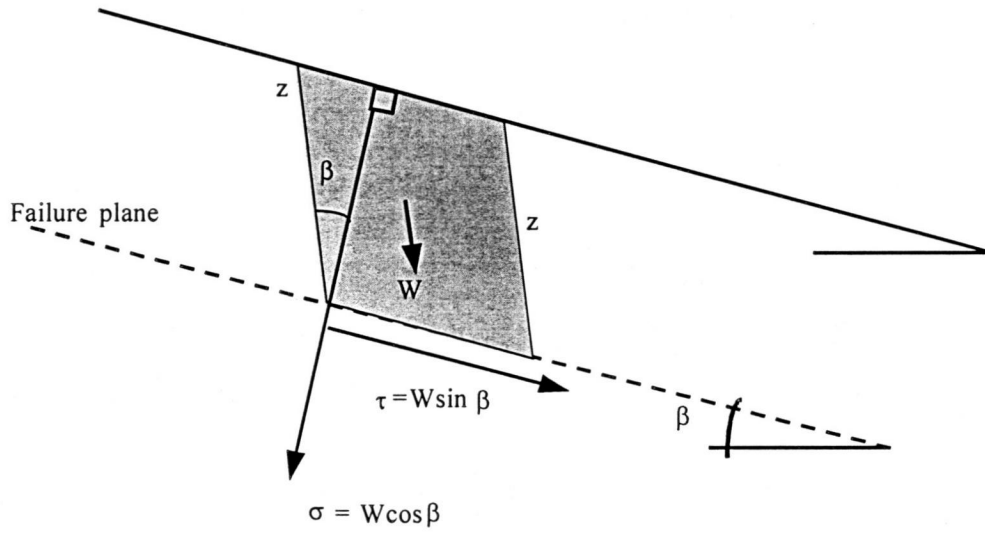


Figure 26. Schematic illustration of the shearing versus resisting forces as they act on a rectangular block resting on a shear plane. β is the slope angle and W is equal to $l\gamma z \cos \beta$.

The driving force (or shearing stress due in part to the weight of the soil) acting on the shear plane that would instigate slope failure is estimated as

$$\tau = W \sin \beta \quad (9)$$

In this study the “block” of soil was taken as part of the C3 hillslope. The location of the failure plane was determined from measurements of the soil profile depth. The soil block was assumed to have unit width.

The magnitude of the pore pressures along the potential failure plane were calculated using:

$$u = (\gamma_w m z \cos^2 \beta) \quad (10)$$

where m is the ratio of the vertical height of the water table as a fraction of the soil thickness above the failure plane, γ_w is the unit weight of the water (M). The fluid pressure data needed for the above calculation is gleaned from the pressure head distributions simulated by NUM5 and VS2DT. It should be noted that u in this portion of the study corresponds to the pore pressure values calculated by (5) and represented by the variable p .

Using the pore pressures that resulted from each simulation, the shear stress along the failure plane was estimated by the Coulomb equation as

$$\tau_f = c' + (\sigma_n - u) \tan \phi' \quad (11)$$

where τ_f is the effective shear strength at any point in the soil, c' is the effective cohesion of the soil (M/L^2), ϕ' is the angle of internal friction, σ_n is the normal stress imposed by the weight of the solids and water above the point in the soil (N/L^2), u is the pore water pressure where $u = (\gamma_w m z \cos^2 \beta)$ (N/L^2).

Because the factor of safety represents the ratio of the sum of the resisting forces to that of the driving forces, the equation for slope stability incorporating the effect of root cohesion is

$$F = \frac{(c' + \Delta c) + (\gamma - m\gamma_w)z \cos^2 \beta \tan \phi'}{\gamma z \sin \beta \cos \beta} \quad (12)$$

where Δc is the root cohesion (M/L^2), and γ is the unit weight of the soil (M/L^3). If the FS is greater than or equal to one, then the slope is considered to be stable. If FS is less than one, then the slope is not stable and is subject to failure.

Sensitivity Analysis

Important factors that control slope stability at a site are (i) the pore water pressure, (ii) the soil strength parameters, (iii) the slope steepness, and (iv) the depth to the potential failure plane. Prior to assessing the vulnerability of the C3 hillslope to failure given the different antecedent and hydrologic conditions simulated in the previous section, the sensitivity of the FS analysis on the C3 hillslope must be discussed. The relative influence of the various soil, slope, and hydrologic variables used in slope stability analysis can be assessed by performing a sensitivity analysis using the infinite slope model. The variables that were considered in this sensitivity analysis were Z (the thickness of the soil layer above the failure plane), Δc (the root cohesion), β (the slope angle), ϕ' (the internal angle of friction), and c' (the soil cohesion). Table 9 gives the reasonable set of variables that were selected as input to the FS equation (i.e., taken as the base case). The base case is used to investigate the impact of increasing or decreasing the individual variables by 10% (keeping everything else constant). The relative change in the FS values is an index of the importance of each parameter, and the relative uncertainty associated with the base case value.

Boundary Value Problem

NUM5

The BVP used for the FS analysis performed for this portion of the study is shown in Figure 27a. The FS was calculated for a homogeneous slope, for a heterogeneous slope, and for a heterogeneous slope with a roadcut. The system was fully saturated so the ratio of the water table height to the above the failure plane to the soil thickness above the failure plane was always equal to one.

A sensitivity analysis investigated the effect that the magnitude of the conductivity contrast along the failure plane had on the FS and pore pressure values. Table 10 summarizes the different case studies that were compared against the base case

Table 9. Parameter values used in this study for the factor of safety analysis at the C3 hillslope.

Parameter	Symbol	NUM5	VS2DT
Hillslope angle	β	20°	30°
Internal angle of Friction	θ'	35	20
Effective cohesion of the soil	c'	1.5	1.5
Root cohesion	Δc	5	5
Hillslope length	l	1250	70
Hillslope thickness	z	24	3
Shear stress	τ	175.25	n/a
Unit weight of soil	γ	19.6	19.6
Unit weight of water	γ_w	9.81	9.81

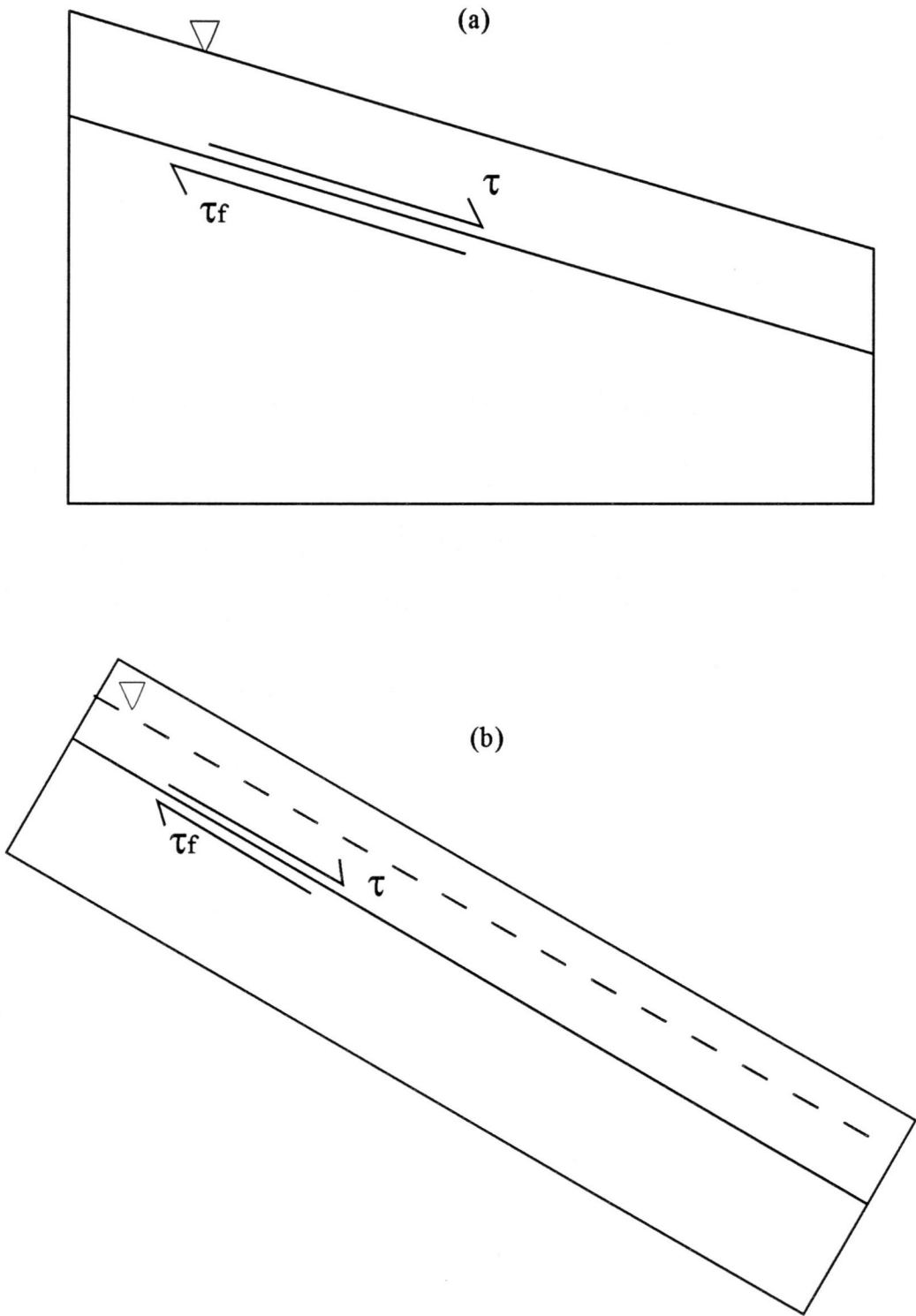


Figure 27. Boundary value problem used in the Factor of safety analysis. (a) The C3 hillslope simulated by NUM5. (b) Portion of C3 hillslope simulated with VS2DT.

Table 10. Summary of the FS input data used in a sensitivity study to assess the sensitivity of (a) Pore pressure development and (b) Factor of safety to the hydraulic conductivity contrast along the failure plane. The K_s value representing the compacted soil beneath the road was 1.0×10^{-7} m/s in the NUM5 simulations.

(a)

Case	WS3 Hillslope	Layer	K_s (m/s)
Case 1	Roadcut	K3	1×10^{-6}
Case 2	Heterogeneous	K3	1×10^{-6}
Case 3	Roadcut	K3	1×10^{-8}
Case 4	Heterogeneous	K3	1×10^{-8}

(b)

Case	C3 Hillslope	Layer	K_s (m/s)
Case 1	Heterogeneous	K3	1×10^{-6}
Case 2	Roadcut	K3	1×10^{-8}
Case 3	Heterogeneous	K3	1×10^{-8}
Case 4	Roadcut	K3	1×10^{-6}

FS and pore pressure results. The sensitivity analysis quantifies the error associated with the uncertainty in the estimates of hydraulic conductivity for the different soils found in WS3 and C3. The conductivity values that were gathered in the field for this study have a high level of confidence associated with them and so the impact associated with altering them was not assessed in this study.

VS2DT

The BVP used for the FS analysis performed for this portion of the study is shown in Figure 27 (b). The water table height varied throughout each storm event and was calculated as a function of the VS2DT output. Cases 1-6 shown in Table 8 act as a sensitivity analysis for this portion of the FS analysis. The purpose was to use each of the cases as an index to identify the conditions for which the C3 hillslope would be prone to failure. The pore pressure distribution and the resultant FS was calculated for each case study.

CHAPTER THREE: RESULTS

FIELDWORK

The site-specific parameters that were estimated during the fieldwork done at C3 and that were used in the NUM5 simulations were the soil depth, the hydraulic conductivity (K_s) of the soil, and the topography. The VS2DT input required C3 field data for K_s , soil moisture, soil depth, soil characteristic curves, and the topography.

NUM5

Soil depth

The soils data used as input for the NUM5 simulations (i) was gleaned from a literature survey of the HJA (see Chapter One) and (ii) the soil depth survey performed at C3. The soil types that dominate the WS3 catchment are listed in Table 11. The dominant soil types at WS3 are Budworm, Limberlost, and Andesite colluvium. The majority of the C3 hillslope contains the Budworm soil, which is characterized as a dark brown shotty loam. Figure 28 summarizes the results of the C3 soil depth analysis. On the ridges, where soils are very shallow (~ 1.0m) with a high stone content, the saprolite layer lies close to the surface. Obviously, erosional processes move sediment from higher elevations to lower elevations. As a result, the soil depth is greater in the C3 convergent hollow than it is on the left and right boundary ridges throughout the entire length of the hillslope. The soil depth also increases down the C3 hillslope from the ridge to the road. Subjected to the right hydrologic conditions (see Chapter One) the thickening of the colluvium layer in the convergent hollow could be a potential debris flow hazard.

Saturated Hydraulic Conductivity

The saturated hydraulic conductivity values used in this study as input for the NUM5 simulations were a result of both fieldwork and a literature search. Table 12 summarizes the saturated hydraulic conductivity data characterizing the layered system used to model the C3 hillslope soil profile and geologic layers. A Guelf permeameter (GP) (Erlick and Reynolds, 1992) was used to measure the saturated hydraulic conductivity (K_s) for the top meter of soil at the C3 hillslope (see Figure 13 for measurement locations). Based on the results from 35 near-surface measurements (see

Table 11. Description of the soil types that dominate WS3 (from Hawk and Dyrness, 1969).

Soil Type	Description	Stone Content (%)	Depth to bedrock (m)	K_s (m/s)
Limberlost	Dark brown fine granular loam	35-50	1.2	$10^{-2} - 10^{-7}$
Budworm	Dark brown silty/shotty loam with a well-developed profile	< 30	0.9-1.2	$10^{-2} - 10^{-8}$
Andesite Colluvium	Loam/sandy loam with fine to medium grains and shotty concretions	25-80	0.5-0.6	$10^{-1} - 10^{-6}$

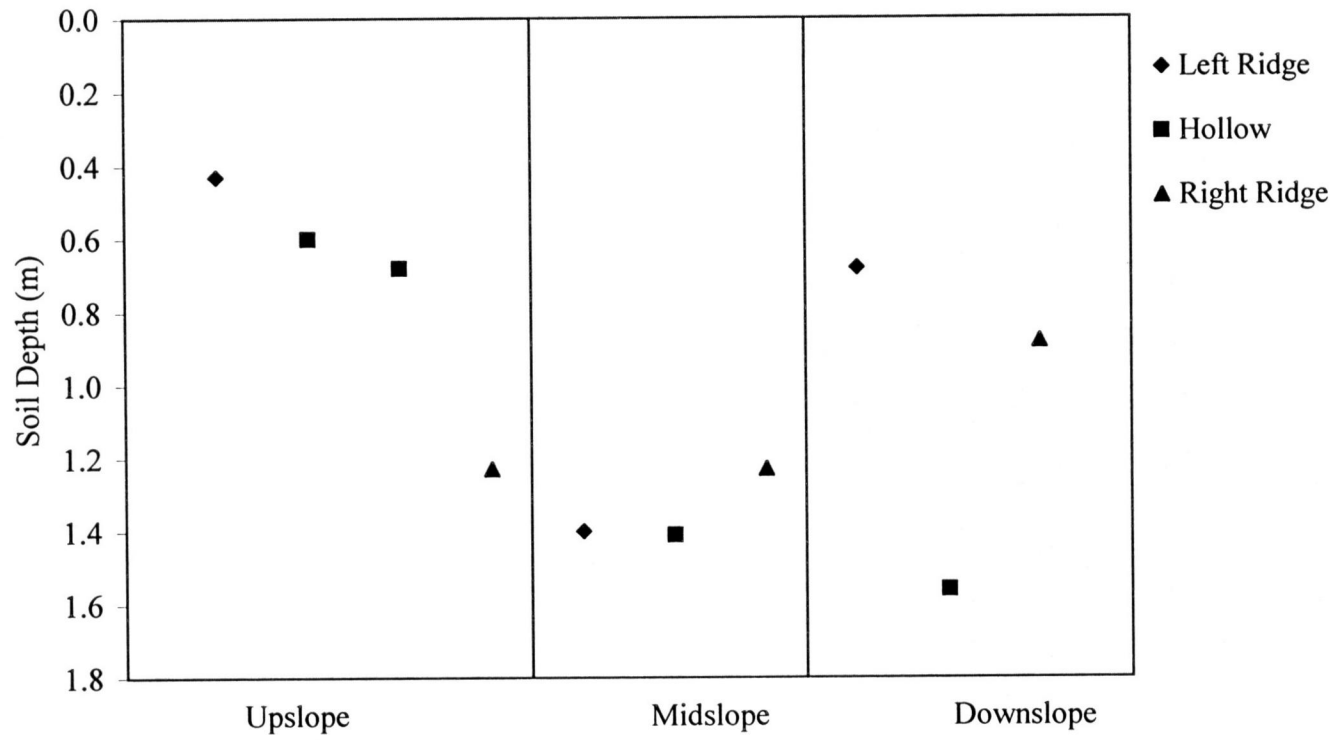


Figure 28. Soil depths measured at C3 using a soil drive probe. See Figure 12 for measurement locations.

Table 12. Saturated hydraulic conductivity values that represent the different geologic layers in the NUM5 simulations.

Soil depth (m)	Model depth (m)	Soil hroizon and geologic layers	K ¹ (m/s)	Number of measurements	Reference
<1	<3	A	1.0x10⁻²	36	Fieldwork ²
			1.0x10 ⁻³	2	Haar(1979)
<3	<6	B	7.0x10⁻⁴	12	Fieldwork
			5.7x10 ⁻⁵	2	Haar(1979)
	<20	Fractured rock	1.0x10⁻⁶	n/a	Freeze and Cherry (1979)
	>20	Unfractured rock	1.0x10⁻¹¹	n/a	Freeze and Cherry (1979)
		Road	1.0x10⁻⁸	n/a	Freeze and Cherry (1979)
			6.7x10 ⁻⁷	n/a	Ziegler et al. (1997)
			1.0x10 ⁻⁸	2	Loague et al.(1997)
		6.7x10 ⁻⁷	6	Ziegler et al. (1995)	

¹ Values in bold were used in this study.

² Fieldwork conducted for this study.

Table 13), a mean K_s value of 0.01 m/s was used to represent the hydraulic properties of the upper soil layer (or A horizon).

To estimate the hydraulic conductivity of the saturated subsurface a series of twelve slug tests were conducted at six piezometers across the C3 and WS3 catchments (see Figure 2 for catchment locations within WS3). The K_s values for the saturated zone (measured at each piezometer) are shown in Table 14. The mean K_s value determined by the slug tests was estimated to be 7.0×10^{-4} m/s. The near-surface and subsurface K_s values estimated from the field experiments in this study are an order of magnitude higher than those found by Harr (1979) for a higher elevation watershed within the HJA. Given that the K_s value of a single material can range over four to five orders of magnitude, a single order of magnitude discrepancy in results was considered to be a close enough match to confirm the accuracy of the measurement techniques used in this study. The K_s values for the fractured bedrock, the bedrock, and the road were estimated for this study from the literature and have a level of uncertainty associated with them that will be addressed later.

VS2DT

Saturated Hydraulic Conductivity

Surface and near-surface

In this study, the C3 catchment is assumed to have uniform surface saturated hydraulic conductivity. The surface infiltration rates for the C3 soils, as measured using the Pressure Infiltrometer (PI), exhibit little variability across the catchment. As seen in Figure 29a, except for a few anonymously high values, the variation of the K_s values over the catchment does not indicate the presence of any spatial trend or any significant disparity between the conductivity values measured on the ridges versus those measured in the hollow. Most infiltration rates were clustered near the mean value of 9.4×10^{-2} m/s, which is effectively the saturated hydraulic conductivity of the surface soils.

As seen in Figure 29b, the K_s value of the top meter of soil, measured using the Guelph permeameter (GP), shows a distinct trend from lower conductivity values measured near the road to higher conductivity values measured towards the top of the ridge. This relationship is correlated to the trend in soil depth from the road to the ridge

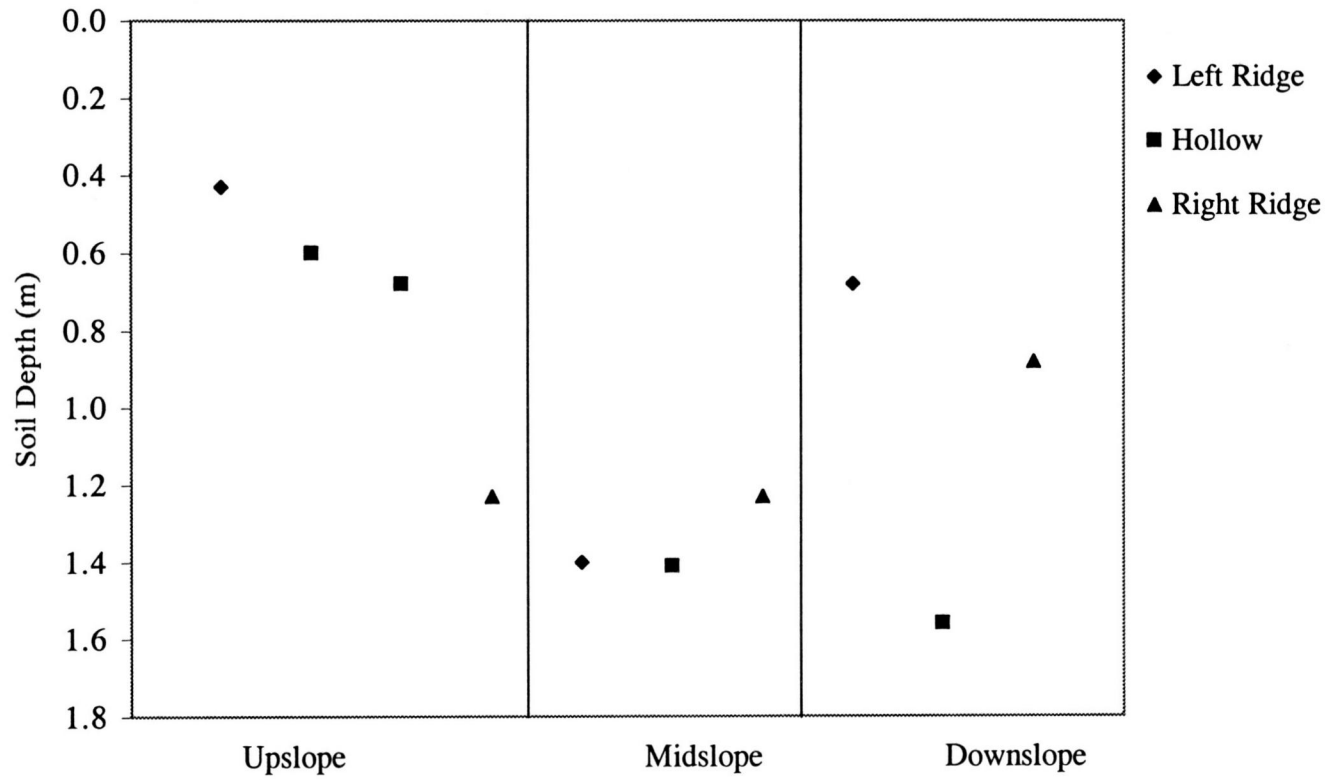


Figure 28. Soil depths measured at C3 using a soil drive probe. See Figure 12 for measurement locations.

Table 14. Saturated hydraulic conductivity (K_s) values estimated using slug tests. The mean value for the C3 hillslope was 7.0×10^{-4} m/s. See Figure 14 for the piezometer locations.

Piezometer	K_s (m/s)
3P4	5.62×10^{-4}
4P1	8.39×10^{-5}
4P2	9.85×10^{-5}
4P3	4.68×10^{-4}
4P4	4.55×10^{-4}
4P1	7.97×10^{-5}
4P2	3.74×10^{-3}
4P3	5.76×10^{-4}
4P4	1.68×10^{-4}

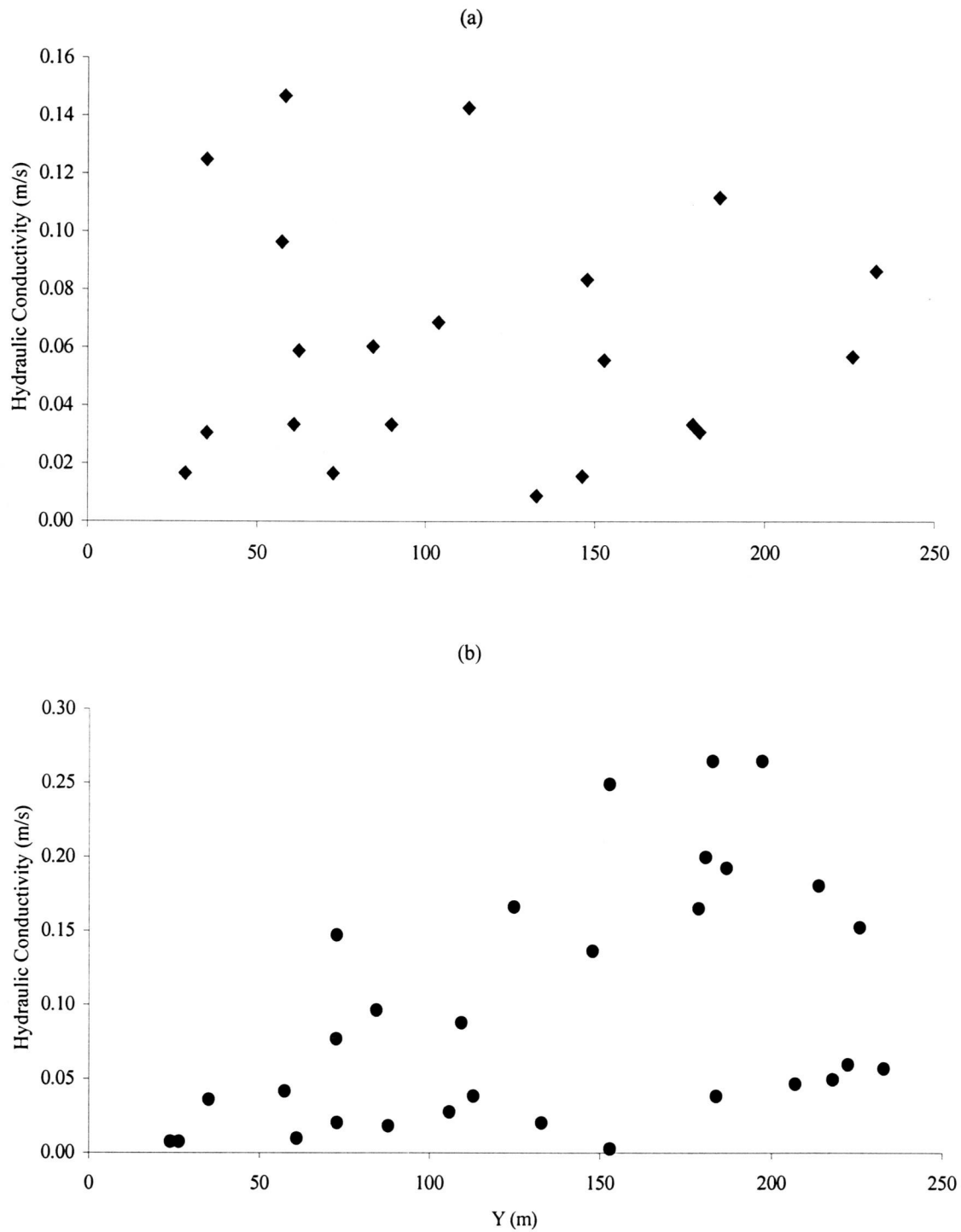


Figure 29. The C3 saturated hydraulic conductivity values. (a) Surface soils as measured with a Pressure Infiltrometer. (b) The top meter of soil as measured using a Guelph Permeameter. See Figure 13 for measurement locations.

(see Figure 28). On the ridge where the saprolite and impermeable bedrock layers are much closer to the surface, soils are very shallow, have a high stone content, and are extremely permeable. In the convergent hollow, and farther downslope in the catchment, the soils are much deeper. While in the hollow the soils can retain higher soil moisture which can in turn increase the hydraulic conductivity, through the process of erosion and soil creep, fine grain soil particles are transported downslope and fill the empty pore spaces between larger grains or aggregates (Loague, personal communication, 1999). This erosion effectively decreases the permeability of the soils in the downslope portion of C3 and locally reduces the value of K_s . Based on the GP results, the spatial distribution K_s is sufficiently complex to require the use of geostatistics to estimate the spatial distribution of the hydraulic conductivity between measurement points.

Figure 30 was generated using a Kriging routine (i.e. a least squares estimation procedure) in GSLIB (Deutsch and Journel, 1992) that determines the distribution of the K_s values over the C3 catchment. The map shows zones of high conductivity in the upper part of the catchment and zones of lower conductivity towards the bottom. This result makes physical sense because, through erosive processes, material is moved from the ridges into the convergent hollow and the downslope of the catchment. This map honors the data, but there is a smoothing effect that is inherent to Kriging. The majority of the map, especially in the areas that were not densely sampled, is green (i.e., the color that represents the mean conductivity value observed at the C3 site). Recall that many of these green areas are outside of the area of interest for this site and are therefore not of importance.

To eliminate the effects of data smoothing that dominate the Kriged results, the geostatistical method of sequential simulation was used study to create alternative, equally probable realizations of the spatial distribution of K_s within C3. Conditional Sequential Gaussian Simulation (Deutsch and Journel, 1992) uses the simple Kriging system to estimate the value of K_s at each point in the grid. The estimated value of K_s at each point is conditioned by surrounding data and the neighboring K_s values that have already been estimated. This point then is added to the hypothetical data set and is used to condition further points in the grid. Figure 31 shows the result of non-Gaussian geostatistical realization of the spatial distribution of K_s based upon the 35 GP

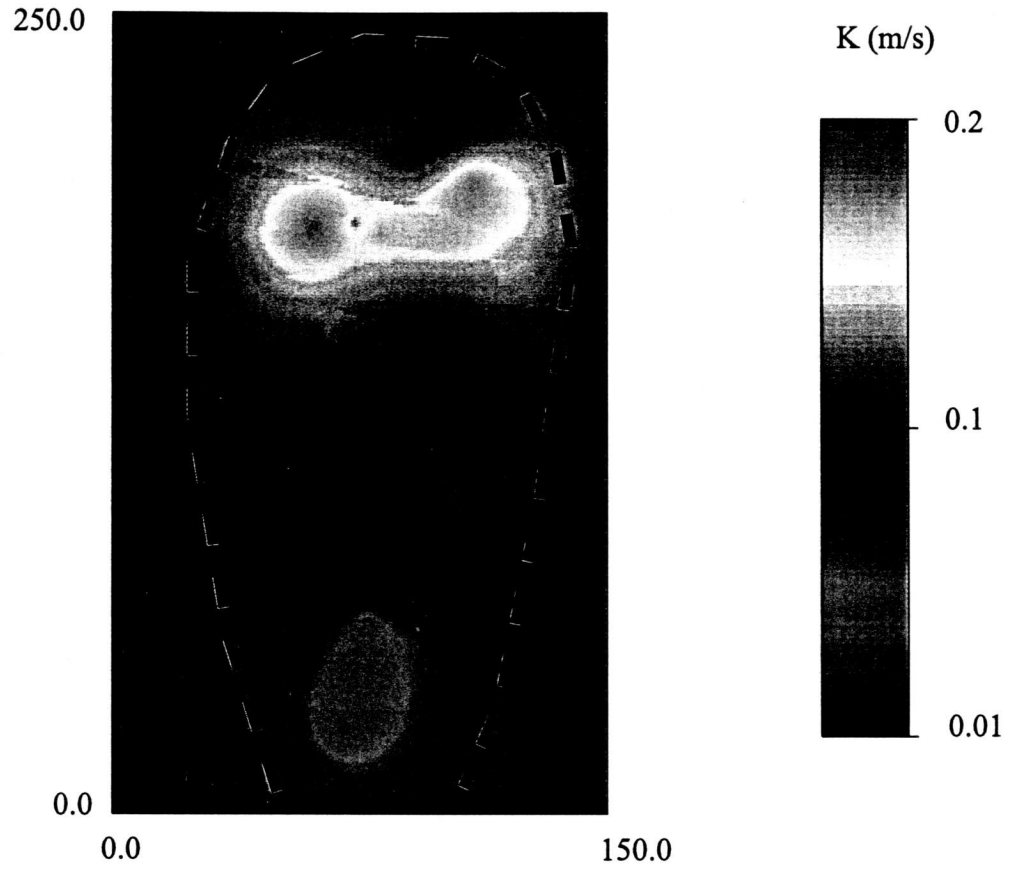


Figure 30. The kriged map of the spatial variation in the hydraulic conductivity values over the C3 hillslope.

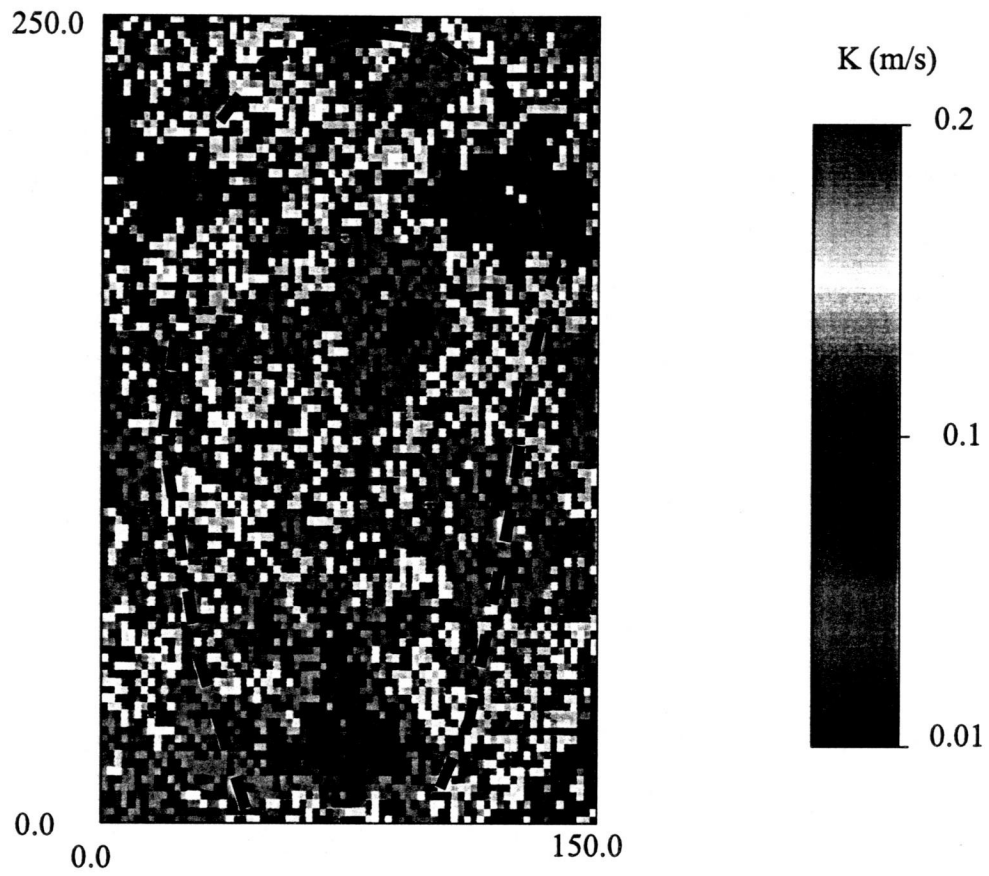


Figure 31. A geostatistical realization of the spatial variation in the hydraulic conductivity values over the C3 hillslope

measurements made across C3 (see Figure 13 for measurement locations) and using GSLIB. In all realizations, the fields were dominated by red and blue, the colors corresponding to high and low conductivities, respectively. As expected, more spatial variability is reflected in these maps than in the Kriged map.

The results from both the Kriged map and the probability map honor the data and the geomorphology of the catchment. According to the data and the resulting geostatistical realizations, the portion of the C3 hillslope modeled in the VS2DT simulations had K_s values that were within the same order of magnitude. Therefore, it was reasonable to represent the near-surface soil hydraulic conductivity as a single value.

Saturated sub-surface

The water table at C3, as measured by the water level in the piezometers, lies approximately two meters below the surface in the convergent axis of the hollow. Any saturated zone that might occur on the C3 boundary ridges is transient or perched above the impermeable bedrock. The value used to estimate the K_s for the subsurface soil layer resulted from a series of twelve slug tests performed in this study (see Figure 14 for measurement locations). Figure 32 shows the results from the slug tests that employed the Hvorslev (1951) method. The mean value of the saturated hydraulic conductivity was estimated to be 7.0×10^{-4} m/s (see Table 14).

Soil-water Content

The estimate for the soil-water content initial conditions throughout C3 are based on the values measured with a TRASE TDR (see Chapter One). As shown in Figure 33, the soil-water content does not follow any noticeable spatial trend throughout the catchment. The average soil-water content does increase with depth, but the variation in soil-water content with measurement depth or location across the C3 hillslope was not significantly different to consider in the initial model testing or subsequent simulations. For the purposes of this study, uniform initial conditions were assumed to exist throughout the catchment and the unsaturated-saturated soil profile.

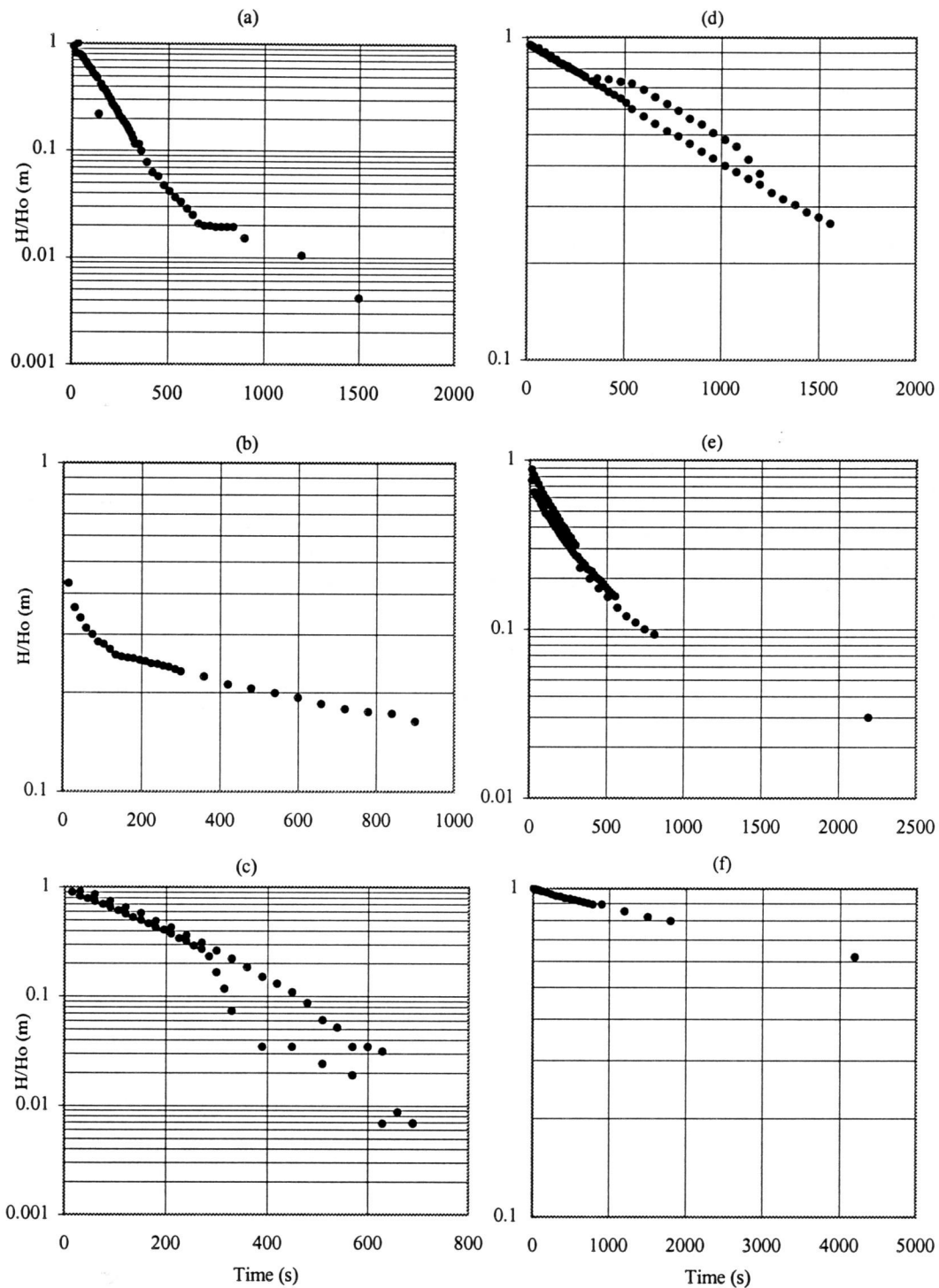


Figure 32. Falling head slug test results for saturated hydraulic conductivity in the saturated zone at five locations. H_0 is the maximum level above the pretest level to which the water level rises after the slug is inserted and H is the water level recorded at subsequent times during the measurement period. The locations are shown on Figure 14. (a) 3P4. (b) 4P2. (c) 4P4. (d) 4P1. (e) 4P3. (f) 3P10.

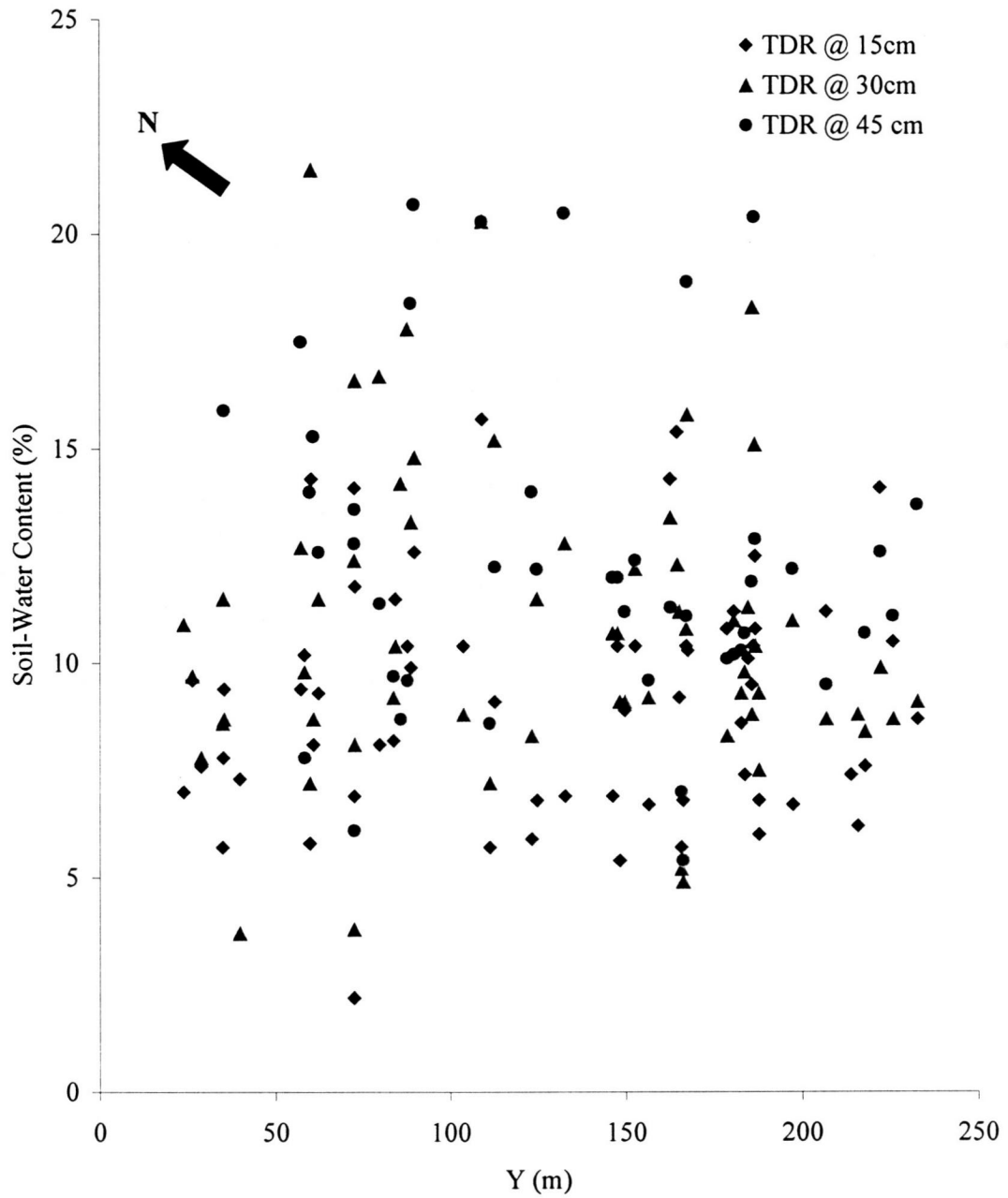


Figure 33. Plan View of the TDR measurements taken at three different depths over C3. The location of the measurement sites is shown on Figure 13.

Characteristic Curves

The $K(\psi)$, $K(\theta)$, and $\theta(\psi)$ characteristic curves describe the hysteretic relationship between soil-water content, tension, and hydraulic conductivity. Based on the timed experiments conducted at C3, a $\theta(\psi)$ characteristic curve was estimated. Figure 34 compares the characteristic curve generated from the work at C3 to the curves characterizing the soil at the Coos Bay (CB) catchment discussed earlier. In general the C3 characteristic curve is not as steep as those measured at CB, implying that while it does have similar hydraulic properties, the soil at C3 is less sandy than the CB soil. Figure 35a shows the six characteristic curves for the CB soils compressed into a single average characteristic curve for the CB soils. The CB wetting curve is compared to the average characteristic curve for C3 in Figure 35b. The CB soil has a steeper slope than the C3 soil, but they reach the same asymptote as they dry. This implies that under unsaturated conditions and at beginning of rainfall events the two catchments might have a similar near-surface hydrologic response.

The points along the averaged soil-water characteristic curve generated for C3 were used to estimate the characteristic curve for the hydraulic conductivity of the unsaturated zone. The Van Genuchten (1980) approach was used to estimate the $K(\psi)$ relationship for the C3 data. The resulting $K(\psi)$ curve is shown in Figure 36. The relationship shown in Figure 36 demonstrates, as expected, that the hydraulic conductivity in the unsaturated zone increases as the soil becomes more saturated. Tension is due to the affinity between water and the soil matrix. When the soil is saturated, all of the pores are water-filled and conducting, while under unsaturated conditions, flow is relegated to the smaller pores, as well as to being held under tension. Thus, desaturation leads to increased tortuosity for soil-water movement.

NUMERICAL MODELING RESULTS

NUM5

The NUM5 simulations conducted for this study represent the hydrologic profile of a vertical slice down the convergent axis of WS3 and the C3 hillslope from the ridgetop to below the road. The effect of a road on the hillslope hydrology in each of these settings (i.e. the regional flow system and the local flow system) was analyzed for

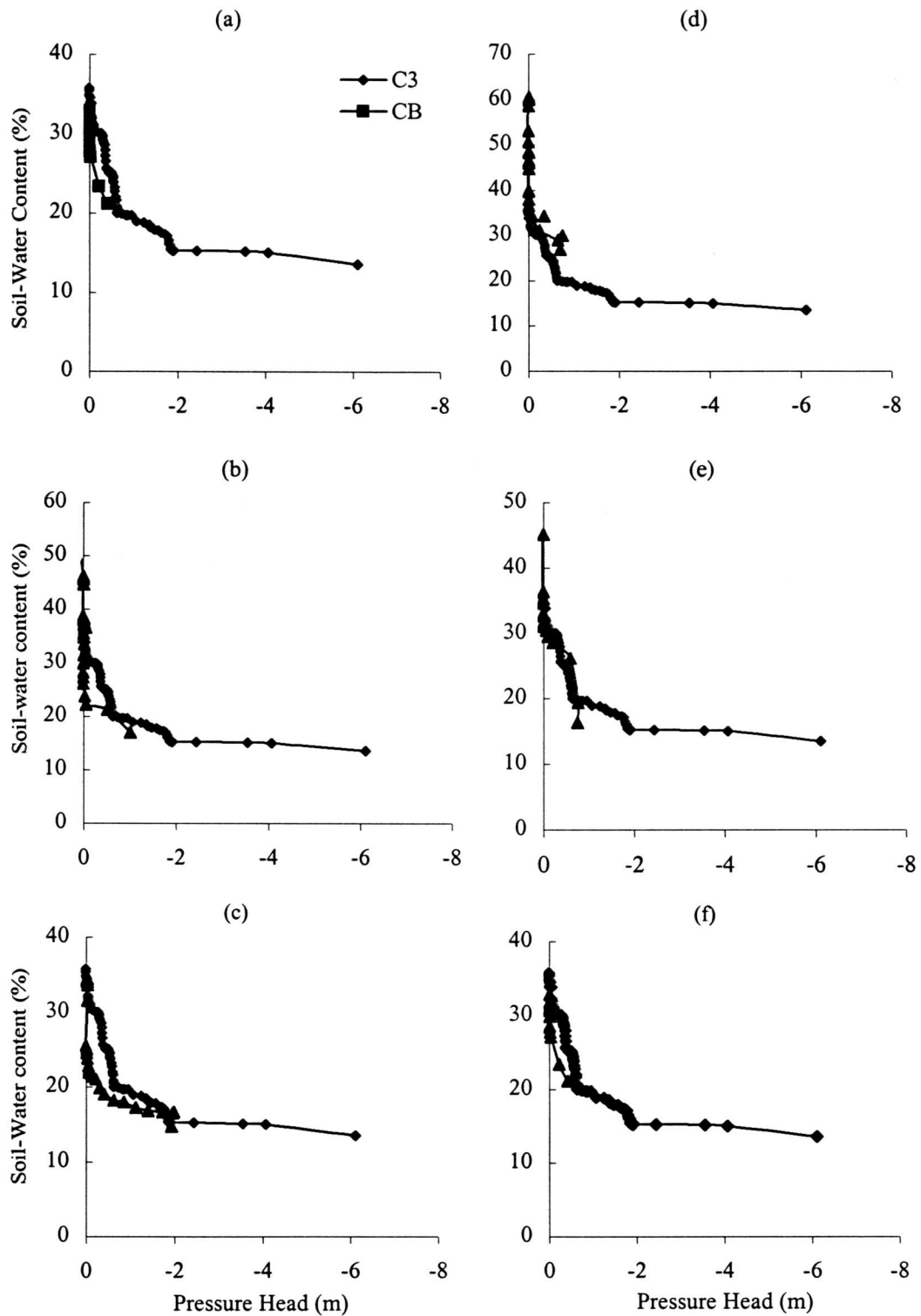


Figure 34. Comparison of the C3 characteristic curve of soil-water retention to the six curves for Coos Bay. (a) CB site 1. (b) CB site 2. (c) CB site 3. (d) CB site 4. (e) CB site 5. (f) CB site 6. The location of the CB sites are given by Torres et al. (1998).

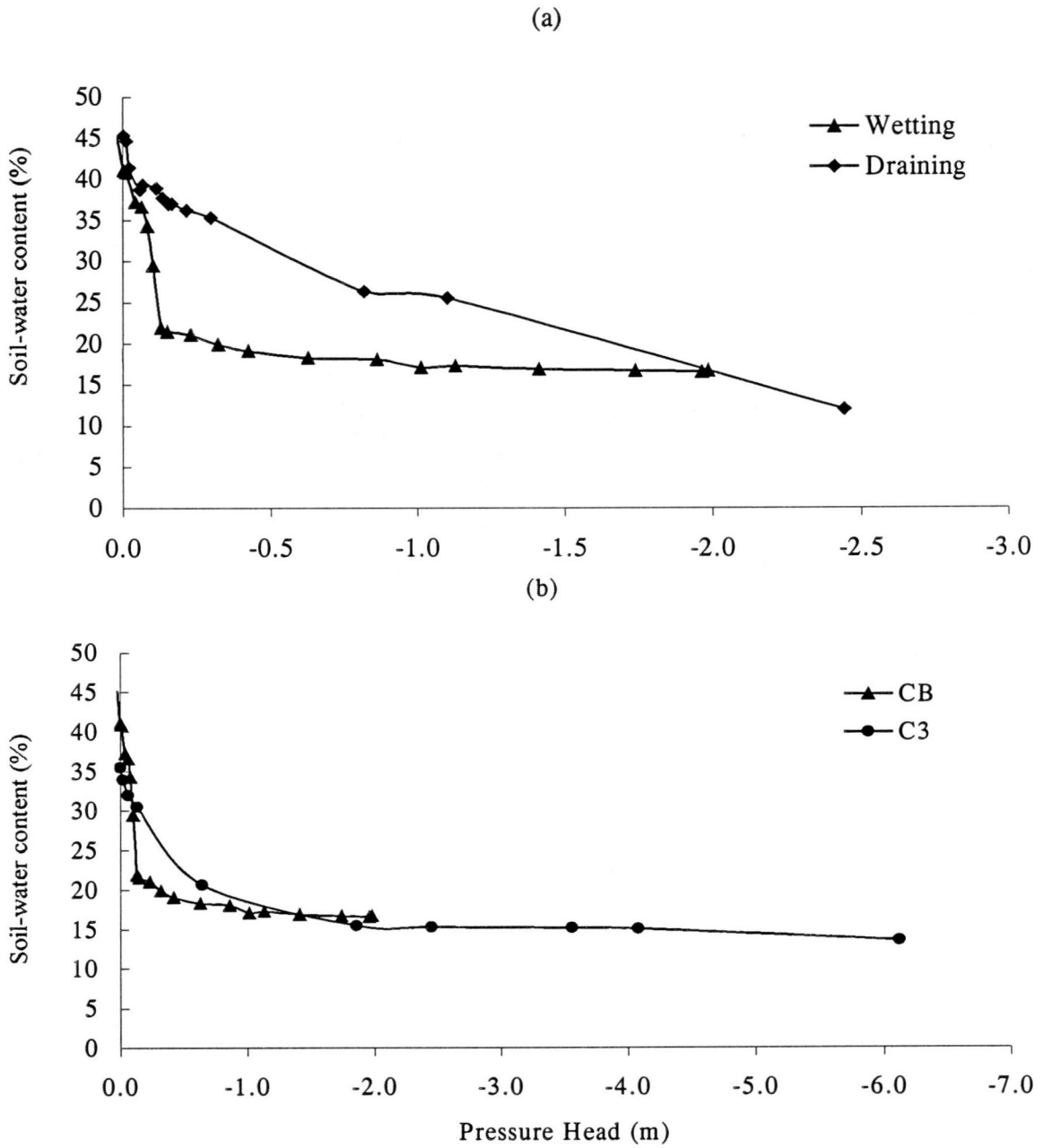


Figure 35. (a) Average characteristic curve of soil-water retention at six Coos Bay (CB) sites, both wetting and drying. See Figure 34 for the original curves. (b) Comparison of characteristic curve of soil-water retention for C3 and the average characteristic curve for CB (wetting).

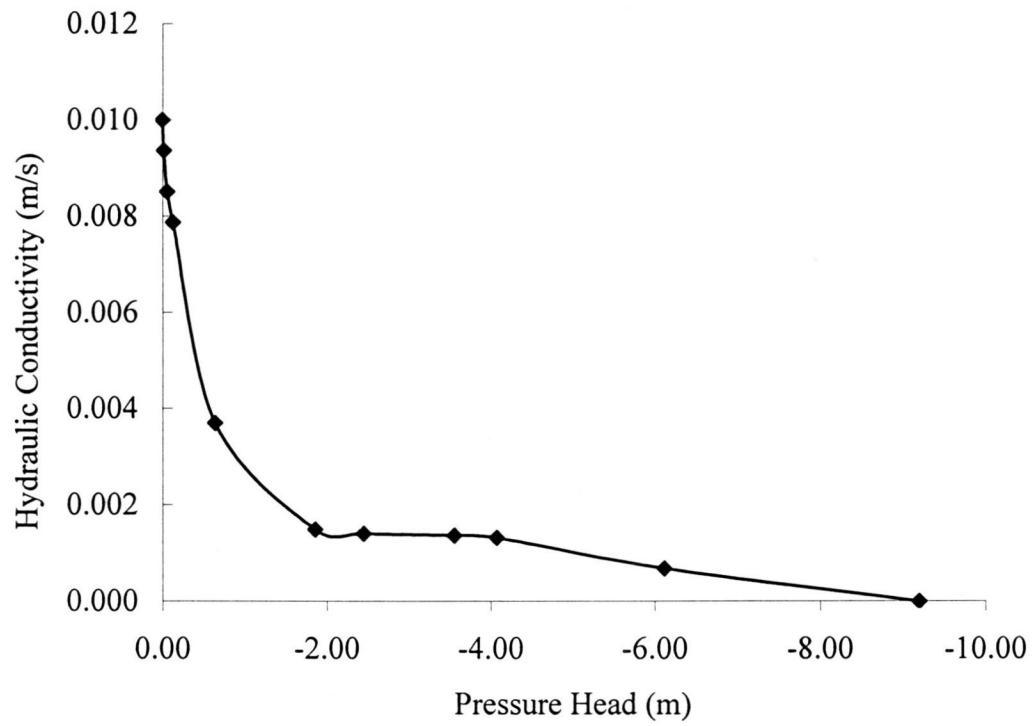


Figure 36. Characteristic curve of hydraulic conductivity as a function of pressure head based upon the Van Genuchten (1980) approach.

the WS3 and C3 systems by comparing simulations that included a roadcut against those without a road. The results from the NUM5 simulations can be summarized as follows:

- Contrasts in hydraulic conductivity result in changes in subsurface flow fields and hydraulic head distributions that significantly differ from the homogeneous case simulations.
 - Groundwater preferentially flows through the high conductivity soils above the bedrock contact.
 - In the near-surface layer (constituting a high conductivity material), groundwater flow is dominantly parallel to the surface slope.
 - The conductivity contrast caused by the compacted soil beneath the road directs flow out across the roadcut face.
- The saturated hydraulic conductivity contrast between the layers dominates the changes in the pore pressure distribution throughout the system.
 - The roadcut acts to increase the pore pressure in the area above the road and to decrease the pore pressures downslope of the road.
 - Pore pressures build up in areas where flow is impeded by a low conductivity layer.

WS3

Hydraulic Head

Figure 37a shows the standard Toth (1963) regional flow result with recharge in the upslope region and discharge in the downslope region of a system defined by impermeable boundaries. When the homogeneous hillslope was saturated to the ground surface (and subject to steady-state, gravity driven groundwater flow), the impact of adding a road, as seen in Figure 37c, had a negligible effect on the hydraulic head distribution relative to the homogeneous case. This result indicates that, when simulated at a large scale in a saturated homogenous system, very small-scale changes in topography have little to no influence on the regional scale flow regime.

Figure 37b, in comparison to Figure 37a, shows the effect that layers of different saturated hydraulic conductivity have on the hydraulic head distribution. The equipotential lines are nearly vertical in the area of higher conductivity and there is a

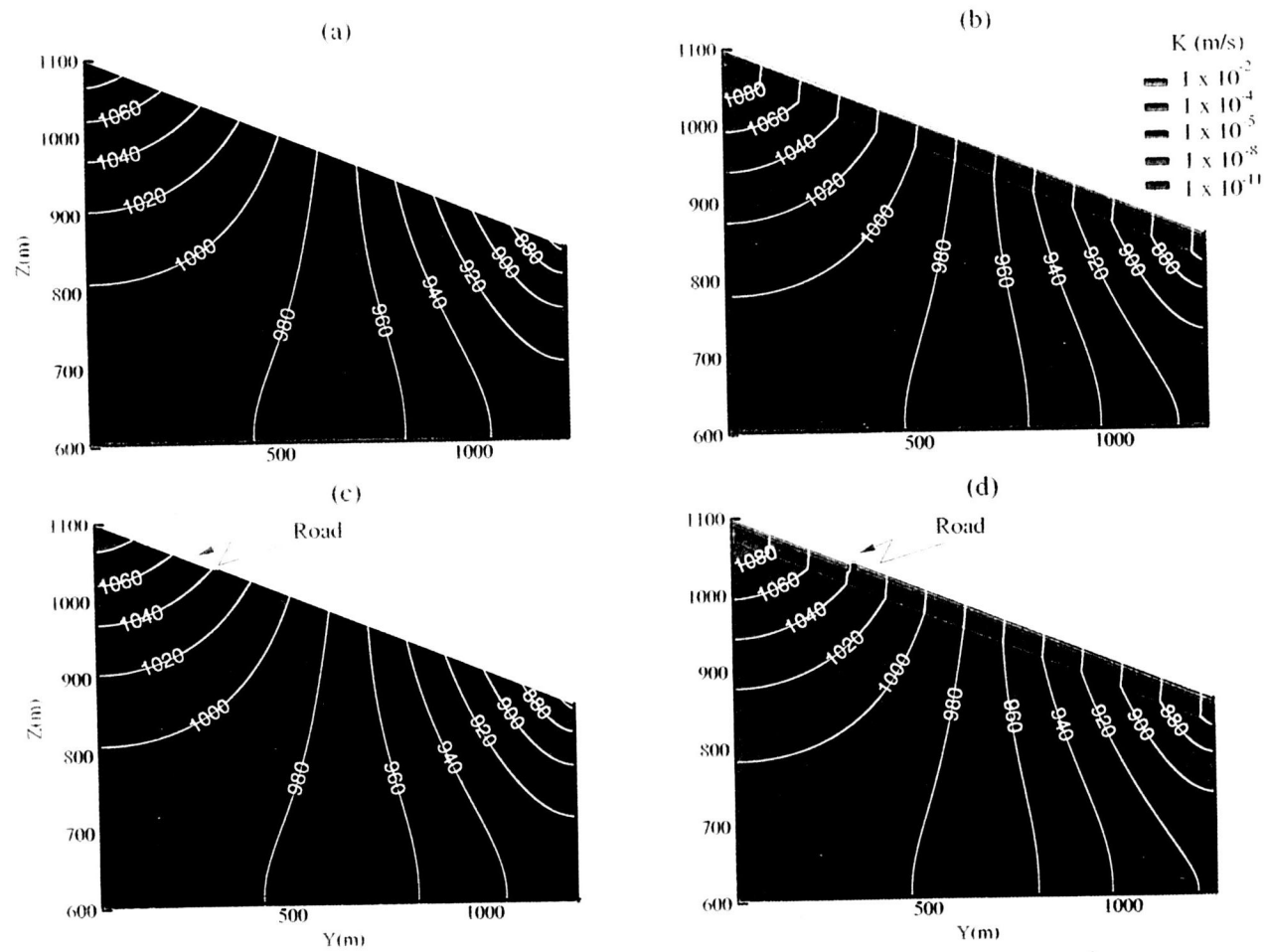


Figure 37. WS3 hydraulic head distribution as estimated from the NUM5 simulations. (a) Homogeneous. (b) Heterogeneous. (c) Homogeneous with road. (d) Heterogeneous with road.

dramatic change in their direction at the bedrock contact. The fact that there is very little differentiation between the higher saturated hydraulic conductivity layers suggests that it is the relative magnitude of the saturated hydraulic conductivity contrast that effects the groundwater flow field, not the actual hydraulic conductivity values. Figure 37d shows that the addition of the road causes a head change only in the area immediately adjacent to the impermeable road. Because the effect of adding the road is not dramatic relative to the regional flow system, the boundary value problem for VS2DT need only incorporate the region of flow directly adjacent to the road.

Flow Paths

Flowlines represent the path a particle of water follows as it flows through a given system. The WS3 system is defined by the hillslope geometry (including the road), the saturated hydraulic conductivity distribution, and the resultant hydraulic head distribution. Figure 38 compares flowlines drawn from the same origin for each of the simulated hillslopes. The flow paths in different parts of Figure 38 change depending on the boundary conditions and heterogeneity. The results in Figure 38(a-d) clearly illustrate the importance of shallow groundwater flow that is "perched" as a transient water table above the impermeable bedrock in WS3. These results also demonstrate how the subsurface flow can become surface flow when the topography lends itself to the formation of a seepage face.

Figure 38a shows the base case (i.e. homogeneous) regional flow system. In comparison, Figure 38c shows how the addition of a road impacts the regional flow. Flow is diverted further downslope than in the homogeneous case. In Figure 38b there is a dramatic alteration in the flow system due to the hydraulic conductivity contrast. Flow is confined to the high conductivity layers and flows along the low conductivity (i.e. bedrock) contact that roughly parallels the ground surface. Another dramatic change in this heterogeneous flow system is caused by the introduction of the road cut as seen in Figure 38d. A seepage face is created along the road cut bank, and all of the intercepted water will potentially flow onto the road (or in a real system be diverted through a ditch or culvert). Below the road cut, water continues to infiltrate and move as subsurface flow along the conductivity contrast between the bedrock and overlying high conductivity

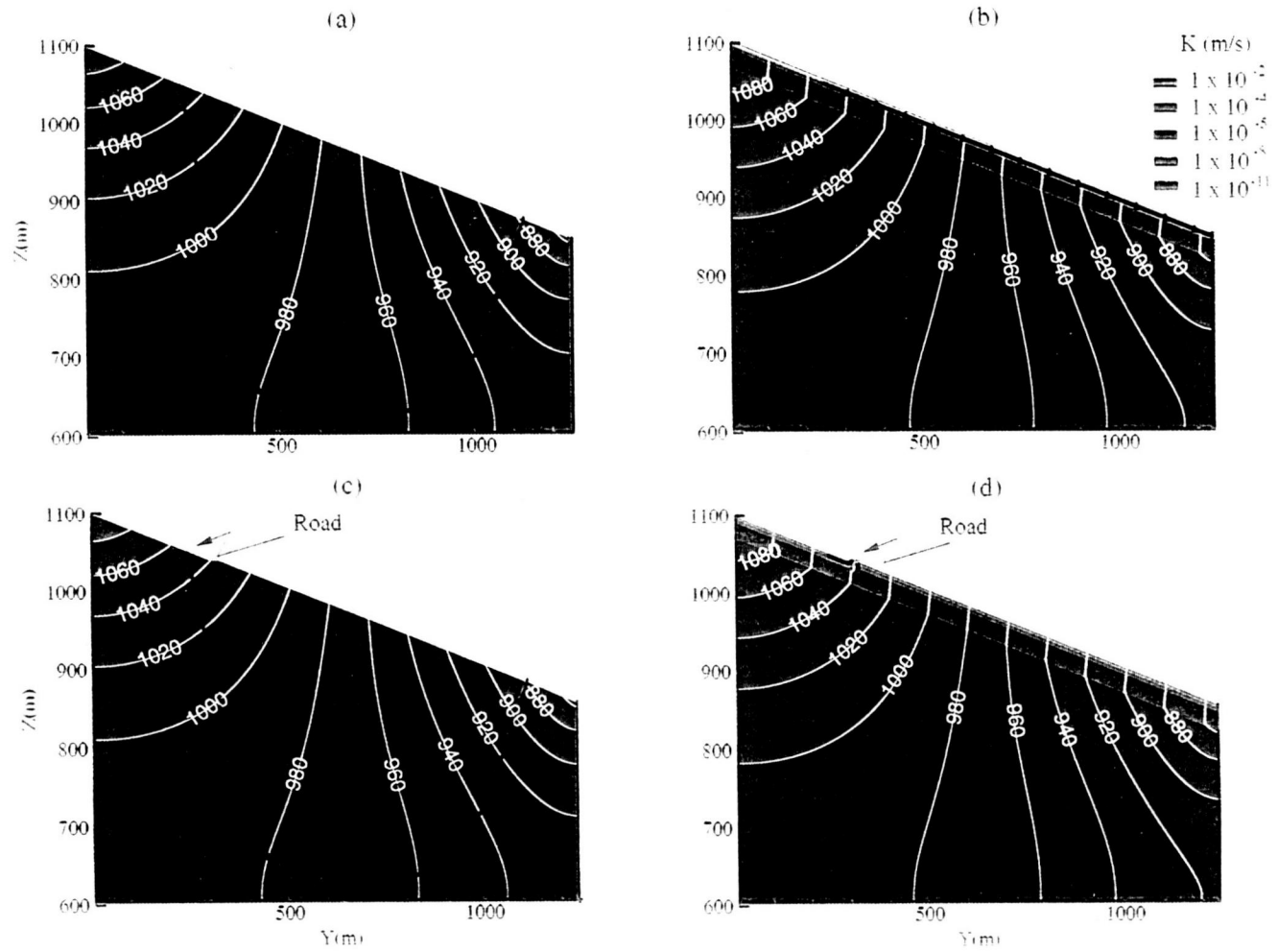


Figure 38. WS3 flowlines estimated from the NUM5 simulations. (a) Homogeneous. (b) Heterogeneous. (c) Homogeneous with road. (d) Heterogeneous with road.

layers. In regions of lower saturated hydraulic conductivity (at depth below the surface layers) the flow system remains unchanged relative to the flow systems simulated for the homogeneous slope.

Pressure Distribution

The impact of the road and the hillslope heterogeneity can also be assessed by the changes in the pore pressure distributions for the different cases simulated by NUM5 and shown in Figure 39. The homogeneous base case is shown in Figure 39a. Due to the weight of the soil and water the high-pressure regions are found at the base of the hillslope. In keeping with the observations made by other workers (Reid et al., 1988; Iverson and Reid, 1992; Reid and Iverson, 1992; Iverson et al., 1997; Iverson and Major, 1986) pore pressures are expected to increase where the seepage velocities are directed outwards from the slope. The results shown in Figure 39c indicate that a road cut into a homogeneous slope amplifies the pressure values above the road. Because the flow region is greatly reduced by the impermeable bedrock layer, zones of high pressure are found much nearer to the surface in the heterogeneous cases shown in Figure 39b than they are in the homogeneous case. Figure 39d shows the influence of the road cut on the pore pressure in the heterogeneous case. The perturbation in the pressure contours that is manifested below the road indicates that the road (and the resultant conductivity contrasts) can locally increase the pressure in the region upslope of the road. This new pore pressure distribution indicates that there is an increased risk of hillslope failure in the upper reaches of the watershed, especially in the vicinity of the roadcut.

C3

Hydraulic Head Distribution

Figure 40a shows the homogenous base case result with recharge in the upslope region and discharge in the downslope region of the hillslope. Adding a road to the base case system, as seen in Figure 40c, has a negligible effect on the hydraulic head distribution. These results indicate that, when modeled at hillslope scale in a saturated homogenous system, small-scale changes in topography exhibit some influence on the flow regime. In contrast to the homogeneous base case, the presence of heterogeneity in

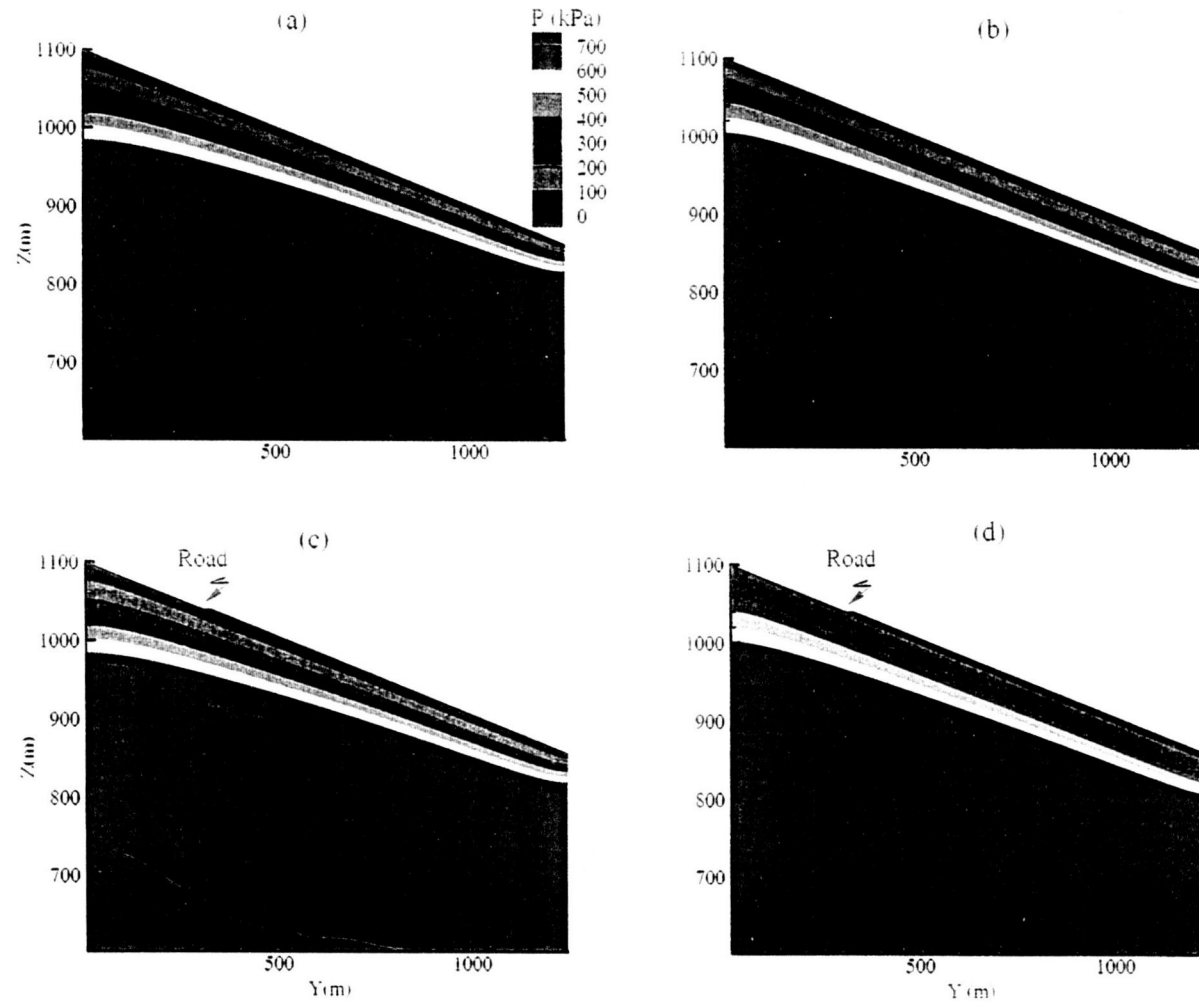


Figure 39. The WS3 pore pressure distribution as simulated using NUM5 (a) Homogeneous. (b) Heterogeneous. (c) Homogeneous with road. (d) Heterogeneous with road.

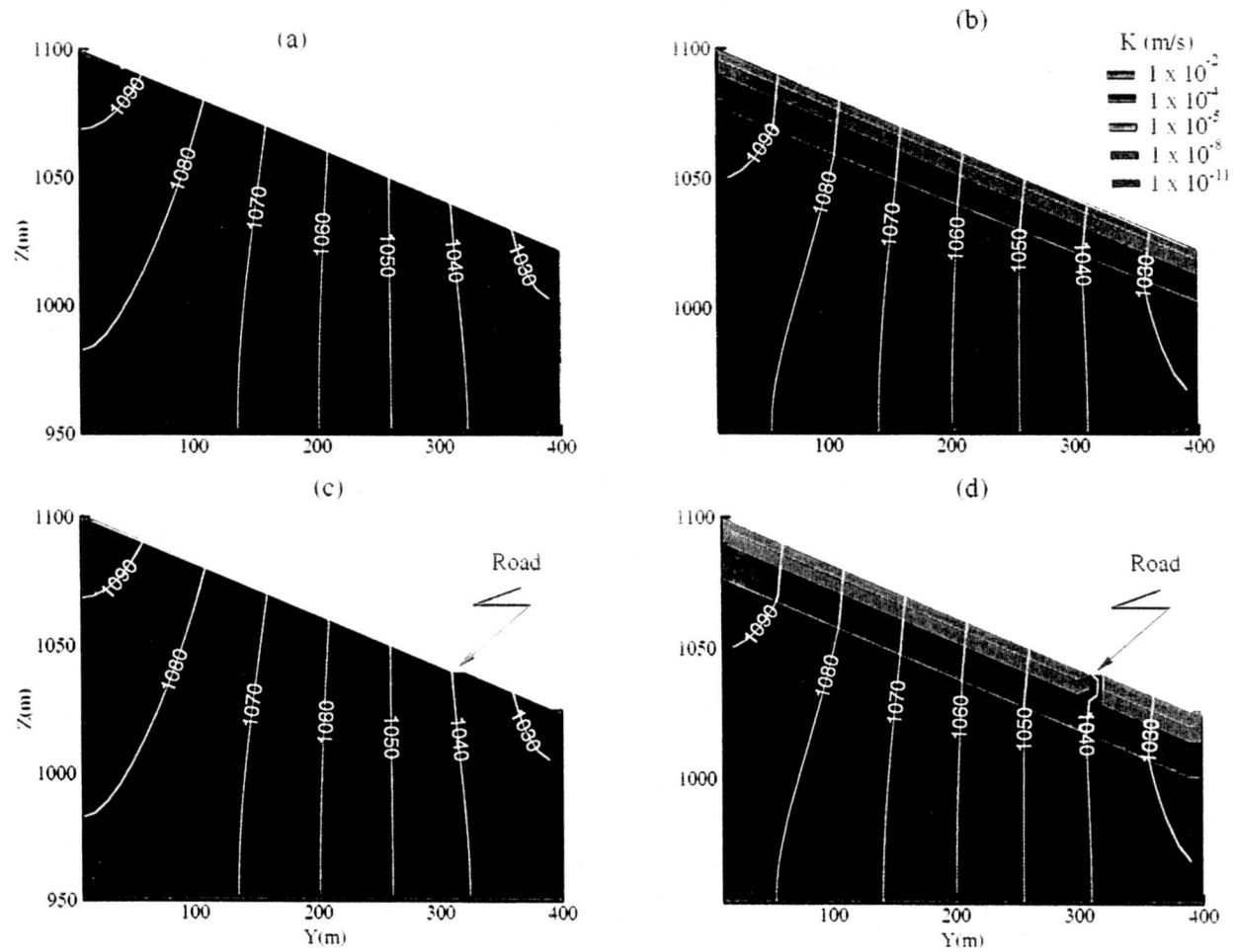


Figure 40. Hydraulic head distribution simulated for the C3 hillslope using NUM5. (a) Homogeneous. (b) Heterogeneous. (c) Homogeneous with road. (d) Heterogeneous with road.

the soil hydraulic properties (i.e. geologic layering) had a significant impact on the hydraulic head distribution. As seen in Figure 40b the hydraulic head contours change direction when they encounter the impermeable bedrock. The refraction of the equipotentials indicates that flow is concentrated in the near surface. Figure 40d shows that the impact of a road in the heterogeneous system is significant, especially in the portion of the C3 hillslope near the road. The change in the shape of the equipotential lines shows the influence of the bedrock contact and the low permeability zone beneath the road.

Flow Paths

Flow lines are defined to be perpendicular to equipotential lines and therefore a change in hydraulic head distribution necessitates a change in the groundwater flow path. The flowlines shown in Figure 41 all started from the same point within the C3 hillslope and represent how a particle of water might move through the prescribed flow system. There is no significant change in the flowlines between the base case (Figure 41a) and the homogeneous system with the addition of a roadcut (Figure 41c). However, in the heterogeneous model of the C3 hillslope, as seen in Figure 41b, flow is constrained to the high conductivity layers perched above the saprolite and bedrock. When a roadcut is introduced into the system, as seen in Figure 41d, a seepage face forms at the roadcut face and water is directed outward from the hillslope to potentially become overland flow.

Pressure Distribution

Another means to assess the impact of the road and the soil heterogeneity is based on the changes in the pore pressure distributions between the different cases. The homogeneous base case is shown in Figure 42a. Because of the increased weight of the overburden, the high-pressure regions are found at the base of the hillslope. Figure 42c shows the minimal impact on the pore pressure distribution associated with a roadcut in a homogeneous system. Relative to the base case, the heterogeneous cases shown in Figure 42b has zones of high pressure much nearer to the surface. Because the size of the flow region is greatly reduced by the impermeable bedrock layer, the pressure of the water

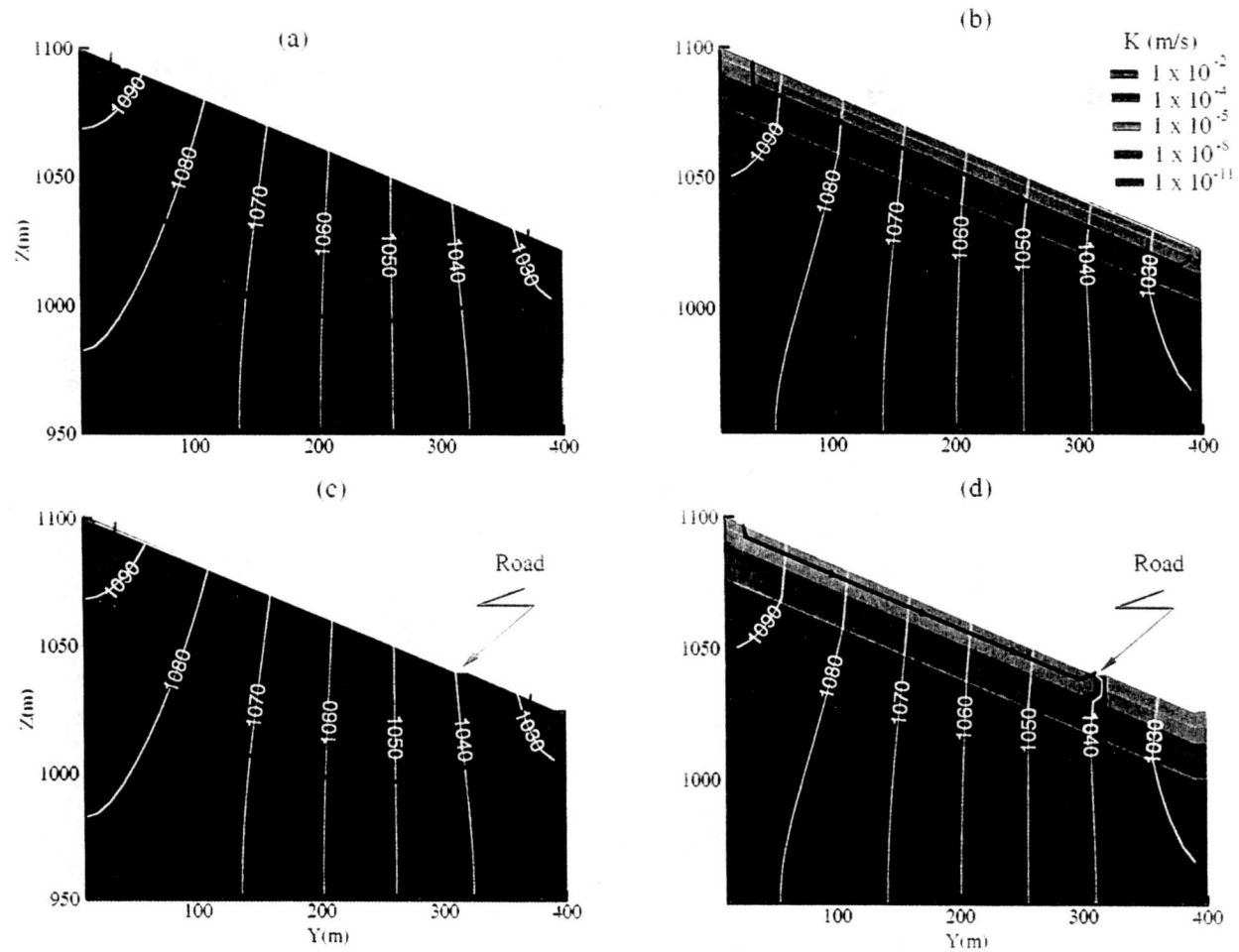


Figure 41. Flowline for the C3 hillslope as simulated by NUM5. (a) Homogeneous. (b) Heterogeneous. (c) Homogeneous with road. (d) Heterogeneous with road.

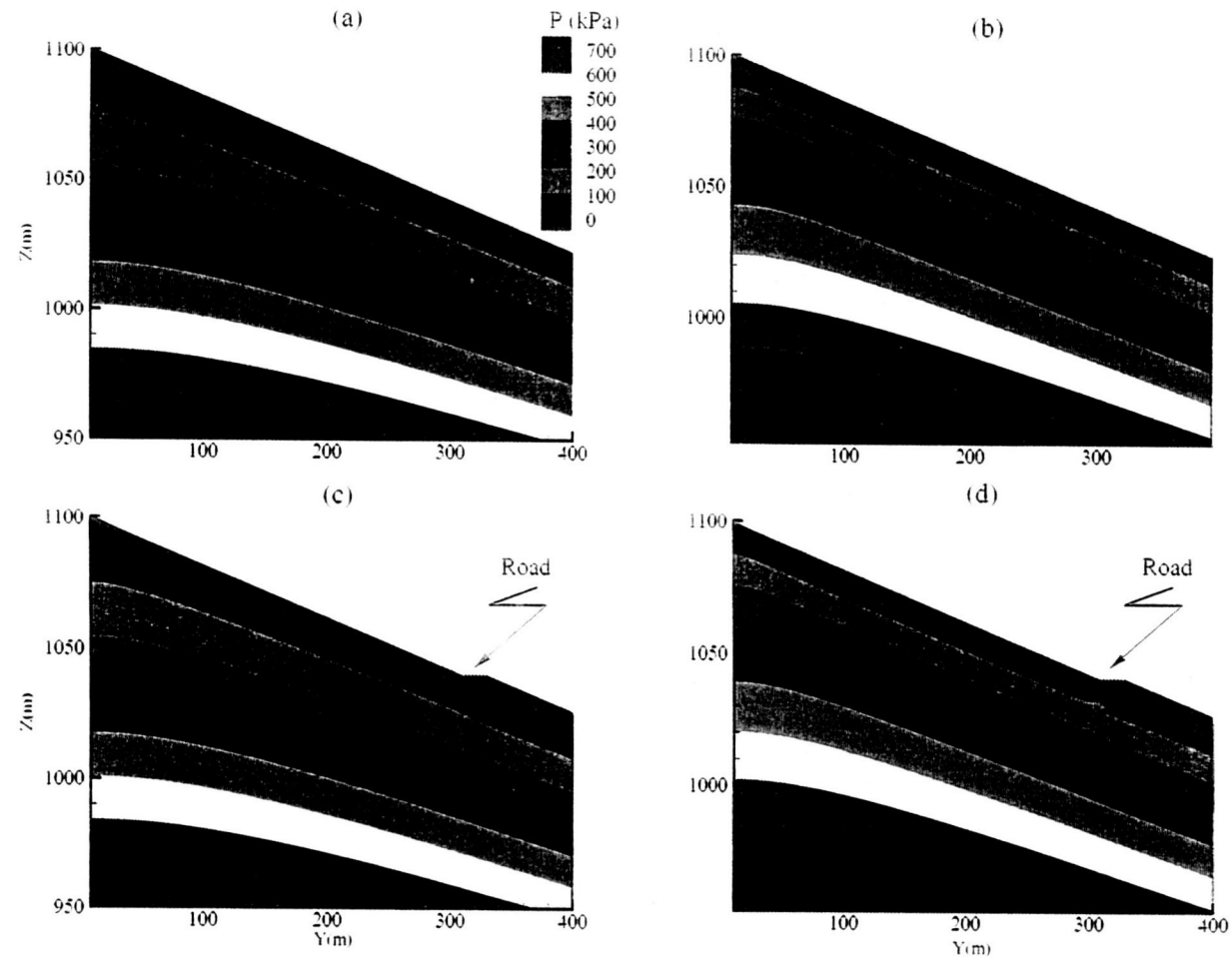


Figure 42. Pore pressure distribution throughout the C3 hillslope as simulated using NUM5. (a) Homogeneous. (b) Heterogeneous. (c) Homogeneous with road. (d) Heterogeneous with road

moving through the newly confined flow system is greater. Figure 42d shows the influence of the road cut that creates a perturbation in the pressure contours below the road. The road and the resultant local conductivity contrasts increase the pressure locally. The high pore pressure buildup and the seepage force directed outward from the hillslope may cause slope instability.

Discussion

The results of the NUM5 simulations determined the upslope and downslope boundary conditions necessary to effectively simulate the local flow system around the road using VS2DT. In the NUM5 simulations for WS3 and C3, contrasts in hydraulic conductivity dominate the changes in subsurface flow fields, hydraulic head, and pore-pressure distributions relative to the homogeneous base case simulations. In the near-surface layer constituting a high conductivity material, groundwater flow is predominantly parallel to the surface slope. In regions of lower saturated hydraulic conductivity, at depth below the surface layers, the flow system was similar to the simulated flow systems for the homogeneous slope (i.e., they have a pronounced vertical component). Given the changes in the hydraulic head contours and the changes in pore pressure during the NUM5 simulations, the most critically impacted region lay upslope of the road. The lower boundary was determined by drawing a flow line from the upper boundary condition through the local system to see where it exited (see Figure 20). In that manner, all of the incoming water was accounted for within a known volume and mass was conserved.

Factor of Safety Analysis

Based on the results of the NUM5 simulations the factor of safety (FS) was calculated for a homogeneous slope, for a heterogeneous slope, and for a heterogeneous slope with a roadcut. The FS equation (12) was applied to the C3 hillslope, using realistic parameter values given in Table 9. Figure 43 shows the results of the FS analysis. A dramatic decrease in the FS occurs above the roadcut, corresponding to the localized rise in pore pressures calculated in that region. Below the road there was a

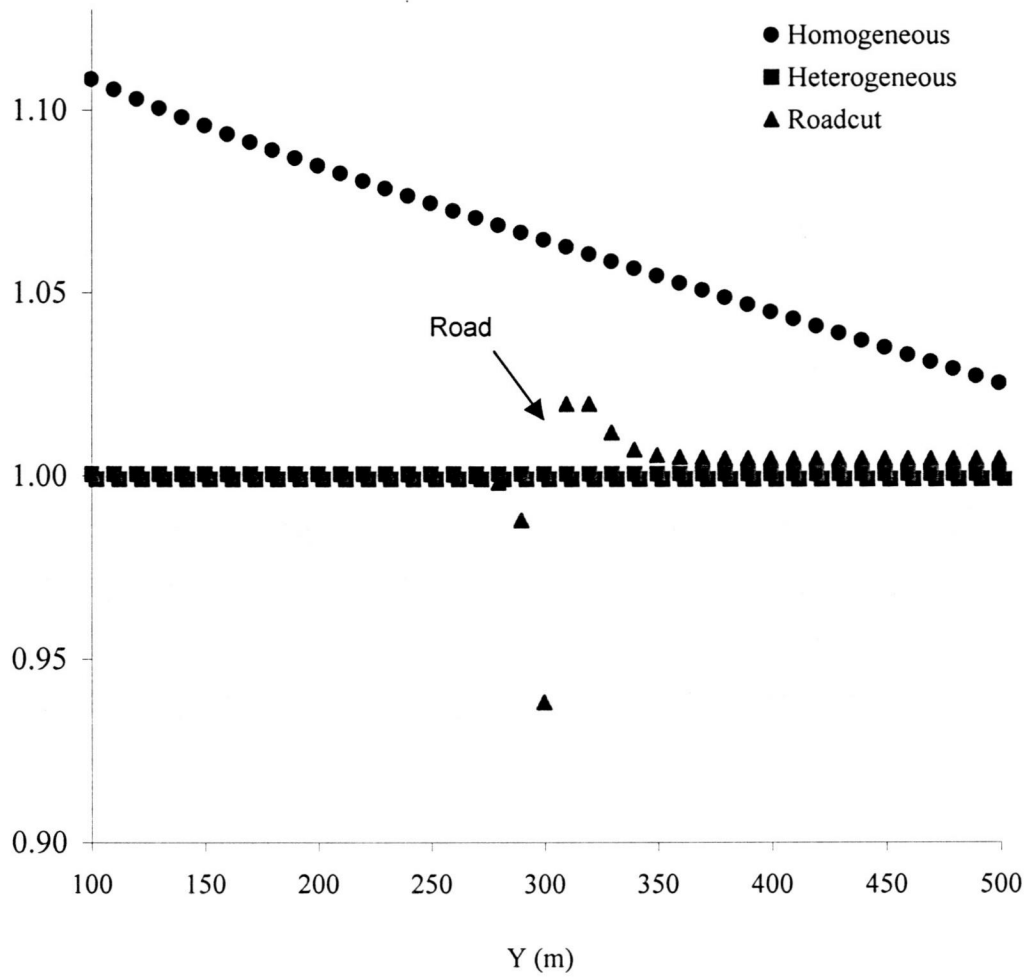


Figure 43. Factor of safety analysis based on the NUM5 simulation results. Above the road FS values are less than one indicating imminent slope failure under fully saturated conditions.

sudden increase in the FS value and this indicates that the pore pressures were abnormally low in this area.

High soil-water pressures indicate high soil-water content and reduced effective stresses i.e. an increased risk of failure. The dramatic increase in pore pressure directly above the road is due to the impact of the low-conductivity zone directly beneath the road that imposes dam-like impedance to the near-surface flow. As a result, FS values decrease below one in the vicinity of the road, (see Figure 43) indicating that failure would be imminent if the hillslope was indeed completely saturated as this model assumed. A physical explanation for the simulated low pore pressures and high FS results below the road is that the lateral subsurface flow was impeded by the compacted soil beneath the road and the hillslope was essentially starved for water. The soil was replenished farther down the slope by surface infiltration or flow that occurred beneath the influence of the roadcut or through the low conductivity barrier.

A sensitivity analysis was performed on the magnitude of the saturated hydraulic conductivity contrast that was taken as the location of the failure plane by varying the contrast by two orders of magnitude (see Table 10). The sensitivity analysis accounted for potential error associated with assuming K_s for the saprolite layer from the literature. The K_s values that were measured in the field had a high level of confidence associated with them and so the impact associated with altering them was not assessed in this study. When the K_s values for the saprolite layer were decreased, even higher pore pressure values were calculated above the road (see Figure 44a). Based on the FS results, a mass movement was more likely to occur by roadcut failure when the K_s was decreased relative to background, homogeneous conditions (see Figure 44b).

Limit equilibrium analysis for potential failure surfaces has engineering utility, but provides a limited view of groundwater influence on slope stability analysis because this method can only assess the net force balance on an isolated piece of slope (Iverson and Reid, 1992). The greatest uncertainties associated with this analytical method are related to estimating the soil-water content. For a given hillslope, a saturated, steady-state groundwater flow field will result in higher pore pressures than a partially saturated, transient flow field (Reid, 1997). Assumptions of homogeneity for properties such as soil depth, soil hydraulic conductivity, and soil density, strength, and cohesion also detract

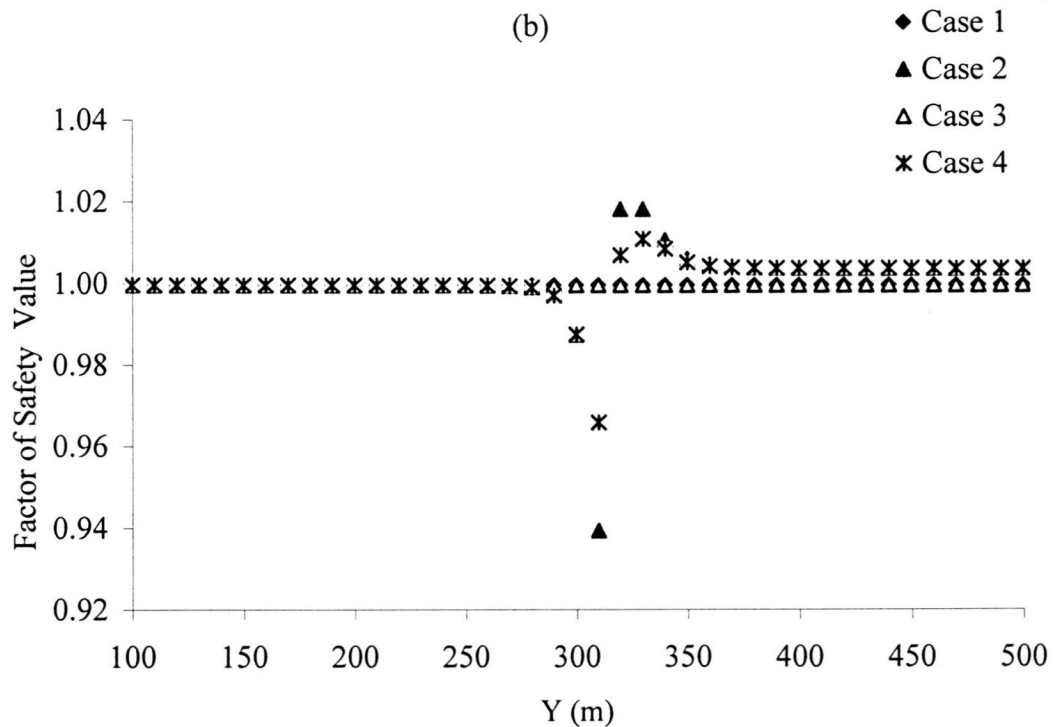
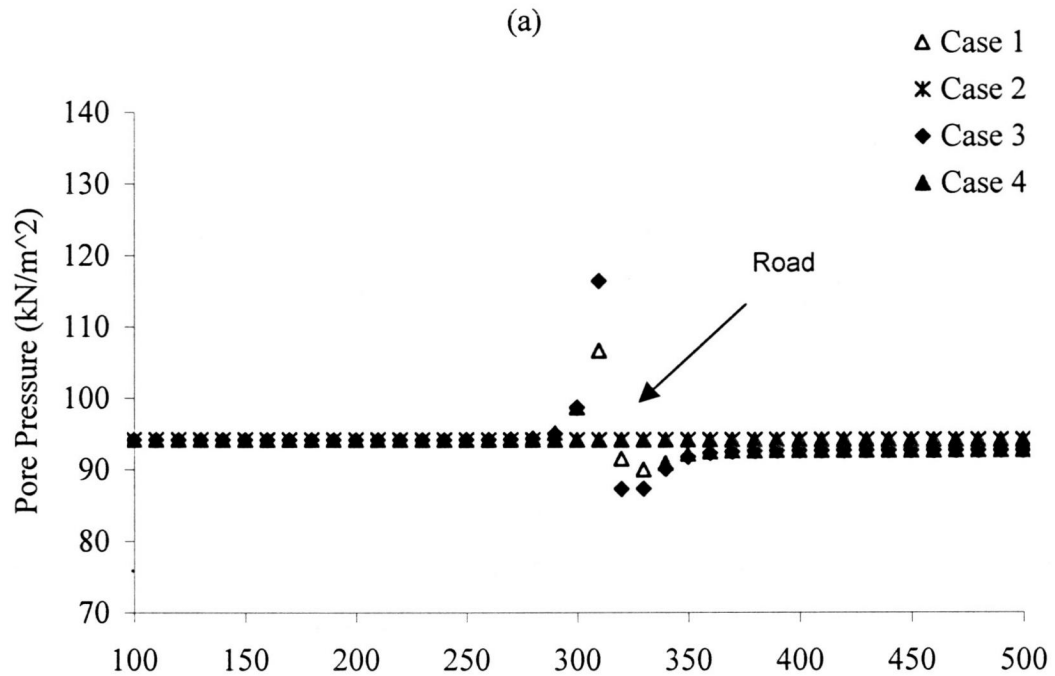


Figure 44. Comparison of the impact that the K_s value for the failure plane has on the (a) Pore pressure distribution and (b) FS values. See Table 10 for case descriptions.

from the influences of spatial variability on the system, and therefore are not a true measure of reality. However, even by simulating a simple uniform groundwater flow field, the significant destabilizing effects of outward directed groundwater flow (i.e. at the roadcut face) can be compared to slope-parallel downward directed groundwater flow. In addition, any larger scale variations in topography or K_s that might impede the downward flow of water and create locally elevated pore pressures warrant special attention in site-characterization and stability analysis.

VS2DT

Model Testing

The first check for the VS2DT model performance was to compare the volume of water that exited the system through the roadcut face. Figure 45a shows the simulated versus the observed volumes of water discharged through the seepage face at the roadcut for the three storm events recorded at C3 during the winter of 1995 (see Table 7 and Figure 23). For this comparison, the model reasonably represented the hydrologic response of the C3 hillslope. It should be pointed out, however, that the height of the seepage face used to determine the discharge through the roadcut face was based upon an estimate of the actual seepage face height. In actuality, the seepage face height varied throughout each storm event based on the storm intensity and the resulting water table response. Therefore, the uncertainty associated with the estimates of the discharge measured at the road can be seen in Figure 45b.

In the sensitivity analysis presented here the minimum and the maximum recorded seepage face heights were used as the basis for estimating the percentage of the total volume of water that was potentially discharged along the roadcut face. There is a significant discrepancy in the results between the simulated discharge results. However, given the nature of the C3 hillslope, the water table is expected to rise during a rainfall event. This being the case, the lower bound on the seepage face height is not likely to be a realistic estimate of the seepage face height during the majority of a storm event and so the error associated with these approximations of the volume of seepage at the roadcut is decreased.

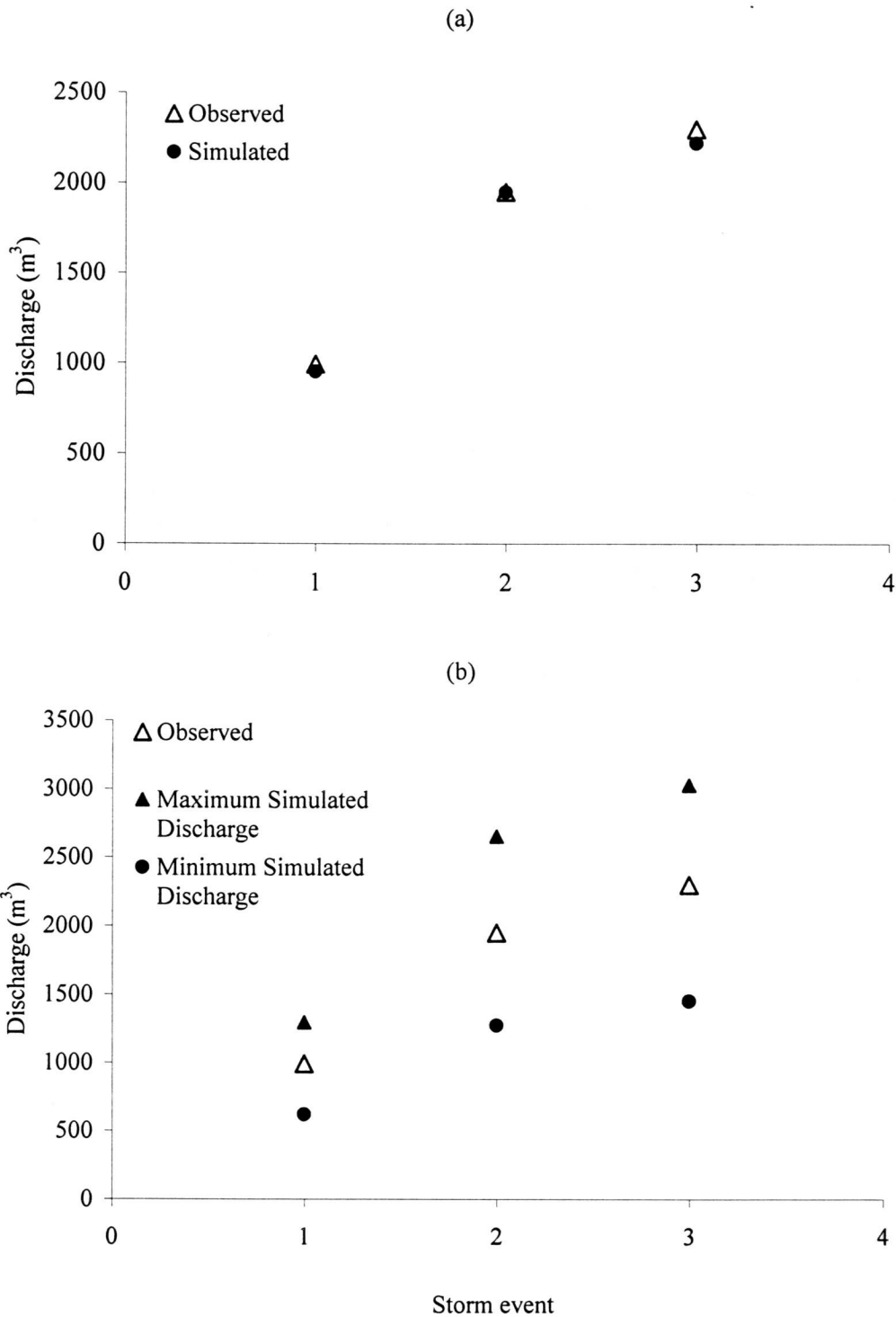


Figure 45. Comparison of VS2DT simulated results to the observed volumetric discharge at the C3 hillslope during the three storm events used for model calibration. (a) Simulated versus observed volumes of water discharged at the roadcut face. (b) Potential error in simulated estimates related to observed data.

The second check on how effectively VS2DT simulated the C3 hillslope was based upon a comparison of the piezometric response from VS2DT and that recorded by the C3 piezometers during each storm event. Figures 46, 47, and 48 show the results of the simulated versus the observed piezometric response during each storm event.

While the matches are not exact between the simulated and the observed piezometric response, for the most part the general trend of the near-surface hydrologic response (i.e. head increases with rainfall intensity and duration) is consistent between the two results. Exact matching of piezometric data at the catchment scale is very difficult (Loague, personal communication, 2000; Stephenson and Freeze, 1974). Piezometric response in the field is highly influenced by local soil heterogeneity, proximity to macropores, and hydraulic conductivity anomalies. In this study there was insufficient data to further constrain the model, especially in terms of the small-scale spatial variability of hydraulic conductivity and macropore distribution. However, enough reasonable matches (see Figure 46a, c, and d, Figure 48a) occurred to confirm that the simulated C3 hillslope was a sufficient representation of the actual C3 system.

Rainfall Events

As an example of the C3 hillslope hydrologic response to the individual storm events Figure 49 shows the simulated hydraulic head distribution throughout the cross-section of the C3 hillslope during the November 24, 1995 storm. The road has a significant impact on changing the distribution of the equipotential lines in the vicinity of the road. The lines of constant head are more closely spaced directly upslope of the road. This local steepening of the hydraulic gradient increases the potential for seepage through the roadcut face.

Figure 50 shows the water table response during the November 24 storm event. In Figure 50 the initial position of the water table, the position of the water table after day one, and the water table location after the third day of the event are superimposed. As the storm duration increases or as the rainfall becomes more intense, the water table rises and the height of the seepage face that forms at the roadcut face increases.

Figure 51 shows a partial flow net constructed for this portion of the C3 system during the November 24 storm. The flow lines show water either being directed out

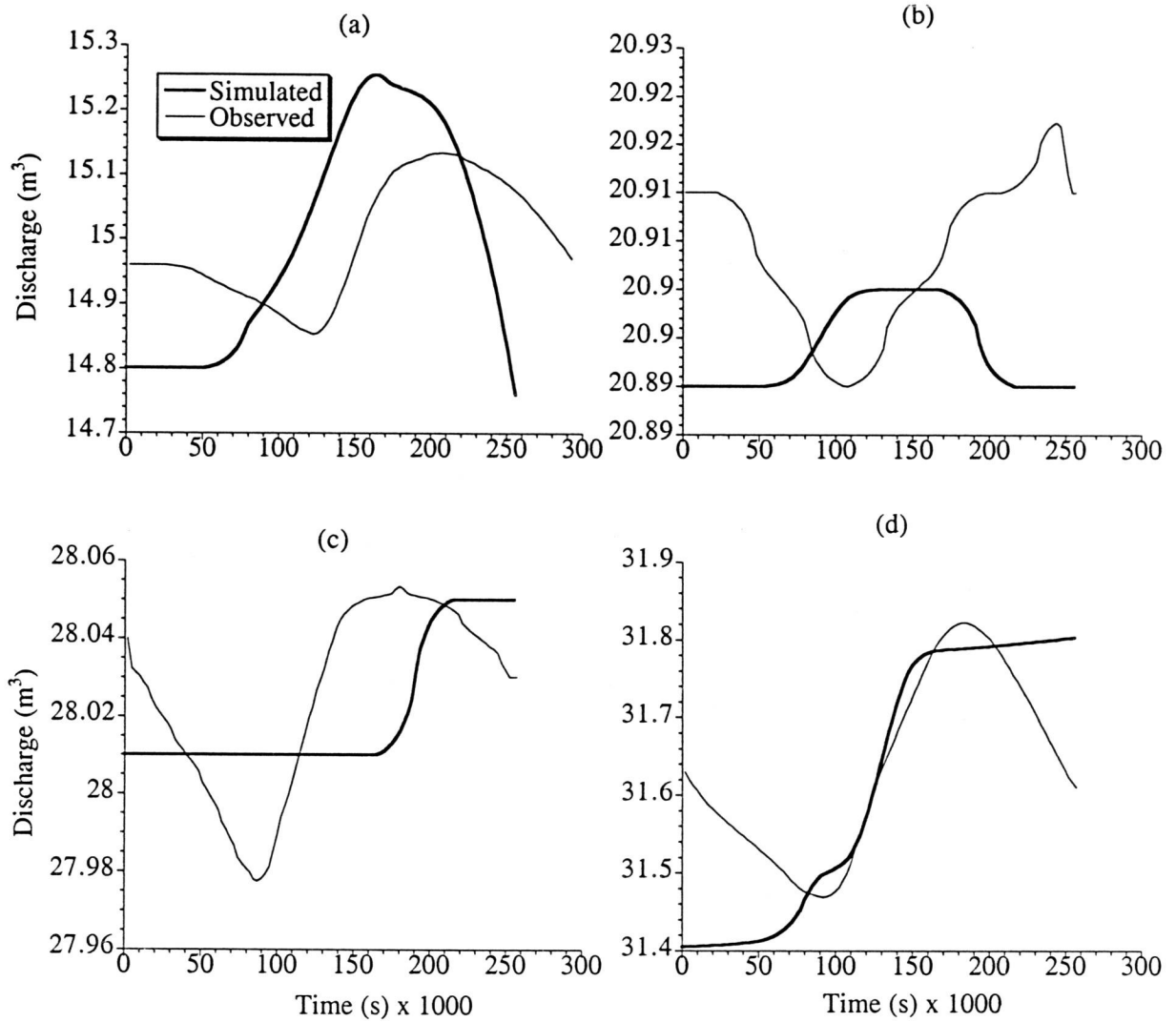


Figure 46. The piezometric response simulated by VS2DT compared to that recorded at C3 during the November 24, 1995 storm event. See Figure 14 for piezometer locations. (a) 3P4. (b) 3P6. (c) 3P8. (d) 3P9.

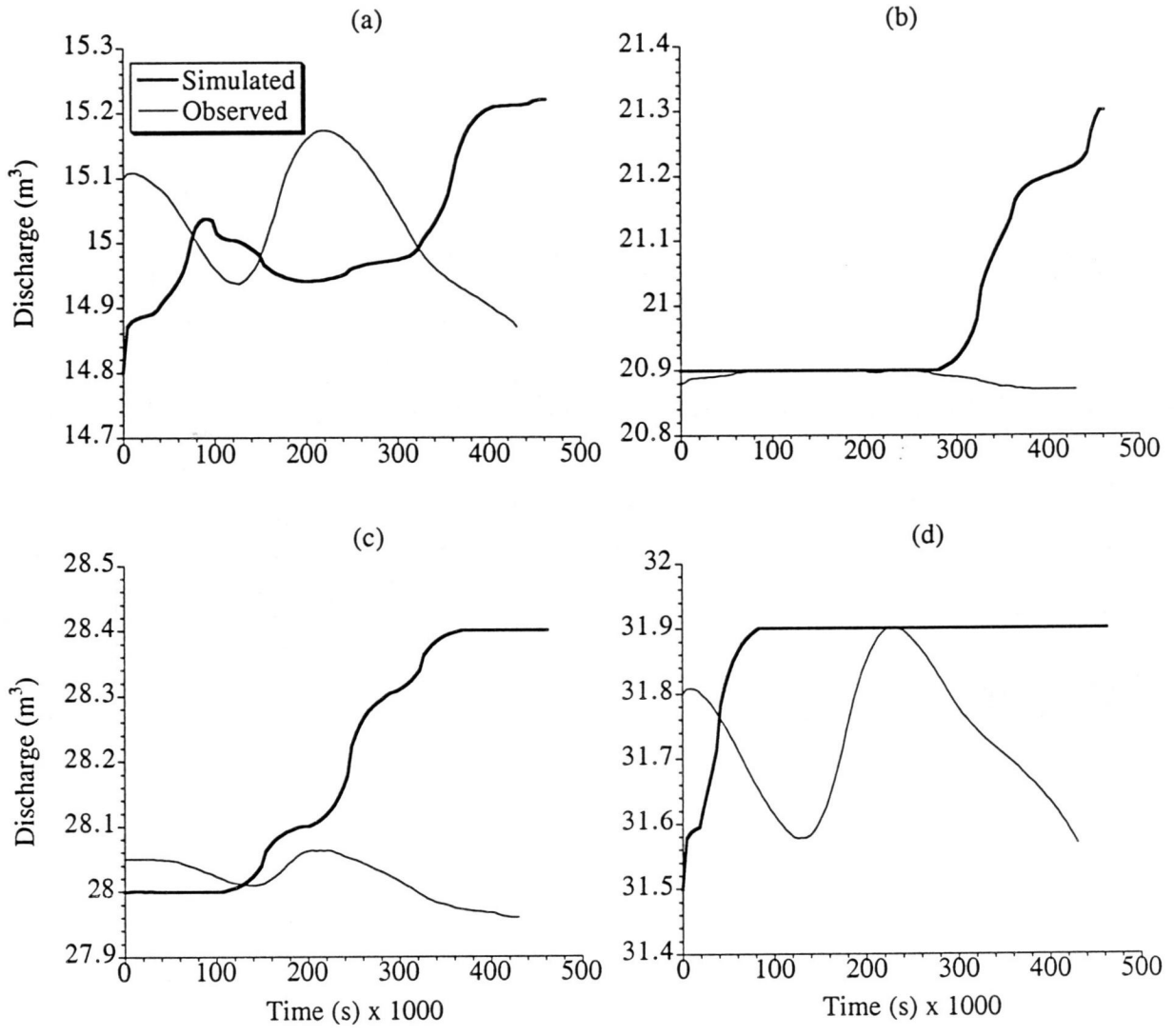


Figure 47. The piezometric response simulated by VS2DT compared to that recorded at C3 during the November 29, 1995 storm event. See Figure 14 for piezometer locations. (a) 3P4. (b) 3P6. (c) 3P8. (d) 3P9.

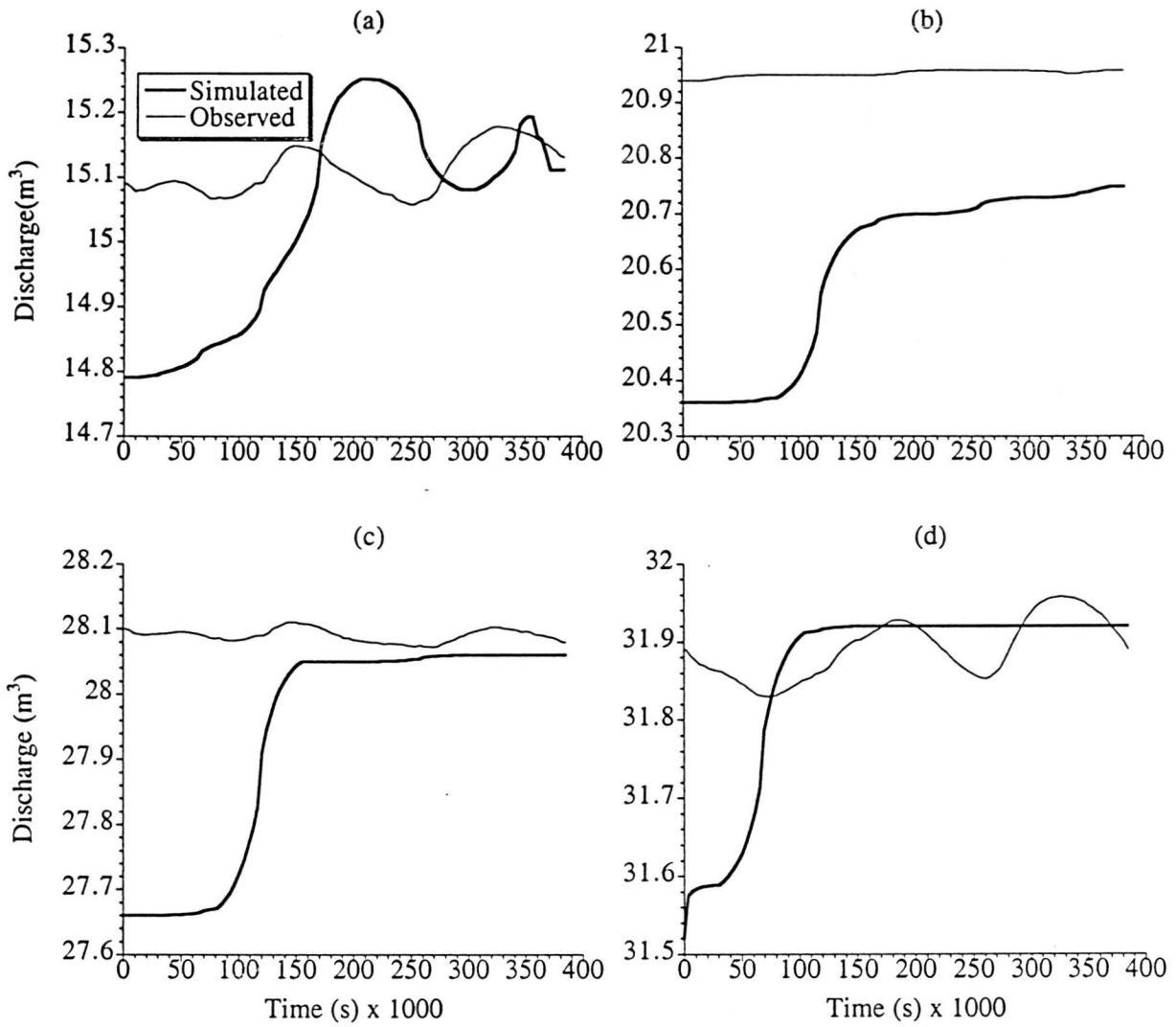


Figure 48. The piezometric response simulated by VS2DT compared to that recorded at C3 during the December 8, 1995 storm event. See Figure 14 for piezometer locations. (a) 3P4. (b) 3P6. (c) 3P8. (d) 3P9.

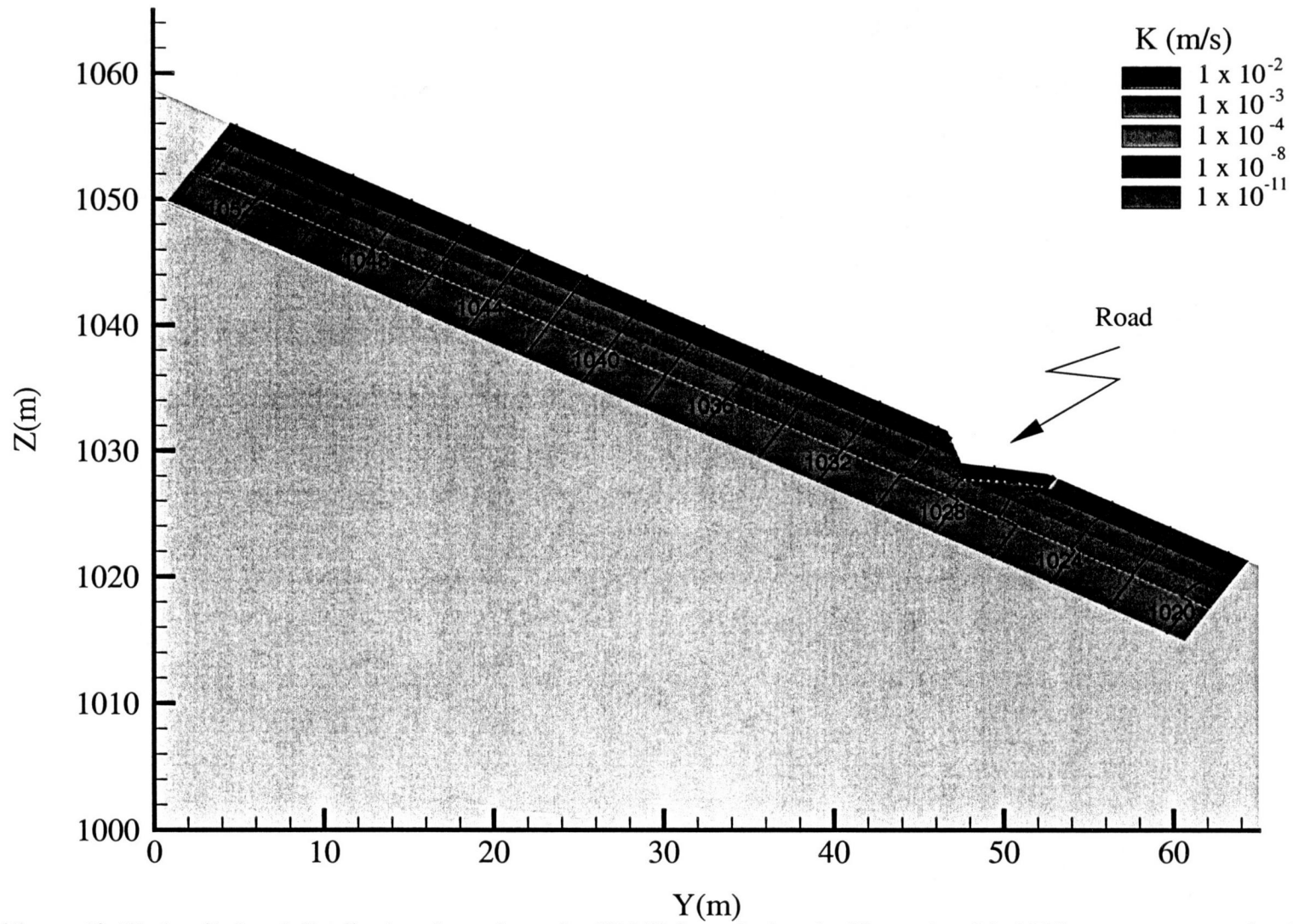


Figure 49. Hydraulic head distribution throughout the C3 hillslope during the November 24, 1995 storm event as simulated using VS2DT.

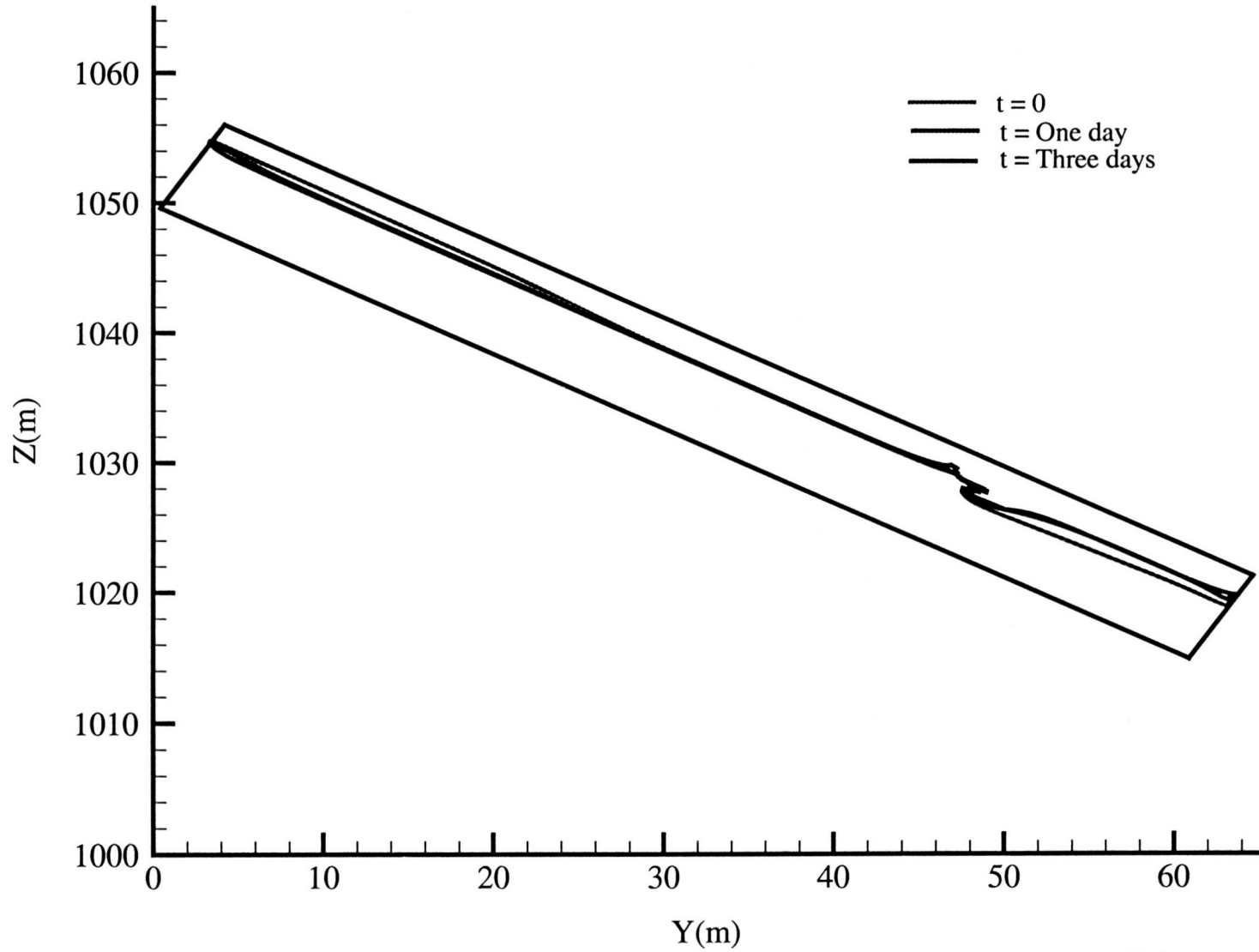


Figure 50. Water table location throughout the C3 hillslope at different times during the November 24, 1995 storm event as simulated using VS2DT.

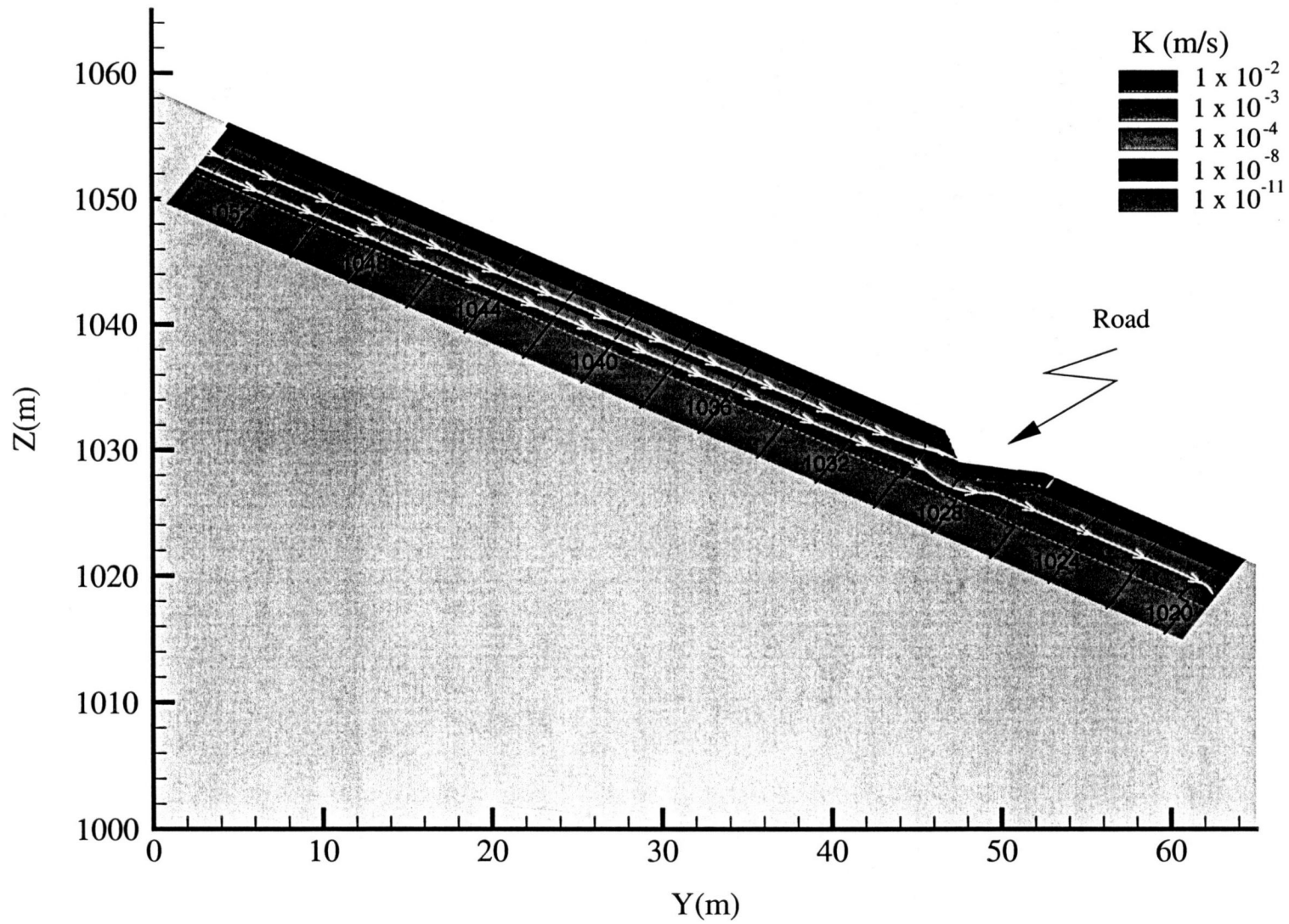


Figure 51. Partial flownet throughout the C3 hillslope during the November 24, 1995 storm event as simulated using VS2DT.

across the seepage face onto the road or being diverted beneath the compacted soil beneath the road. There are two mechanisms by which water could potentially exit the system at the roadcut face. One means would be to overcome the atmospheric pressure at the roadcut face (i.e. the pore pressures of the saturated zone above the road would have to be larger than the air-entry value at the soil-air interface to drive the flow out of the system). Flow could also leave the system by flowing through the macropores that are prevalent in forested systems (Smetten et al., 1991; Jones and Grant, 1996). In the case of macropore flow the soil does not have to be saturated for seepage to occur. However, for the purposes of this study, the influence of macropore flow was not addressed and so all flow exiting the roadcut face is assumed to be through a saturated seepage face.

Figure 52 shows the pore pressure distribution throughout this portion of the C3 hillslope during the November 24 storm event. There is a significant increase in the pore pressure values in the region upslope of the road. This local increase in pore pressure is related to the barrier to slope-parallel subsurface flow that is created by the impermeable zone beneath the road. Water builds up behind the low permeability zone and creates a region of groundwater mounding and increased pore pressure that propagates upslope. Zones of high pore pressure are often areas that are prone to slope failure or other types of mass movement.

Factor of Safety Analysis

A factor of safety analysis was performed on the simulated C3 hillslope after each day during the three individual storm events. Figure 53 shows the results of the FS analysis after each day during the events. Typical forested slopes have an FS value that lies between 1.0-1.5 (Sidle et al., 1985) and the C3 hillslope falls within this range. As the C3 hillslope did not fail during any of the 1995 events, the marginal stability of the slope exhibited in Figure 53 is to be expected. An important trend in the FS results during the rainfall events that were simulated was the sharp decrease in the FS values directly above the road and a sharp increase in the FS values at and below the road. These results mimic those for the fully saturated system modeled by NUM5 (see Figures 43 and 44b) where the regions of local instability occurred upslope of the road.

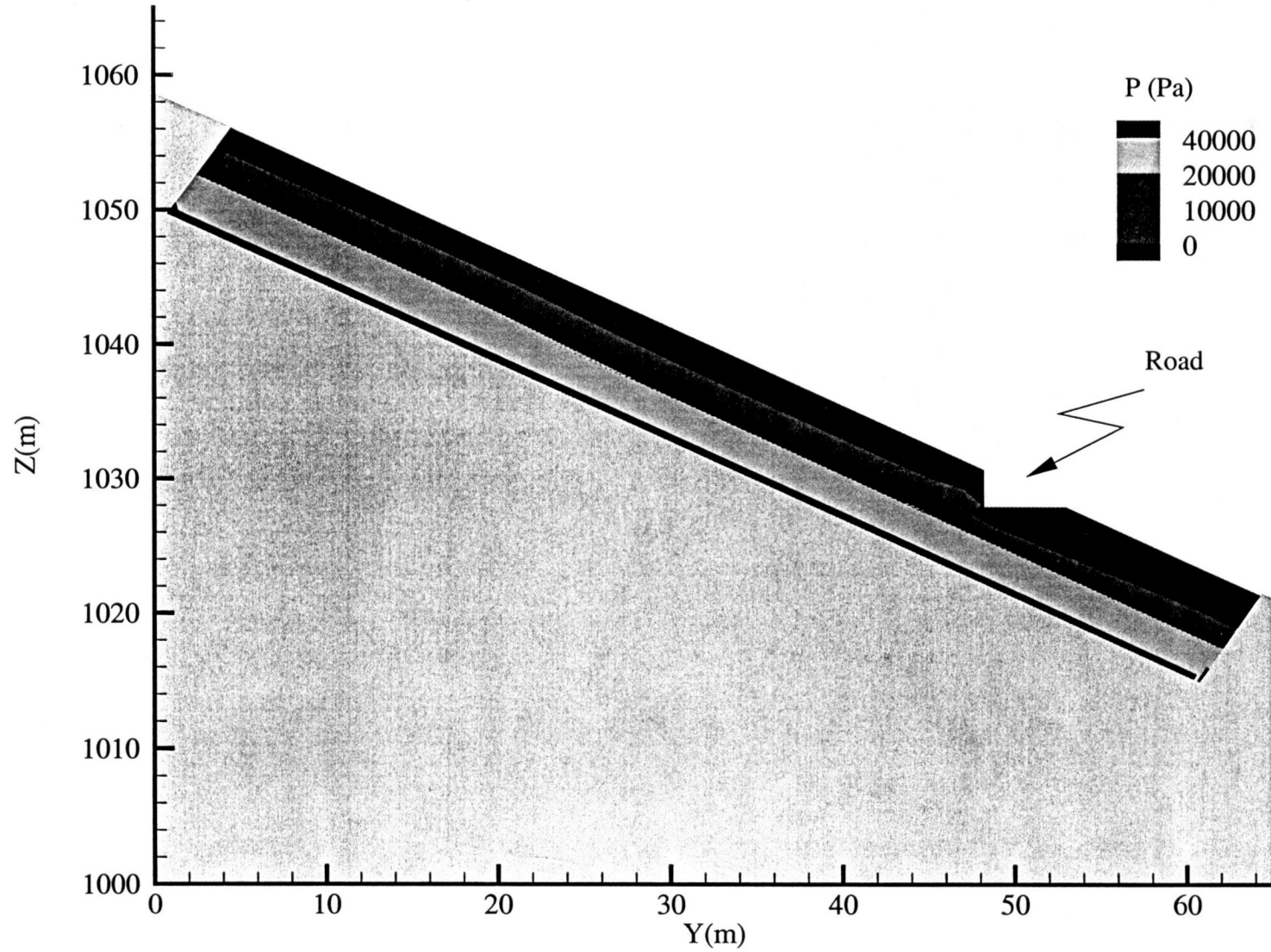


Figure 52. Pore pressure distribution through the C3 hillslope during the November 24, 1995 storm event as simulated by VS2DT.

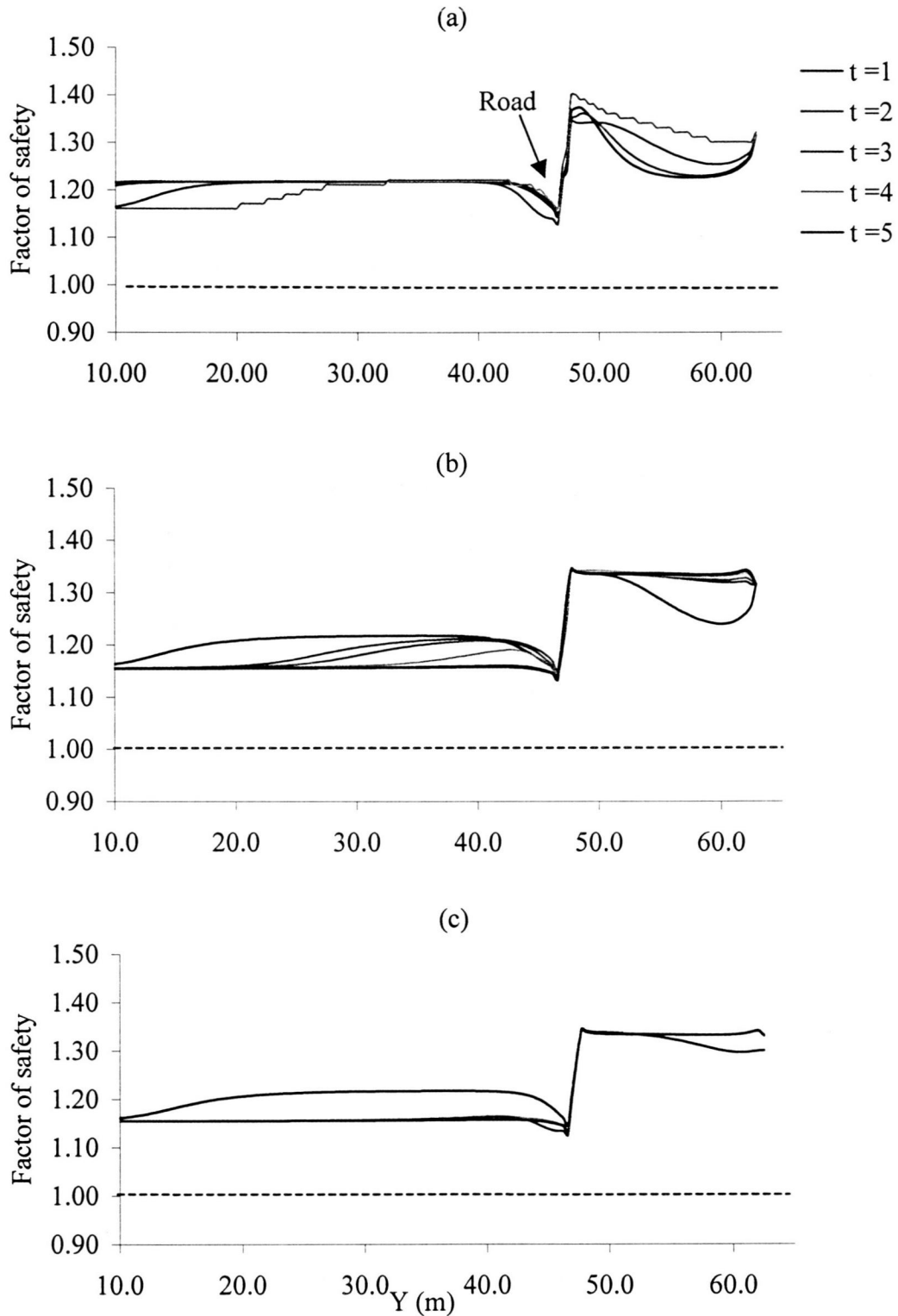


Figure 53. Factor of safety values measured at one day intervals along the potential failure plane during the simulated 1995 storm events. (a) November 24 storm event. (b) November 29 storm event. (c) December 28 storm event.

The FS results shown in Figure 53 are attributed to the impact that the compacted soil beneath the road has on impeding the groundwater flow and locally elevating the pore pressure. Below the road the soil is effectively starved as the water table is diverted away from the impermeable zones (see Figure 53a,c). The results of the FS analysis also correspond to the findings by other researchers that the discharge rate of water through or from unstable soils is a significant hydrologic function affecting soil mass movement (Sidle et al., 1985; Rulon et al. 1985; Rulon and Freeze, 1985; Reid et al., 1995; Montgomery et al., 1997). The zones where the seepage is directed outward from the slope (i.e. the seepage face at the roadcut; see Figure 51) are areas that are most likely to fail.

Simulated Events

The focus of the study reported here was to understand the hydrologic response of the C3 hillslope relative to different rainfall events and to assess under what conditions slope failure is imminent. Based on the match between the volume of water discharged at the roadcut face and the piezometric response during the three storm events described above, the BVP simulated by VS2DT was assumed to be a reasonable approximation of the C3 hillslope system. Under this assumption, the sensitivity of the C3 system to different factors that would influence slope stability could be assessed.

A series of hypothetical events (i.e. rainfall events of different intensity and duration) were imposed upon the C3 system and the hydrologic response was evaluated in terms of the volumetric flux discharged at the roadcut face and the slope stability. The impact of the rainfall intensity on the hydrologic response was estimated by simulating four rainfall events of increasing magnitude (i.e. 0.36, 3.60, 36.0, and 360 mm/hr) for a one-day duration during which the rainfall rate remained uniform. These rainfall rates served as the input against which other physical perturbations to the system were evaluated. The effect of rainfall duration on the hydrologic response and the resultant slope stability was determined by extending a rainfall event of constant intensity to encompass two, three, and four consecutive days.

Several model input parameters (i.e. slope gradient, hydraulic conductivity contrasts, and initial conditions) were evaluated in terms of their influence on the

hydrologic response simulated by the model (see Table 8). The resultant FS value was calculated for each hillslope scenario. Figure 24 shows the location of the six measurement points established throughout the vertical cross-section of the C3 hillslope, both upslope and downslope of the road. The pore pressure response at these locations was calculated four times during each rainfall event to assess how the different combinations of rainfall intensity and different sets of boundary or initial conditions impacted the pore pressure development throughout the slope. The total volumetric discharge from the system for each simulated event was recorded as well.

The results of the VS2DT simulated events for the C3 system can be summarized as follows:

- Volumetric discharge increases with increased slope angle.
- Volumetric discharge increases as a function of rainfall intensity and/or duration.
- Volumetric discharge increases with higher antecedent soil-water content conditions.
- Slope stability decreases with increased slope angle.
- Slope stability decreases with increased saturated hydraulic conductivity contrast between the high conductivity soil and the low conductivity compacted soil beneath the road.
- Slope stability decreases as a function of rainfall intensity and/or duration.
- Slope stability decreases with higher antecedent soil-water content conditions.

Rainfall Events

Hydrologic Response

As shown in Figure 54, the volume of water discharged after a single day event increases with increasing rainfall intensity. This relationship is expected because, given a proper mass balance, any water input to the system must either go into storage (i.e. increase the height of the water table) or flow through the system. Because the hydraulic conductivity of the soil is not the limiting factor in terms of how much water can infiltrate the C3 system (i.e. the rainfall rate is always less than the saturated hydraulic conductivity of the surface soil), the subsurface flow rate becomes the controlling factor

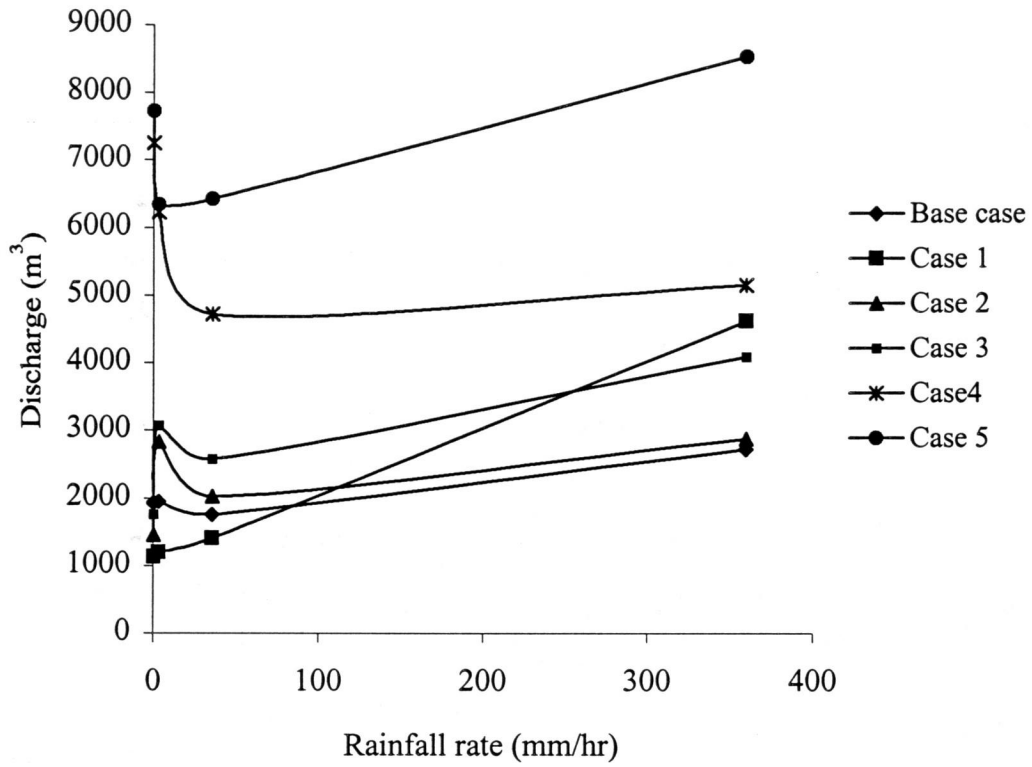


Figure 54. Total volumetric discharge recorded at the C3 hillslope as the rainfall rate varied over four orders of magnitude. (a) Base case. (b) Case 1. (c) Case 2. (d) Case 3. (e) Case 4. (f) Case 5. See Table 8 for case descriptions.

for slope stability. Water flows through saturated soil faster than through unsaturated soil because under saturated conditions the water is held with less tension to the grains (see the characteristic curve in Figure 36). Therefore, if an increased volume of recharge is entering the system, the water table is expected to respond more rapidly and allow water to flow through the system at a greater rate.

The pore pressure development at the six measurement sites within the C3 BVP is shown in Figure 55 (a-e) and in Table 15. In general, the pore pressures throughout the system increase with increasing rainfall intensity. The vertical conductivity contrast below the road acts to impede the slope-parallel groundwater flow and the soil remains predominately unsaturated below the road. The decrease in pore pressure values simulated at the measurement sites below the road indicates that the area below the road is significantly impacted by the presence of the impermeable zone beneath the road.

Case 1

One physical factor that will significantly influence the hydrologic response of the C3 hillslope is the slope angle. The hydraulic gradient increases as the slope angle increases and so, based on Darcy's law (4), an increased volume of water can be forced through the system. This relationship is shown in Figure 54 where the discharge simulated through the system during the base case is compared to the discharged simulated when the C3 hillslope was inclined at an angle of 35° . Although the volume of water discharge through the Case 1 system is smaller under light rainfall conditions, the volume of water discharged increases at a much greater rate as the rainfall intensity increases. The low intensity event results may be an artifact of the model, but in general, steeper slope is correlated to an increase in discharge.

As seen in Table 15 and in Figure 55b the pore pressures simulated throughout the Case 1 system were lower than those simulated for the base case (see Figure 55a). The lower pore pressures may be because water is draining more rapidly through the system when the slope is increased. In a real system, the water table will be deepest in convergent hollows or depressions in a hillslope (i.e. areas where the gradient is shallow), not on steep slopes.

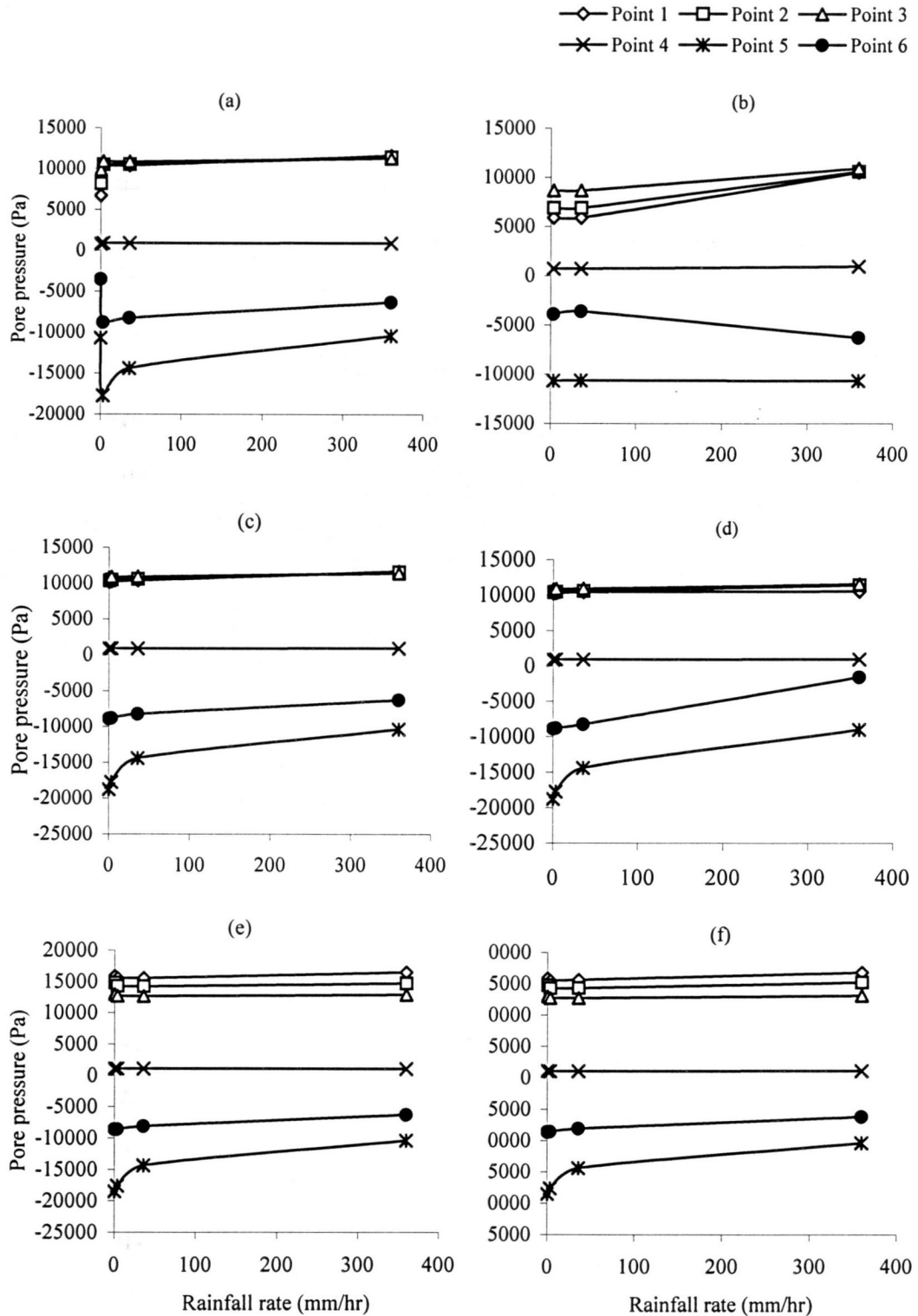


Figure 55. Pore pressure values simulated at six points on the C3 hillslope as the rainfall rate varied over four orders of magnitude. (a) Base case. (b) Case 1. (c) Case 2. (d) Case 3. (e) Case 4. (f) Case 5. See Figure 25 for the locations of the measurement points. See Table 8 for case descriptions.

Table 15. Pore pressure simulated at each measurement point throughout the C3 hillslope when the system was subject to different initial conditions and/or rainfall rates. See Table 8 for case descriptions and Figure 25 for measurement locations.

Case	Precipitation rate (mm/hr)	Pore pressure (Pa)					
		Point1	Point2	Point3	Point4	Point5	Point6
Base case	0.36	6733.6	8207.5	9868.6	830.6	-10672.2	-3506.4
	3.60	10270.4	10495.8	10917.2	921.0	-17738.0	-8777.9
	36.0	10407.6	10535.0	10897.6	918.1	-14396.2	-8218.3
	360	11701.2	11495.4	11368.0	959.4	-10368.4	-6247.5
Case 1	0.36	5810.4	5784.0	5441.0	-314.4	-10525.2	-1758.1
	3.60	5914.3	6897.2	8667.1	727.6	-10642.8	-3869.0
	36.0	5911.4	6900.2	8683.8	730.8	-10623.2	-3581.9
	360	10525.2	10633.0	10946.6	965.1	-10642.8	-6275.9
Case 2	0.36	10231.2	10388.0	10819.2	910.8	-18757.2	-8857.2
	3.60	10270.4	10495.8	10917.2	921.0	-17738.0	-8777.9
	36.0	10427.2	10613.4	10966.2	925.6	-14396.2	-8213.4
	360	11730.6	11613.0	11466.0	969.3	-10358.6	-6245.5
Case 3	0.36	10241.0	10407.6	10838.8	912.8	-18747.4	-8855.3
	3.60	10270.4	10495.8	10917.2	921.0	-17738.0	-8777.9
	36.0	10427.2	10613.4	10966.2	925.6	-14396.2	-8213.4
	360	10554.6	11407.2	11583.6	985.9	-8954.3	-1526.8
Case 4	0.36	15885.8	14788.2	12975.2	1100.5	-18473.0	-8589.7
	3.60	15552.6	14278.6	12720.4	1078.0	-17581.2	-8559.3
	36.0	15582.0	14219.8	12681.2	1075.1	-14366.8	-8072.3
	360	16503.2	14729.4	12887.0	1091.7	-10358.6	-6218.1
Case 5	0.36	15885.8	14788.2	12975.2	1100.5	-18473.0	-8589.7
	3.60	15542.8	14259.0	12710.6	1078.0	-17581.2	-8560.3
	36.0	15640.8	14317.8	12730.2	1079.0	-14366.8	-8068.3
	360	16856.0	15248.8	13141.8	1113.3	-10358.6	-6213.2
Case 6	0.36	6733.6	8207.5	9868.6	830.6	-10672.2	-3506.4
	0.36	6733.6	8207.5	9868.6	830.6	-10672.2	-3506.4
	0.36	6733.6	8207.5	9868.6	830.6	-10672.2	-3506.4
	0.36	6733.6	8207.5	9868.6	830.6	-10672.2	-3506.4

Case 2

The compacted area beneath the road serves as a vertical impediment to flow. A water table mound forms upslope of the road and creates a saturated zone through which water is discharged across the roadcut face and exits the system. Although the road permeability is very low relative to the surrounding soil mantle, a certain volume of water does saturate and flow through the low conductivity zone. In Case 2 the conductivity of the road is decreased by an order of magnitude and the expected effect is to increase the height of the groundwater mounding upslope of the barrier and as a result increase the discharge recorded at the roadcut face. Figure 54 shows the impact that decreasing the conductivity of the road has on the volume of water discharged through the C3 system. In all of the simulated rainfall events, the discharge recorded from Case 2 is greater than that recorded for the base case.

The hypothesized increase in water table height recorded above the road is evident in the increase in pore pressures recorded at the measurement points above the road for Case 2. In Figure 55c and in Table 15 it can be seen that for all of the rainfall events the pore pressures above the road increased and the pore pressures below the road dramatically decreased. If the K_s value of the compacted soil below the road is decreased, the low K_s zone acts as a dam against which water builds up, locally increasing the pore pressures. This damming effect will naturally prove a more effective barrier to subsurface flow, thus “drying out” the area of the hillslope below the road.

Cases 3-5

Initial conditions (i.e. water table height and soil-water content) are largely responsible for the outcome of any rainfall event in terms of the volume of discharge recorded, water table height, and slope stability. Figure 54 shows the impact that the position of the initial water table height has on the volume of discharge simulated at C3. There are two reasons why, as expected, more water is discharged through the simulated C3 system when the water table is closer to the surface (i.e. Cases 3-5). For one, based on Darcy's law (4), the cross-sectional area through which water can be discharged through the system increases as the water table height increases. Secondly, the tortuosity of the potential flow paths for the water is decreased under saturated conditions.

An increase in water table height directly influences the pore pressures throughout the C3 system. As seen in Figure 55(d-f) and Table 15, the pore pressures dramatically increase relative to the base case (see Figure 55a) when the water table is closer to the surface (Cases 3-4) or the initial soil-water content is greater (Case 5).

Case 6

Figure 56a demonstrates that the volume of water discharged from the simulated C3 system increased proportionally to the increased duration of the constant intensity rainfall event. It is interesting to note, however, that the pore pressures simulated for the different events (see Figure 56b and Table 15) did not change relative to each other. One would expect that, especially with the saturated hydraulic conductivity contrast below the road acting as a vertical impediment to flow, that the water table would rise with time, thus increasing the pore pressures throughout the hillslope. However, in steep forested hillslopes Dunne overland flow is an unlikely phenomenon because the hydraulic conductivity of the soil is usually much higher than the rainfall rate. It appears that in Case 6 the rainfall rate (0.36 mm/hr) is so low relative to the hydraulic conductivity of the soil, that the influx of water just flows through the simulated C3 system and is not sufficient to raise the water table.

Factor of Safety Analysis

Sensitivity analysis

Important factors that control slope stability at a site are the pore water pressure, the soil strength parameters, the slope steepness, and the depth to the potential failure plane (Sidle et al., 1985). Prior to assessing the vulnerability of the C3 hillslope to failure given the different antecedent and hydrologic conditions simulated in the previous section, the sensitivity and accuracy of performing an FS analysis on the C3 hillslope must be discussed. The relative influence of the various soil, slope, and hydrologic variables used in slope stability analysis can be assessed by performing a sensitivity analysis using the infinite slope model (Gray and Megahan, 1981). A reasonable set of variables (shown in Table 9) was selected as input to the FS equation for this study. The FS values that resulted from using the parameters listed in Table 9 served as the base case

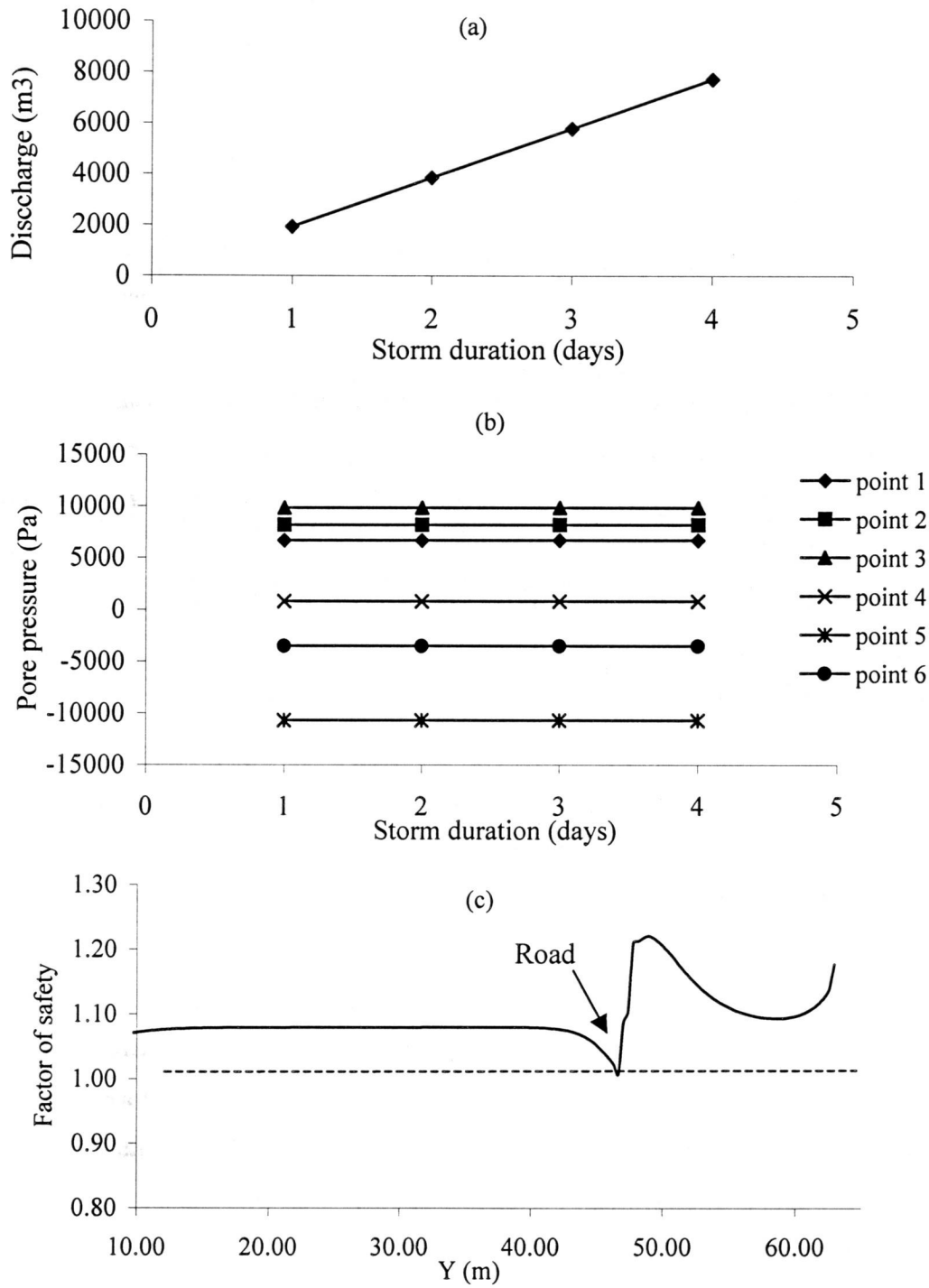


Figure 56. Impact of storm duration on the C3 hydrologic response. (a) Volumetric discharge recorded at C3 at the end of each event. (b) Pore pressure response to each storm event. See Figure 24 for the location of the measurement points.(c) Factor of safety distribution over the C3 hillslope.

to which the FS values that result from increasing or decreasing the individual variables by 10%, keeping everything else constant, can be compared to. The relative change in the FS values is an index for how important each parameter, and the uncertainty associated with its value, is on the results and validity of any FS results.

Figure 57(a–e) shows the impact of varying the different input variables to the FS equation. The variables that were considered in this sensitivity analysis were Z (the thickness of the soil layer above the failure plane), ΔC (the root cohesion), β (the slope angle), ϕ' (the internal angle of friction), and C (the soil cohesion). Figure 57(a–e) shows the relative effect that modifying each of these variables has on the final FS result compared to the mean FS values. Based upon the position of the lower bound of the FS values, the significance associated with decreasing the root cohesion (Figure 57b), the angle of internal friction (Figure 57d), and the soil cohesion (Figure 57e) on destabilizing the slope is apparent. Conversely, if the thickness of the soil above the failure plane (Figure 57a) or the slope angle is increased (Figure 57c), the slope also becomes increasingly unstable.

Natural slopes exhibit a high degree of heterogeneity and stability is often linked to the type and condition of the site vegetation. Root cohesion is extremely important in stabilizing slopes because roots provide artificial cohesion on slopes where the soil itself might be effectively cohesionless and can increase the shear strength at a site (Gray and Megahan, 1981; Zeimer, 1981). Roots can be especially effective at preventing mass movements if they cross the critical surface plane on which sliding might occur, therefore bonding unstable soils to the more stable underlying strata. In areas where land use activities such as clear-cutting remove the vegetation, the roots that formerly maintained the stability of the slope decay and no longer maintain the hillslope integrity. As a result, the area becomes more prone to sliding and mass movements happen more frequently (Swanson et al., 1977; Zeimer, 1981; Montgomery et al., 1998).

Hillslope morphology is also an important component in slope stability and its influence can be analyzed by studying the effect of changing the parameters of slope steepness and soil thickness. Hillslope gradient is important to maintaining slope stability because, the steeper the slope, the more force the gravitational component has on influencing a block of soil to move downslope. If the hillslope in question is concave the

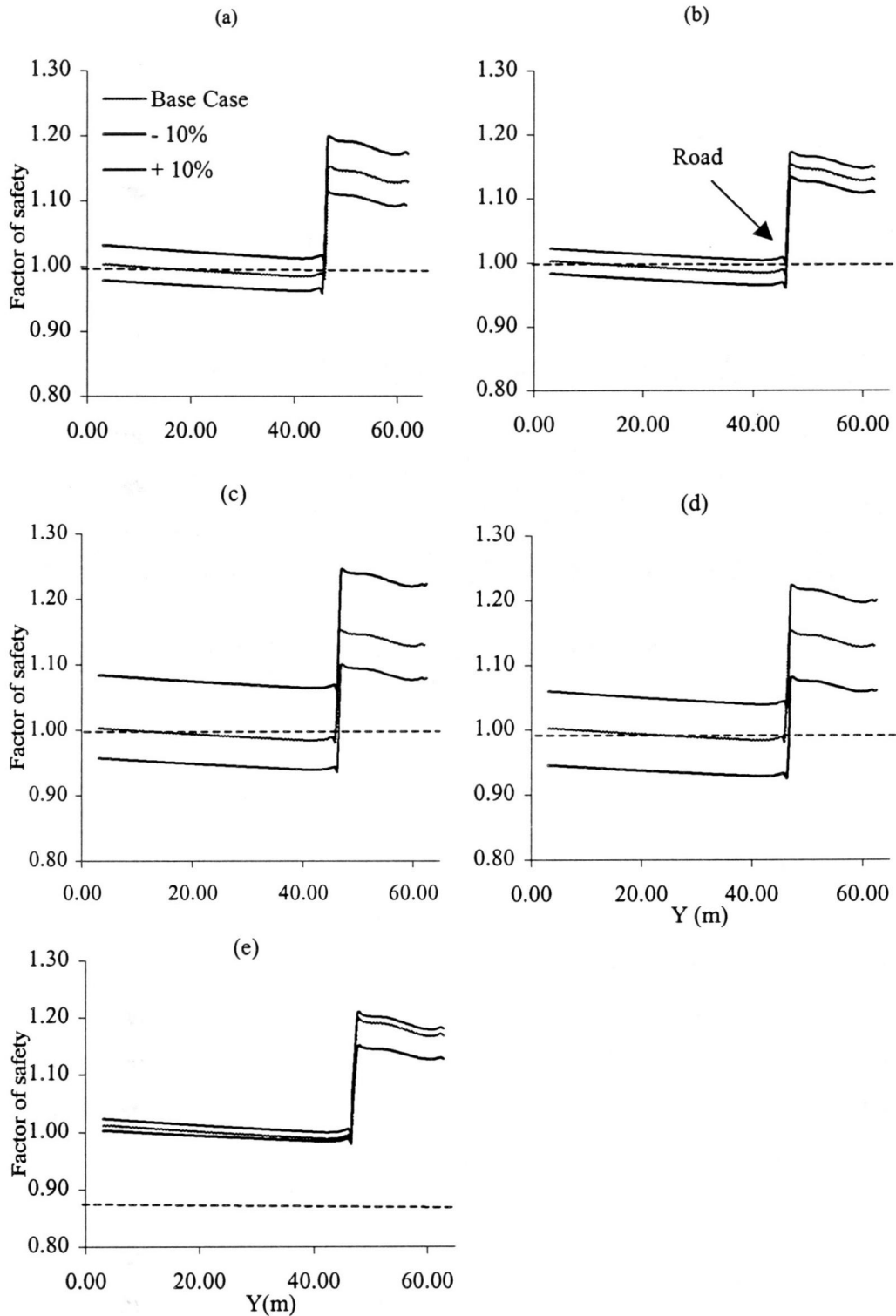


Figure 57. Sensitivity of the Factor of safety values to adjusting individual parameters by +10% and -10%. (a) The thickness of the failure slab. (b) The root cohesion. (c) The slope angle. (d) The angle of internal friction. (e) The soil cohesion.

soil thickness is generally greater in the hollows than on the bounding ridges (see Figure 28) and groundwater flow tends to concentrate in these topographic depressions. Increased weight of the soil column (i.e. increased soil thickness or saturation) tends to increase the shear stresses that can induce movement along a failure plane, especially in the event of a sharp increase in the pore pressures along the failure surface.

Rainfall Events

The impact of rainfall intensity and duration on hillslope stability is illustrated in Figure 58. At lower rainfall intensities (0.36 and 3.60 mm/hr) the FS values are relatively similar to each other and only approach the failure criterion directly upslope of the road. There is a dramatic increase in FS at and below the road due to the local seepage face created at the cut face that diverts flow outward from the system. However, at the highest rainfall intensity simulated (360 mm/hr) the FS decreases to be less than or equal to one. The propagation of the low FS values upslope of the road indicates that the road has more than a localized influence on slope stability.

Case 1

The impact of increasing the mean C3 hillslope angle from 30° to 35° on the hillslope stability is shown in Figure 58b. Especially at the high rainfall intensities, increasing the slope gradient drastically effects the susceptibility of the hillslope to a mass movement. When the rainfall rate is 360 mm/hr the FS drops below one along the entire length of the C3 hillslope above the road. At intensities of 36 mm/hr the portion of the hillslope falling below the stability threshold propagates further upslope from the road than the base case. The FS below the road decreases relative to the base case scenario shown in Figure 58a but never falls below one.

Case 2

Decreasing the conductivity of the zones directly beneath the road also decreases the FS locally as is shown in Figure 58c. Subject to the higher rainfall intensities the local pore pressure increase above the road upsets the already tenuous equilibrium of the cutslope. Because of the dam-like impedance of the low conductivity zone beneath the

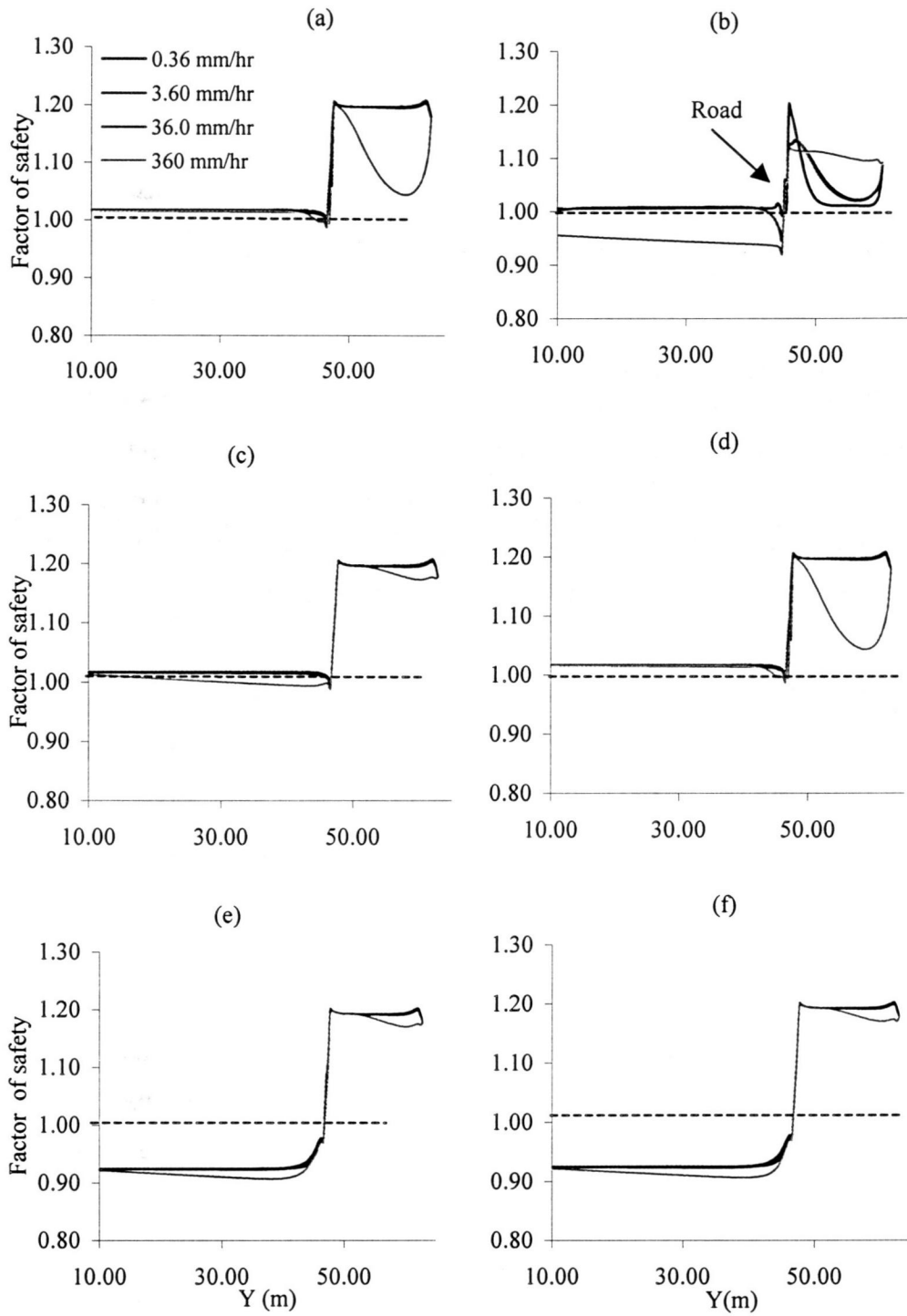


Figure 58. Factor of safety values simulated at the C3 hillslope as the rainfall rate varied over four orders of magnitude. (a) Base case. (b) Case1. (c) Case 2. (d) Case 3. (e) Case 4. (f) Case 5. See Table 8 for case descriptions.

road the portion of C3 downslope of the road is predominately unsaturated and the FS values are consistently higher than those simulated in the base case.

Cases 3-5

When the water table is near the surface (i.e. the hillslope is very saturated) the potential for slope failure can be amplified. As shown in Figure 58(e-f), the FS of the C3 hillslope is close to a value of 0.9 when subject to the initial and boundary conditions described in Cases 4 and 5. This low value of FS indicates that the C3 slope, by this criterion, should have failed. Figure 58(e-f) also confirms the relationship between the increased risk of slope failure and conditions of high soil-water content (Sidle et al., 1985). Because of the increased volume of interstitial water the soil cohesion is reduced and as a result saturated slopes are more likely to fail as unsaturated slopes.

Case 6

The impact of rainfall duration on slope stability is shown in Figure 56c. It is interesting to note that independent of the length of the rainfall event, the FS throughout the simulated C3 hillslope remained constant. In this instance the rainfall rate (0.36 mm/hr) was insufficient to drive any significant hydrologic or geomorphic change. One would expect that if the rainfall intensity were increased, as well as the duration of the event, that the likelihood for failure would also increase. In fact, many researchers have documented that mass movements can be triggered by “spikes” of high intensity rainfall falling on nearly saturated slopes that have been receiving lower, but longer duration levels of precipitation (Sidle et al., 1985; Coughlin, 1985; Coughlin, 1995; Montgomery et al., 1997; Torres et al., 1998).

Case 7

All of the simulations discussed thus far have concentrated on the potential for hillslope failure in the region above the road. An issue that has not yet been addressed in this study is the potential for fillslope failure, or the occurrence of a mass movement downslope of the road. The importance of fillslope failure was not apparent based on the VS2DT results because the water that was discharged from the roadcut face was not

routed to re-infiltrate elsewhere in the system, but was assumed to have exited the active domain. However, many researchers have noted the importance of road drainage in terms of rerouting flow and creating zones of concentrated recharge that can saturate fillslopes and cause slope failure below the roads (Swanson and Dyrness, 1979; Megahan, 1972; Wemple, 1996). In the case of the C3 hillslope, a culvert runs underneath the road and routes all of the water that is discharged along the cut slope to the downslope side of the road. To simulate this increase in local recharge on the downslope side of the road, the volumetric flux from the cutslope face was added to the rainfall rate at the first three nodes below the road. This process was repeated for each of the four simulated rainfall events of increasing intensity.

Figure 59 shows the impact on the pore pressure distribution throughout this portion of the C3 hillslope of effectively “re-routing” the water discharged at the roadcut to the downslope side of the road. Figure 60 shows the resultant FS for the Case 7 C3 hillslope. Whereas in all of the prior simulations the FS increased downslope of the road, these simulations show the FS also decreasing in proximity to the area of increased recharge i.e. the area below the culvert outlet where concentrated flow would be re-entering the system. The potential instability of the fillslope could be augmented if the volume of water recharging the system reflected the cumulative seepage from several different hollows that the road might intercept. If proper drainage conditions did not exist, flow could converge either on the road surface or in a drainage ditch until it reached a low point in the road or a culvert that would allow an ever increasing volume of water to locally saturate a downslope portion of the hill.

Discussion

The results of the VS2DT simulations conducted in the study supported the hypothesis that roads have a significant impact on the near-surface hydrologic response of a steep forested catchment. Coupled with the FS analysis and a sensitivity analysis of the different model inputs, the some of the conditions under which the C3 hillslope were susceptible to failure could be assessed. In summary, it seems that initial water table height has the largest impact on determining the slope stability. If an event was long enough and at high enough intensity to raise the water table height past a critical height,

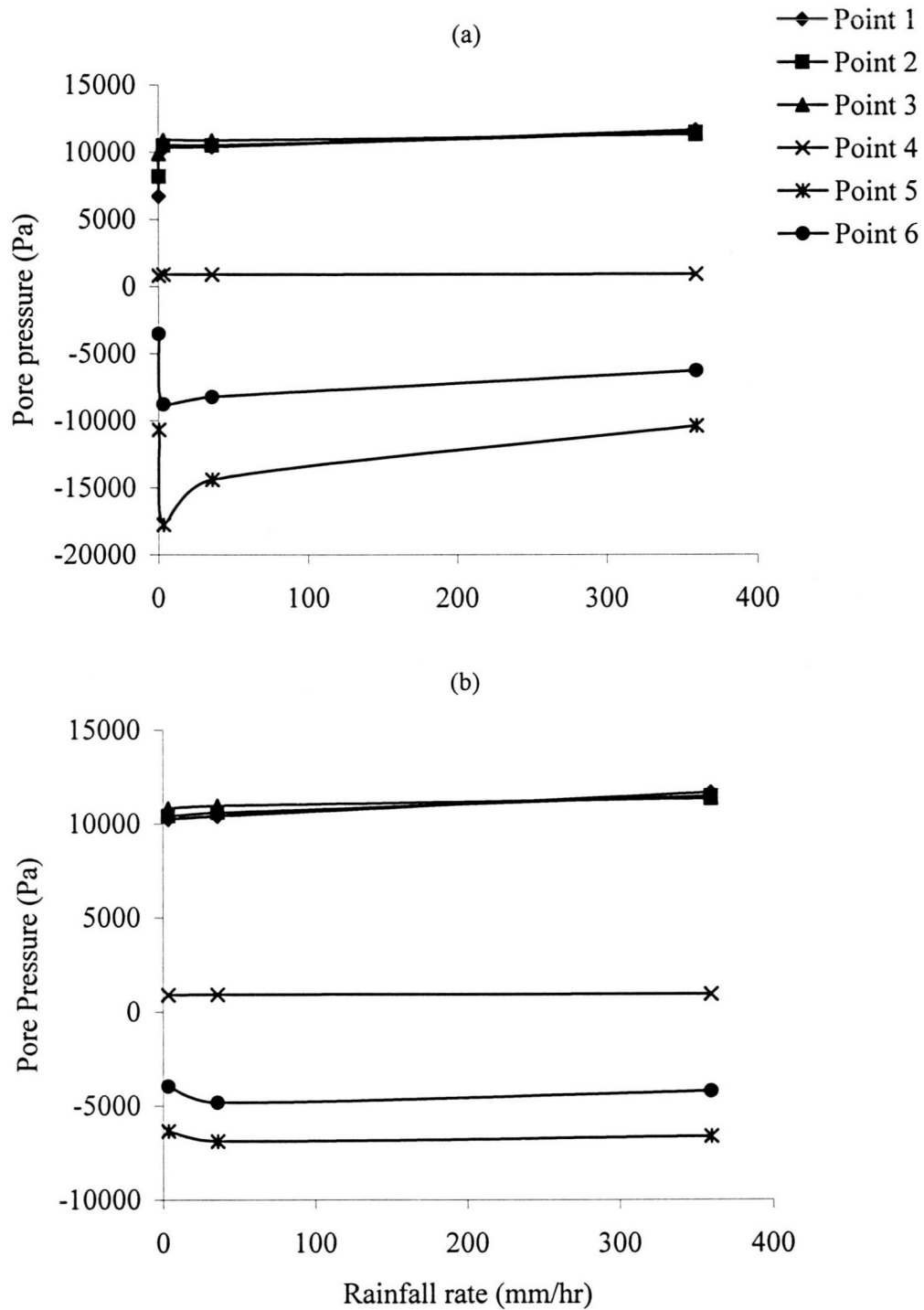


Figure 59. Pore pressure values simulated throughout the C3 hillslope subject to rainfall events varying over four orders of magnitude. (a) Base case. (b) Discharge at the roadcut face routed over the road to recharge the downslope side of the C3 system. See Figure 24 for the location of the measurement points.

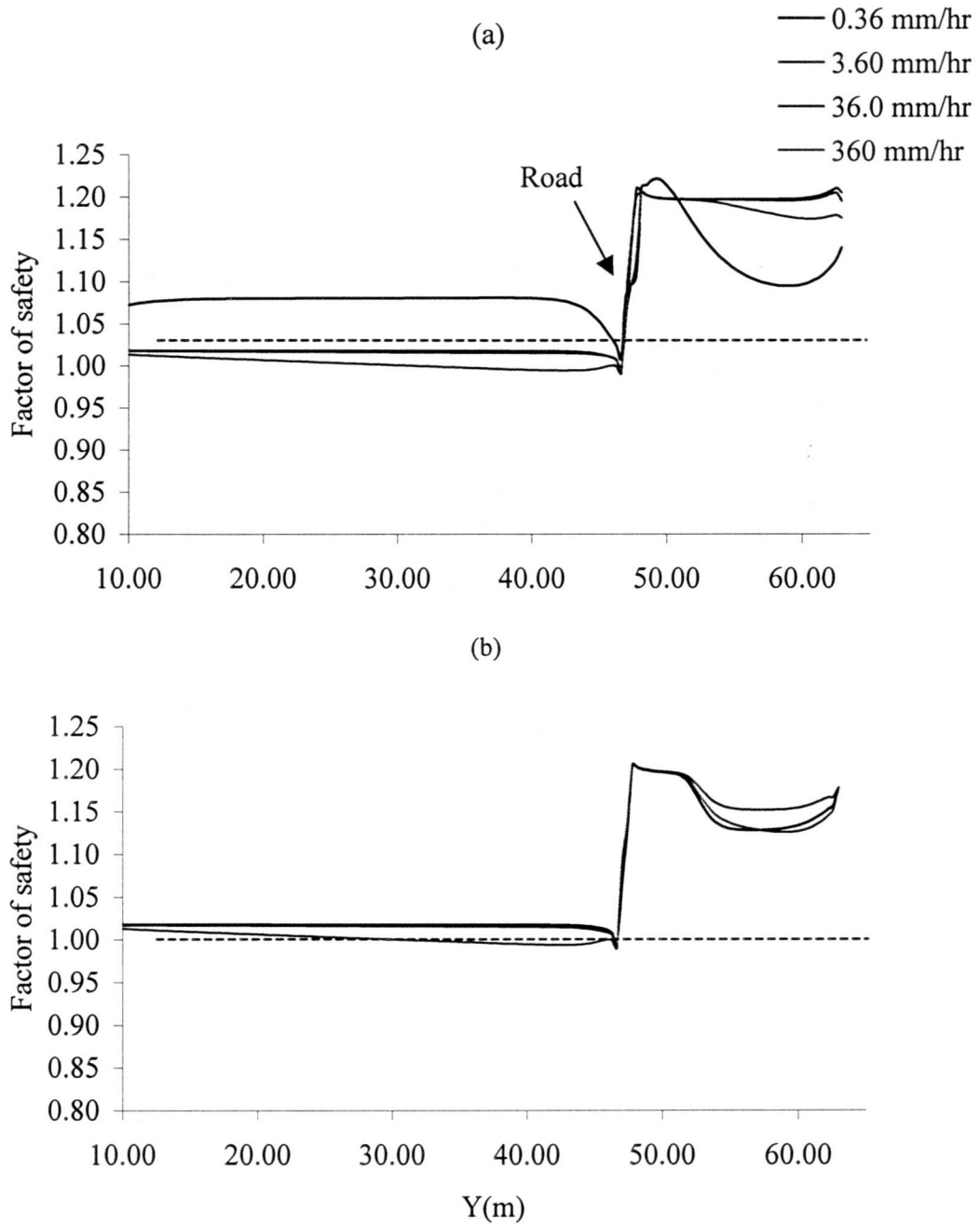


Figure 60. Factor of safety values as the rainfall rate varied over four orders of magnitude. (a) Base case. (b) Water routed over the road and recharging the system on the downslope side.

then any additional rainfall could imbalance the equilibrium and cause slope failure. The results also demonstrate that the impact of the road on hydrologic response is not just a localized phenomena, but that the impact can propagate up and down the hillslope.

CHAPTER FOUR: CONCLUSION

SUMMARY

The suite of hydrologic and geomorphic processes operating in steep, forested catchments is exceedingly complex. Recognition of the feedback loop between slope form, hydrologic response, runoff generation, and shallow landsliding is fundamental to understanding the geomorphology of mountain watersheds.

To assess the susceptibility of a hillslope to shallow landsliding, one must have a thorough knowledge of the hydrology, the near-surface and hydrogeologic properties, the topography, the failure plane, and the land use history. This study builds upon the work done by others, including prior studies at the H.J. Andrews (HJA) Experimental Forest Blue River, OR, on the general subject of accelerated landscape evolution related to land use. The objective of this study was to understand the physical, topographic, and hydrologic controls that control subsurface flow at Watershed 3 (WS3) in the HJA, and what role logging roads play in altering the hydrologic processes. This study combines a field component, process-based numerical simulation of near-surface hydrologic response, and slope stability analyses to address the impact of a road in a typical steep forested catchment.

The fieldwork conducted at WS3 characterized hillslope morphology, soil depth, and soil properties of a single hillslope (C3) within WS3. The modeling component of this study had four objectives: (i) identify what part of the WS3 and C3 hillslope systems were most drastically affected by the presence of a road using NUM5, a simple 2-D finite-difference model; (ii) isolate that portion of the flow domain for more detailed simulation with VS2DT, a 2-D transient, saturated-unsaturated, finite-difference model; (iii) compare the results from the VS2DT simulations with observed piezometric levels and hydrograph data for precipitation events in 1995; (iv) assess if pore pressure buildup in specific areas of C3 during a series of hypothetical events would be enough to trigger a mass movement event based on the factor of safety (FS) criterion.

The fieldwork conducted in the study reported here is documented in Chapters Two and Three. The general results from the field component of this work can be described as follows:

- The two-hectare C3 hillslope is concave with slopes ranging from 20-45%.

- The two-hectare C3 hillslope is concave with slopes ranging from 20-45%.
- The soils are deeper in the convergent hollow than on the bounding ridges.
- The soils have very high saturated hydraulic conductivities relative to the underlying saprolite and bedrock layers.
- Horton overland flow is never observed at C3.
- The roadcut intercepts a significant volume of water during rainfall events.

The characterization of the C3 hillslope could easily be used to describe most of the convergent hollows in the Western Cascades and makes the results from this study somewhat general for at least this region of the Pacific Northwest. The concave topography and the saturated hydraulic conductivity (K_s) contrast at the soil-bedrock contact noted at C3 (and the other catchments within the HJA) are conducive to the formation of elevated pore pressures. Depending on the soil-water content, the soil thickness, the slope steepness, and the intensity and/or duration of a given rainfall event, a hillslope failure can be expected to occur. The conversion of subsurface flow to surface flow at the roadcut may instigate cutslope or fillslope failure or create new channels and gullies that accelerate the movement of both sediment and water downslope.

The results from the numerical simulations performed in this study are described in Chapters Two and Three. The simulations support the hypothesis made in this study that roads have a significant impact on the near-surface hydrologic response of a steep forested catchment. Some of the most important findings are summarized below:

- The K_s , caused by the compacted soil beneath the road, directs flow out across the roadcut face.
- The roadcut acts to increase the pore pressure in the area above the road and to decrease the pore pressures below the road.
- Volumetric discharge increases with increased slope angle.
- Volumetric discharge increases as a function of rainfall intensity and/or duration.
- Volumetric discharge increases with higher antecedent soil-water content conditions.
- Slope stability decreases with increased slope angle.
- Slope stability decreases with increased K_s contrast between the high K_s soil and the low K_s compacted soil beneath the road.

- Slope stability decreases with higher antecedent soil-water content conditions.

In the NUM5 simulations for WS3 and C3, contrasts in K_s dominated the changes in the subsurface flow fields, and the hydraulic head and pore-pressure distributions relative to the homogeneous base case simulations. Based on the VS2DT simulations and sensitivity analysis, the initial water table height had the greatest impact on the slope stability. Both the NUM5 and VS2DT results, when coupled with the FS analysis demonstrated that the impact of the road on hydrologic response was not just a localized phenomenon, but that the impact could propagate up and down the hillslope.

DISCUSSION

While the results in this study quantitatively illustrate the impacts that different antecedent soil-water contents, rainfall intensities, and physical scenarios (i.e. slope angle and K_s) had on slope stability, the true applicability of any of these results to a real system must be discussed. To simulate the actual complexity of a system, taking into account both large scale and small-scale heterogeneity, was not feasible in this study. Therefore, both of the two-dimensional flow models (NUM5 and VS2DT) employed in this study represent simplified versions of the actual WS3 and C3 systems. The fact that the WS3 and C3 systems were modeled in two dimensions removes an entire element of lateral flow related to the convergent topography that might be important in terms of slope stability. Small-scale topography along the axis of the hillslope was not accounted for in the field mapping or in the simulations.

The parameters used as model input (e.g. K_s) can vary significantly spatially and with depth. Assumptions of homogeneity for properties such as soil depth, soil-water content, density, strength, and cohesion minimize their influences on the system, and therefore are not a true measure of reality. Averaging the rainfall over a minimum of half-hour intervals smoothed out some of the high intensity rain rainfall spikes that might have triggered failure in a real system.

Perhaps the biggest assumption made in this study was to concentrate the simulation efforts on cutslope and hillslope slides rather than fillslope slides. In terms of land use management issues, it is also very important to consider the potential for fillslope failure because in actual systems this type of road-related failure is very

prevalent and a significant source of sediment (see Dyrness, 1967; Swanson and Dyrness, 1975; Wemple, 1998). The subsurface flow models employed in this study could not route water over the road surface, as would occur in a real system.

IMPLICATIONS

It is important to understand how pervasive the impact of a land use change is on the hydrologic system of a watershed. It is now widely recognized that forest management practices, including timber harvesting and road construction, can significantly affect the hydrologic response, accelerate the near-surface evolution of a hillslope catchment, and increase sediment loading to downstream areas. However, depending on what geologic and topographic setting a road is constructed in, the impacts can be extremely variable. Slope profiles and K_s contrasts have a pronounced and diverse effect on groundwater seepage forces, effective stresses, and slope failure potentials. These issues are especially prevalent on steep hillslopes and they can be compounded by road building. Therefore, it is important to assess where, given a set of conditions, a road can be built while mitigating its impact on the local hydrology and geomorphology.

No study conducted thus far has been able to determine the exact conditions under which a hillslope will fail. Researches have (i) inventoried hillslopes to determine the relationships between road location and slide frequency, (ii) attempted to establish empirical relationships between rainfall events, slope angle and the type of resultant mass movement, and (iii) monitored a slope under natural and applied rainfall to determine the hydrologic conditions that served as precursors to failure. The study presented here sheds some insight into what can be done to avoid anthropogenically induced mass movements.

Midslope roads are the most likely to fail and this type of failure has the most impact on contributions to disturbance cascades and cumulative watershed effects. The results from this study suggest that if a road is built along a ridgeline or higher on the slope, it will have less of an impact on the watershed in terms of both volume of water intercepted at the roadcut and slope stability. In this study the area above the road (where the FS value dropped below 1.0 during some of the simulations) would decrease reducing both the area impacted and the volume of sediment released.

The work reported here also suggests that if the soil beneath the road were less compacted (i.e. traffic density was decreased, or the weight of the vehicles driven on the roads was reduced) then the vertical K_v contrast would not be as significant. As a result, the pore pressures would not increase so rapidly directly upslope of the road. Another alternative might be to use a different material to surface the road that is not so easily compacted (e.g., gravel). Materials such as gravel are highly porous, providing good drainage and trapping some of the fine-grain sediment that is easily eroded from the road surface. The depth to which the roadcut intercepts the water table also effects the slope stability and the results presented here suggest that a shallower roadcut would have less impact on the near-surface hydrologic response and on the volume of water intercepted at the roadcut.

Obviously, improved road designs that would avoid wider than necessary roads, avoid oversteepening of cut and fill slopes, and provide for adequate drainage (e.g. culverts that are big enough to handle the volumes of water and sediment discharged through them) would be beneficial. Some means of mitigating the potential impact that roads have on watershed functioning are:

- Improved engineering and design of roads.
- Improved drainage.
- Recognition and accounting for site geology.
- Placement of road on slopes to minimize impact.
- Aggressive action to “restore” the roaded areas to pre-disturbance conditions after they are no longer in active use.

A study performed at the level of detail described here highlights the significance of road positioning on a hillslope and the role of geology on determining slope stability. Larger scale variations in topography or K_v that might impede the downward flow of water and create locally elevated pore pressures warrant special attention in site-characterization and stability analysis. As demonstrated in this study, simple groundwater flow and slope stability models, can be used in a risk-adverse manner by the design community to identify the potential destabilizing effects of discharging groundwater flow (i.e. at the roadcut face) can be addressed in a risk-adverse manner. For example, prior to road construction, techniques similar to those employed in this study, could be used to

assess if a given area could support a road. Although this type of study might be expensive, it would likely be more cost-effective than trying to mitigate problems of unfavorable ecosystem impacts that might arise later as the result of improper road location and design.

REFERENCES

- Anderson, M.G. 1972. Forecasting the trafficability of soils. *Geomorphology and soils*. K.S. Richards, R.R. Arnett, S. Ellis (editors). George Allen & Unwin.
- Anderson, M.G. and T.P. Burt. 1978. The role of topography in controlling throughflow generation. *Earth Surface Processes* 3: 331-344.
- Anderson, S.P., W.E. Dietrich, R. Torres, D.R. Montgomery, and K. Loague. 1997. Concentration-discharge relationships in runoff from a steep unchanneled catchment. *Water Resources Research* 33: 211-225.
- Anderson, S.P., W.E. Dietrich, R. Torres, D.R. Montgomery, and K. Loague. 1997. Subsurface flow paths in a steep, unchanneled catchment. *Water Resources Research* 33: 2637-2653.
- Beven, K. 1977. Hillslope hydrographs by the finite element method. *Earth Surface Processes*. 2:13-28.
- Beven, K. 1981. Kinematic subsurface flow. *Water Resources Research* 17(5): 1419-1424.
- Bilby, R.E., K. Sullivan, and S.H. Duncan. 1989. The generation and rate of road-surface sediment production in forested watersheds in southwestern Washington. *Water Resources Research* 14: 1011-1016.
- Bosch, J.M. and J.D. Hewlett. 1982. A review of catchment experiments to determine the effect of vegetation changes on water yield and evapotranspiration. *Journal of Hydrology* 55: 3-23.
- Campbell, R.H. 1975. Soil slips, debris flows and rainstorms in the Santa Monica mountains, Southern California. U.S. Geological Survey Professional Paper 851. U.S. Geological Survey. Denver, CO. 51p.
- Cederholm, C.J., L.M. Reid, and E.O. Salo. 1981. Cumulative effects of logging road sediment on salmonoid populations in the Clearwater River, Jefferson County, Washington. *In Salmon-spawning gravel: A Renewable Resource in the Pacific Northwest?* 39: 38-74. Pullman, WA, USA: Washington Water Research Center.
- Coates, D.R. 1990. The relation of subsurface water to downslope movement and failure. *Geological Society of America, Special Paper* 252: 51-76.
- Cullen, S.J., C. Montagne, and H. Ferguson. 1991. Timber harvest trafficking and soil compaction in Western Montana. *Soil Science Society of America* 55: 1416-1421.
- Deustch, C.V. and A.G. Journel, 1992. *GSLIB- Geostatistical software library and users guide*. Oxford University Press. New York.

- Dunne, T., T.R. Moore et al. 1975. Recognition and prediction of runoff-producing ones in humid regions. *Hydrological Sciences Bulletin* 20(3): 305-327.
- Dietrich W.E; T. Dunne, N. Humphrey, and L. Reid. 1982, Construction of sediment budgets for drainage basins. In *Sediment budgets and Routing in Forested Drainage Basins*; Swanson, F.J.; Janda, R.J.; Dunne T.; and Swanston, D.N. (editors). U.S. Department of Agriculture, Forest service General technical Report PNW-141, Pacific Northwest Forest and Range Experiment Station: Portland, OR, p. 5-23.
- Dietrich, W.E., C.J. Wilson, and S.L. Reneau, 1986, Hollows, colluvium, and landslides in soil-mantled landscapes. In *Hillslope Processes*. Abrahams, A.D. (editor): Allen and Unwin Ltd.: 361-388.
- Dietrich, W.E., R. Preiss, M. Hsu, D.R. Montgomery. 1995. A process-based model for colluvial soil depth and shallow landsliding using digital elevation data. *Hydrological Processes* 9: 383-400.
- Dunne, Thomas. 1978. Field studies of hillslope flow processes. *Hillslope Hydrology* edited by M.J. Kirkby, p. 227-293. Wiley-Interscience. New York.
- Dyrness, C.T. 1967. Mass soil movements in the H.J. Andrews Experimental Forest. Pacific Northwest Forest and Range Experiment Station. USDA, USFS, PNW-42.
- Dyrness, C.T. 1969. Hydrologic properties of soils in three small watersheds in the Western Cascades of Oregon. USFS Research Note. PNW-111.
- Erlick, D.E. and W.D. Reynolds. 1992. Infiltration from constant head well Permeameters and Infiltrimeters. Soil Science Society of America. *Advances in Measurement of Soil Physical Properties: Bringing theory into Practice*. SSSA Special Publication 30:1-24.
- Freeze, R.A. 1971. Three-dimensional, transient, saturated-unsaturated flow in a groundwater basin. *Water Resources Research* 7: 347-366.
- Freeze, R.A. 1972. Role of Subsurface Flow in Generating Surface Runoff 1. Base Flow Contributions to Channel Flow. *Water Resources Research* 8: 609-623.
- Freeze and Cherry, 1979. *Groundwater*. Prentice Hall, Inc.
- Freeze, R.A., 1980, A stochastic-conceptual analysis of rainfall-runoff processes on a hillslope. *Water Resources Research* 16: 391-408.

- Grayson, R.B., S.R. Haydon, M.D.A. Jayasuriya, and B.L. Finlayson. 1993. Water quality in mountain ash forests - separating the impacts of roads from those of logging operations. *Journal of Hydrology* 150: 459-480.
- Harden, C.P. 1992. Incorporating roads and footpaths in watershed-scale hydrologic and soil erosion models. *Physical Geography* 13: 368-385.
- Harr, R.D., W.C. Harper, J.T. Krygier, and F.S. Hsieh. 1975. Changes in storm hydrographs after road building and clear-cutting in the Oregon Coast Range. *Water Resources Research*. 11:436-444.
- Harr, R.D. 1976. Forest practices and stream flow in western Oregon. Pacific Northwest Forest and Range Experiment Station. Portland, OR.
- Harr, R.D. 1977. Water flux in soil and subsoil on a steep forested hillslope. *Journal of Hydrology*. 33:37-58.
- Harr, R.D., and F.M. McCorison. 1979. Initial effects of logging on size and timing of peak flows in a small watershed in western Oregon. *Water Resources Research*. 15: 90-94.
- Hawk, G. and C.T. Dyrness, unpublished report. Vegetation and soils of watersheds 2 and 3. H.J. Andrews Experimental Forest. USFS Internal Report 49.
- Healy, 1987. Simulation of solute transport in variably saturated porous media with supplemental information on modification to the U.S. Geological Survey's computer program VS2D.
- Hodge, R.A. and R.A. Freeze, 1977. Groundwater flow systems and slope stability. *Canadian Geotech Journal* 14: 466-476.
- Humphrey, N.F., 1982. Pore pressures in debris failure initiation. State of Washington Water Research Center Rep. 45, Pullman WA, 169p.
- Iverson, R.M. and M.E. Reid. 1992. Gravity-driven groundwater flow and slope failure potential 1. Elastic effective stress model. *Water Resources Research*. 28: 925-938.
- Iverson, R.M. and J.J. Major, Groundwater seepage vectors and the potential for hillslope failure and debris flow mobilization, *Water Resources Research*. 22: 1543-1548.
- Jones, J.A. and G.E. Grant. 1996. Peak flow responses to clear-cutting and roads in small and large basins, Western Cascades, Oregon. *Water Resources Research*. 32: 959-974.

- King, J.G. and L.C. Tennyson. 1984. Alteration of streamflow characteristics following road construction in North Central Idaho. *Water Resources Research*. 20:1159-1163.
- Lappala, E.G., R.W. Healy, and E.P. Weeks, 1987. Documentation of computer program VS2D to solve the equations of fluid flow in variably saturated porous media. *Water Resources Investigation Report 83-4099*, USGS Open File Reports.
- Loague, K. and P.C. Kyriakidis. 1997. Spatial and temporal variability in the R-5 infiltration data set: Deja vu and rainfall-runoff simulations. *Water Resources Research* 33, 2883-2895.
- Megahan, W.F. and W.J. Kidd. 1972. Effect of logging roads on sediment production rates in the Idaho Batholith. Research paper INT-123. Ogden, Utah: U.S. Department of Agriculture, Forest research, Intermountain Forest and Range Experimental Station. 14p.
- Megahan, W.F. 1972, Subsurface storm flow interception by a logging road in mountains of central Idaho, paper presented at National Symposium on watersheds in Transition. American Water Resources Association, Minneapolis, Minn.
- Megahan, W.F. Deep-rooted plants for erosion control on granitic road fills in the Idaho batholith. Research paper INT-156. Ogden, Utah: U.S. Department of Agriculture Forest Service, Intermountain Forest and Range Experimental Station.
- Megahan, W.F. 1978. Erosion processes on steep granitic road fills in central Idaho. *Soil Science Society of America*. 42: 350-357.
- Megahan, W.F. and J.L. Clayton. 1983. Tracing subsurface flow on roadcuts on steep, forested slopes. *Soil Science Society of America Journal* 47(6):1063-1067.
- Megahan, W.F. 1987. Effects of forest roads on watershed function in mountainous areas. USDA, USFS, Intermountain Forest and Range Experiment Station. *Environmental Geotechnics and Problematic Soils and Rocks*. Balasubramanian et al. (editors) Balkems, Rotterdam. ISBN 90 6191 785 9.
- Montgomery, D.R. 1994. Road surface drainage, channel initiation, and slope instability. *Water Resources Research*. 30:1925-1932.
- Montgomery, D.R., W.E. Dietrich, R. Torres, S.P. Anderson, J.T. Heffner, and K. Loague. 1997. Hydrologic response of a steep unchanneled valley to natural and applied rainfall. *Water Resources Research*. 33: 91-109.

- Montgomery, D.R, R.H. Wright, and T. Booth 1991. Debris flow hazard mitigation for colluvium-filled swales. *Bulletin of the Association of Engineering Geologists*. 28: 303-323.
- Neary, D.G. and L.W. Swift, Jr. 1987. Rainfall thresholds for triggering a debris avalanching event in the southern Appalachian Mountains. *Geological Society of America, Reviews in Engineering Geology*. 7: 81-92.
- O'Loughlin, C.L. A preliminary study of landslides in the coast mountains of south western British Columbia. In *Mountain Geomorphology*; O. Slaymaker, H.J (ed.). MacPherson, 14:101-11.
- Reid. L.M. 1981. Sediment production from gravel-surfaced forest roads, Clearwater basin, Washington. Seattle, University of Washington Fisheries research institute.
- Reid, L.M., T. Dunne, and C.J. Cederholm. 1981. Application of sediment budget studies to the evaluation of logging road impacts. *Journal of Hydrology (NZ)* 29: 49-62.
- Reid, L.M. and T. Dunne. 1984. Sediment production from forest road surfaces. *Water Resources Research*. 20:1753-1761.
- Reid, M.R., H.P. Nielson, and S.J. Dreiss, 1988. Hydrologic factors triggering a shallow hillslope failure. *Bulletin of the Association of Engineering Geologists*. 25: 349-361.
- Reid, M.E. and R.M. Iverson. 1992. Gravity driven groundwater flow and slope failure potential, 2. Effects of slope morphology, material properties, and hydraulic heterogeneity, *Water Resources Research*. 28: 939-950.
- Rothacher, J., C.T. Dyrness, and R.L. Fredricksen. 1967. Hydrologic and related characteristics of three small watersheds in the Oregon Cascades. Pacific Northwest Forest and Range Experiment Station. USFS, USDA. PNW-111.
- Rulon, J.J. and R.A. Freeze. 1985. Multiple seepage faces on layered slopes and their implications for slope stability analysis. *Canadian Geotechnical Journal*. 22(3): 347-356.
- Rulon, J.J., R. Rodway, and R.A. Freeze. 1985. The development of multiple seepage faces on layered slopes. *Water Resources Research*. 21:1625-1636.
- Selby, M.J. 1993. *Hillslope Materials and Properties*. Oxford University Press.
- Sidle, R.C., A.J. Pierce, and C.L. O'Loughin. 1985. Hillslope stability and land use. American Geophysical Union. Water resources Monograph.

- Smetten, K.R.J., D.J. Chittleborough, B.G. Richards, and F.W. Leaney, 1991, The influence of macropores on runoff generation from a hillslope soil with contrasting textural class, *Journal of Hydrology*. 122: 235-252.
- Soilmoisture Equipment Corp. 1989. TRASE instruction manual and technical information. Santa Barbara, CA.
- Stephenson, G.R., and R.A. Freeze. Mathematical simulation of subsurface flow contributions to snowmelt runoff, Reynolds creek watershed, Idaho. *Water Resources Research* 10: 284-294.
- Swanson, F.J. and C.T. Dyrness. 1975. Impact of clear-cutting and road construction on soil erosion by landslides in the Western Cascade Range, Oregon.
- Swanson, F.J. and M.E. James. 1975. Geology and geomorphology of the H.J. Andrews Experimental Forest, Western Cascades, Oregon. Pacific Northwest Forest and Range Experiment Station. USDA, USFS, PNW-188.
- Swanston, D.N. 1970. Mechanics of debris avalanching in the shallow till soils of south east Alaska, research paper PNW-103, 17 p. Forest Service, U.S. department of Agriculture. Portland, OR.
- Swanston, D.N. 1974. Slope stability problems associated with timber harvesting in mountainous regions of the western United States. General technical Report. PNW-21, 41 pp. Forest Service, U.S. department of Agriculture. Portland, OR.
- Swanston, D.N. 1981. Creep and earthflow erosion from undisturbed and management impacted slopes in the coast and Cascade range of the Pacific Northwest, U.S.A., IAHS AISH Publication. 132, 76-194.
- Thomas, R.B. and W.F. Megahan. 1998. Peak flow response to clear-cutting and roads in small and large Basins, Western Cascades, Oregon: A second opinion. *Water Resources Research* 34: 3393-3403.
- Toth, J., 1963, A theoretical analysis of groundwater flow in small drainage basins, *Journal of Geophysical Research* 68: 4795-4812.
- Torres, R., W.E. Dietrich, D.R. Montgomery, S.P. Anderson, and K. Loague. 1998. Unsaturated zone processes and the hydrologic response of a steep, unchanneled catchment. *Water Resources Research* 34:1865-1879.
- Van Genuchten, M. Th. 1980. A closed form equation for predicting the hydraulic conductivity of unsaturated soils. *Soil Science Society of America Journal*. 44: 892-898.

- Wemple, B.C., J.A. Jones, and G.E. Grant. 1996. Channel network extension by logging roads in two basins, Western Cascades, Oregon. *Journal of the American Water Resources Association* 32:1195-1207.
- Wemple, B.C. 1998. Investigations of runoff production and sedimentation on forest roads. PhD Dissertation. Oregon State University.
- Wieczorek, G.F., 1987. Effect of rainfall intensity and duration on debris flows in central Santa Cruz Mountains, California. *Geological Society of America, Reviews in Engineering Geology* 7, 93-114.
- Wilson, C.J. and Dietrich, W.E., 1987. The contribution of bedrock groundwater flow to storm runoff and high pore pressure development in hollows. In Beschta, R.L, Blinn, T., Grant, G.E., Ice, G.G., and Swanson F.J. (editors), *Erosion and sedimentation in the Pacific Rim*; IAHS Publication No. 165, Washington DC, pp.49-60.
- Wright, K.A., K.H. Sendek, R.M. Rice, and R.M. Thomas. 1990. Logging effects on streamflow: Storm runoff at Caspar Creek in Northwestern California. *Water Resources Research* 26:1657-1667.
- Ziegler, A.D. and T.W. Giambelluca, 1997. Importance of rural roads as source areas for runoff in mountainous areas of northern Thailand. *Journal of Hydrology* 196: 204-229.
- Ziemer, R.R. 1981. Storm flow response to road building and partial cutting in small streams of Northern California. *Water Resources Research* 17:907-917.